REPUBLIC OF TURKEY
YILDIZ TECHNICAL UNIVERSITY
GRADUATE SCHOOL OF NATURAL AND APPLIED SCIENCES

THE DESIGN AND DEVELOPMENT OF NOVEL ULTRA-WIDE BAND (UWB) ANTENNA AND FILTER UNITS FOR RF FRONT-END APPLICATIONS

MUSTAFA İLARSLAN

PhD. THESIS

DEPARTMENT OF ELECTRONICS AND COMMUNICATION ENGINEERING
PROGRAM OF ELECTRONICS ENGINEERING

ADVISER
ASSIST. PROF. DR. HAMİD TORPİ

CO-ADVISER
ASSIST. PROF. DR. SALİH DEMİREL

İSTANBUL, 2014

REPUBLIC OF TURKEY

YILDIZ TECHNICAL UNIVERSITY

GRADUATE SCHOOL OF NATURAL AND APPLIED SCIENCES

THE DESIGN AND DEVELOPMENT OF NOVEL ULTRA-WIDE BAND (UWB) ANTENNA AND FILTER UNITS FOR RF FRONT-END APPLICATIONS

A thesis submitted by Mustafa İLARSLAN in partial fulfillment of the requirements for the degree of **DOCTOR OF PHILOSOPHY** is approved by the committee on 30.12.2014 in Department of Electronics and Communication Engineering, Electronics Engineering Program.

Thesis Adviser

Assist. Prof. Dr. Hamid TORPİ

Yıldız Technical University

Co- Adviser

Assist. Prof. Dr. Salih DEMİREL

Yıldız Technical University

Approved By the Examining Committee

Assist. Prof. Dr. Hamid TORPİ

Yıldız Technical University ______________________

Assist. Prof. Dr. Salih DEMİREL

Yıldız Technical University ______________________

Prof. Dr. Filiz GÜNEŞ, Member

Yıldız Technical University ______________________

Prof. Dr. Sedef KENT, Member

İstanbul Technical University ______________________

Prof. Dr. Ahmet Serdar TÜRK, Member
Yıldız Technical University ______________________

Assoc. Prof. Dr. Mesut KARTAL, Member
İstanbul Technical University ______________________

Assist. Prof. Dr. Ahmet ÖNCÜ, Member
Bosphorus University ______________________

ACKNOWLEDGEMENTS

Bu zorlu ve uzun süreçte her zaman yanımda olan, destek ve dualarını esirgemeyen Annem'e, Babam'a ve özellikle kendileri de bu yoldan çoktan geçmiş olan kardeşlerim Kazım ve Kenan hocalara en derin şükranlarımı sunmak istiyorum.

Her şeyin bir bedeli olduğu gerçeğinden hareketle bu bedeli benimle birlikte çektikleriyle ve yaptıkları fedakârlıklarla ödeyen eşim Çiğdem hanıma ve çocuklarım Ahmet, Şevval ve Vasfi'ye nasıl teşekkür edeceğimi ise bilemiyorum. Hakları ödenemez.

Bu çileli yolculukta beni yalnız bırakmayan, rehberlik görevlerinin ötesinde beni sürekli motive eden, zorlukları kolaylaştıran, danışman hocalarım Sayın Yrd. Doç. Dr. Hamid TORPİ ve Yrd. Doç. Dr. Salih DEMİREL'e sonsuz teşekkür ediyorum. Sizler olmadan bu çalışmayı sonuçlandırmamın imkânı yoktu.

Yine bu zorlu süreçte her zaman destek ve yardımlarını gördüğüm, yapıcı eleştiri ve önerilerinden istifade ettiğim Tez İzleme Komitesi üyeleri, Sayın Prof. Dr. Filiz GÜNEŞ, Prof. Dr. Sedef KENT ve Prof. Dr. Ahmet Serdar TÜRK hocalarım ile değerli arkadaşlarım Yrd. Doç. Dr. Mustafa Emre AYDEMİR ve Ahmet Kenan KESKİN'e teşekkürü bir borç bilirim.

Burada isimlerini tek tek sıralayamadığım, samimi yardım ve desteklerini sürekli hissettiğim yakın çevremdeki ve mesai ortamındaki dost ve arkadaşlarıma da şükranlarımı sunmadan geçemeyeceğim.

Hepiniz sağ olun, var olun..!

30 Aralık 2014

Mustafa İLARSLAN

TABLE OF CONTENTS

Page

LIST OF SYMBOLS ... vii

LIST OF ABBREVIATIONS ... vii

LIST OF FIGURES ... x

LIST OF TABLES ... xiiii

ABSTRACT ... xiii

ÖZET ... xv

CHAPTER 1

INTRODUCTION ... 1

1.1 Literature Review ... 1
1.1.1 What is RF Front-End ? ... 1
1.1.2 Building Blocks of RF Front-End ... 2
1.1.3 Basic Receiver Architectures ... 4
1.1.3.1 AM Detector Receivers ... 5
1.1.3.2 TRF Receiver ... 6
1.1.3.3 Direct Conversion Receiver ... 7
1.1.3.4 Superheterodyne Receivers ... 8
1.1.4 Advanced Architectures ... 8
1.1.4.1 Software Defined Radios ... 10
1.1.5 The trends for RF Front-End ... 11
1.2 Objective of the Thesis ... 13
1.2.1 Issues with RF Front-end Design ... 13
1.2.2 The Motivation and Research Goals ... 15
1.3 Hypothesis ... 15

CHAPTER 2

UWB RF FRONT-END ... 17

2.1 Wireless Revolution ... 17
2.2 The History of UWB ... 20
2.3 The Definition of UWB ... 21

2.4 UWB Target Applications 21
2.5 UWB Communication Technology 23
2.6 The Impact of UWB Technology on RF Front-End Design 25

CHAPTER 3

THE UWB ANTENNA DESIGN...30

3.1 Introduction 30
3.2 Antenna Design 32
3.2.1 The Effect of Partial Dielectric Loading 32
3.2.2 Antenna Implementation 34
3.3 The Simulation and Measurement Results 37
3.4 Results and Conclusions...41

CHAPTER 4

THE UWB FILTER DESIGN 42

4.1 Introduction 42
4.2 Classification 43
4.3 Base Elements..45
4.4 Design Synthesis and Optimization Process 47
4.4.1 Mathematical Bases of Support Vector Regression 47
4.4.2 3D EM Simulation-based SVRM Microstrip Modeling....................48
4.4.3 Cuckoo Search Algorithm 50
4.4.4 Cost function Evaluation and Updating Process 52
4.5 Design and Comparison of UWB Bandpass Filter 53
4.6 Results and Conclusions...57

CHAPTER 5

SYSTEM LEVEL TESTING 58

5.1 Simulations 58
5.2 Measurements 61
5.3 Results and Conclusions...67

CHAPTER 6

RESULTS AND DISCUSSION 68

REFERENCES..71

CURRICULUM VITAE...75

LIST OF SYMBOLS

b	Bias parameter
B	Bandwidth
C	Channel capacity
C	The positive parameter that is a measure of the trade-off
D	Antenna Aperture Depth
f	Frequency
f_l	The lower frequency of the operation band.
f_h	The higher frequency of the operation band.
f_c	The center frequency of the operation band.
h	Substrate thickness
K	Kernel function
n	Fixed number of available host nests
n_{sv}	The number of the Support Vectors
$\vec{\ell}_{ss}$	Length
P_a	Fraction probability (the probability of the egg laid by a cuckoo is discovered)
S/N	Signal to Noise Ratio (SNR)
S_{ij}	S-parameters
t	Thickness
Tanδ	Tangent loss
$[T]^n$	ABCD matrix of n^{th} element
$\vec{W}_{ss}$	Width
ϵ	Insensitive loss parameter
ε_r	Relative Permittivity
λ	The size of the training data
γ	The variance of the kernel function
α_i	Lagrange multipliers
ω_i	Weight coefficients of the cost function

LIST OF ABBREVIATIONS

2/3/4G	Second/Third/Fourth Generation
3D	Three Dimensional
ADC	Analog-to-Digital Converter
AM	Amplitude Modulation
bps	bits per second (aka b/s)
BER	Bit-Error Rate
BPF	Band Pass Filter
BPSK	Binary Phase Shift Keying
BSF	Band Stop Filter
CDMA	Code Division Multiple Access
CMOS	Complementary Metal Oxide Semiconductor
CPU	Central Processing Unit
CQP	Constrained Quadratic Programming
CS	Cuckoo Search
CSA	Cuckoo Search Algorithm
CST MWS	Computer Simulation Technology Microwave Studio
DAC	Digital-to-Analog Converter
DC	Direct Current
DCR	Direct Conversion Receiver
DGS	Defected Ground Structure
DSP	Digital Signal Processing
DS-UWB	Direct-Sequence Ultra-wideband
EM	Electromagnetic
EMC	Electromagnetic Compatibility
ESS	Etched Square Stub
FCC	US Federal Communications Commission
FDMA	Frequency Division Multiple Access
FET	Field Effect Transistor
GA	Genetic Algorithm
GaAs	Gallium Arsenide
GHz	Giga-Hertz
GPR	Ground Penetrating Radar
GSM	Global System for Mobile Communications
HDTV	High-Definition TV
HPF	High Pass Filter
HS	Harmony Search

IC	Integrated Circuit
IEEE	Institute of Electrical and Electronics Engineers
IF	Intermediate Frequency
IIP3	Third order Intercept Point
IoT	Internet of Things
IR	Impulse Radio
ISM	Industrial Scientific
I/Q	In / Quadrature
LNA	Low Noise Amplifier
LO	Local Oscillator
LPF	Low Pass Filter
LTE	Long-Term Evolution (aka 4G)
MB-OFDM	Multi-band Orthogonal Frequency Division Multiplexing
MCM	Multi-chip Module
mW	milliwatt
OOK	On Off Keying
PC	Personal Computer
PCB	Printed Circuit Board
PDTEM	Partially dielectric loaded TEM Antenna
PDVA	Partially dielectric loaded Vivaldi Antenna
PEC	Perfect Electric Conductor
PN	Pseudorandom
PPM	Pulse Position Modulation
PSO	Particle Swarm Optimization
Q	Quality Factor
RF	Radio Frequency
RF/D	RF-to-Digital
SATCOM	Satellite Communication
SDR	Software-Defined Radio
SNR	Signal-to-Noise Ratio
SiGe	Silicon Germanium
SIP	System-in-Package
SoC	System on a Chip
SS	Shunt Stub
SV	Support Vector
SVRM	Support Vector Regression Machine
TDMA	Time Division Multiple Access
TEM	Transverse Electro-Magnetic
TRF	Tuned-Radio-Frequency
USB	Universal Service Bus
UWB	Ultra-wide Band
VS-PDL	Vivaldi Shaped Partially Dielectric Loaded
VSWR	Voltage Standing Wave Ratio
WCDMA	Wideband CDMA
Wi-Max	Worldwide Interoperability for Microwave Access
WLAN	Wireless Local Area Network (aka Wi-Fi)
WPAN	Wireless Personal Area Network
YTU	Yıldız Technical University

LIST OF FIGURES

Page

Figure 1.1 Tear down of modern mobile device reveals several RF Front-end chips...2
Figure 1.2 Block diagram of an RF transceiver 4
Figure 1.3 Block diagram of RF front-end 5
Figure 1.4 Simple amplitude modulation (AM) radio architecture 6
Figure 1.5 Tuned-Radio-Frequency (TRF) architecture..6
Figure 1.6 Direct-Conversion Receiver (DCR) architecture 7
Figure 1.7 Superheterodyne architecture 8
Figure 1.8 Block diagram of a modern RF communication receiver 9
Figure 1.9 Generic block diagram of the receiver portion of a SDR.......................11
Figure 2.1 Various wireless systems along with data rates and distances 18
Figure 2.2 Allotted spectrum of various applications...19
Figure 2.3 FCC spectral mask for indoor UWB systems 21
Figure 2.4 UWB receiver block diagram..25
Figure 2.5 IR-UWB transceiver 26
Figure 2.6 DS-UWB transceiver 27
Figure 2.7 MB-OFDM Transceiver..27
Figure 3.1 The impact of dielectric loading on the antenna performance 34
Figure 3.2 Vivaldi Shaped TEM Horn Antenna 35
Figure 3.3 The variation of gain with respect to frequency for various aperture depth (D) values (simulation only)..36
Figure 3.4 VS-PDL TEM horn antenna design with its dimensions 36
Figure 3.5 The manufactured antenna 36
Figure 3.6 The simulated radiation patterns of the VS-PDL TEM Horn antenna for “boxed” and “un-boxed” configurations at various frequencies 38
Figure 3.7 Measured E-plane and H-Plane (Normalized) Radiation Patterns of the proposed antenna 39
Figure 3.8 Gain performance of the antenna for simulation (both boxed and un-boxed) and actual measurement cases. 39
Figure 3.9 Simulated and Measured (for both boxed and un-boxed cases) VSWR plots of the antenna 40
Figure 3.10 Time-domain characteristic of the proposed antenna measured on received pulse for various angles and for 1.5-11.0 GHz. 40
Figure 4.1 Shunt stub base element 46
Figure 4.2 Etched Square stub base element 46
Figure 4.3 Defected Ground Structure with microstrip line base element 46
Figure 4.4 Flow chart of the conventional Cuckoo Search Algorithm 51
Figure 4.5. General Design Procedure for the BPF..54
Figure 4.6 Scaled filter drawing with grid background 55

Figure 4.7 Photographs of the fabricated UWB BPF 55
Figure 4.8 Simulated and measured S parameters of the designed UWB BPF. 56
Figure 4.9 Measured group delay of the designed UWB BPF 56
Figure 5.1 Antenna and the filter as attached to it...58
Figure 5.2 Simulation set-up...59
Figure 5.3 Transmitted Signal...60
Figure 5.4 Received signal by the Antenna only...60
Figure 5.5 Received signal by the Antenna and the filter..61
Figure 5.6 Antenna and filter units in concanetation...62
Figure 5.7 Measurement set-up...63
Figure 5.8 Transmitted Pulse 63
Figure 5.9 The signal fed-back thru the cables 64
Figure 5.10 The signal picked-up by the antenna only and the antenna in concatenation with the filter 64
Figure 5.11 Transmitted Pulse 65
Figure 5.12 The signal fed-back thru the cables 65
Figure 5.13 The signal picked-up by the antenna only and the antenna in concatenation with the filter 66
Figure 5.14 The stop-band (a) and the transition-band (b) performance of the filter and its effect on the overall system performance..66

LIST OF TABLES

Page

Table 1.1 Overview of the main trends in the field of wireless communications, IC technology and packaging 12
Table 2.1 Candidate UWB systems specifications 27
Table 3.1 Frequency bands of some of popular wireless communication systems ... 38
Table 4.1 Dimensional range of Base Elements for training data 49
Table 4.2 Accuracy with respect to SVRM parameters 50
Table 4.3 Solution of the base elements. 55
Table 4.4 Comparison of the CSA performance with the Standard Meta-Heuristic Algorithms. 57

ABSTRACT

THE DESIGN AND DEVELOPMENT OF NOVEL ULTRA-WIDE BAND (UWB) ANTENNA AND FILTER UNITS FOR RF FRONT-END APPLICATIONS

Mustafa İLARSLAN

Department of Electronics and Communication Engineering

PhD. Thesis

Adviser: Assist. Prof. Dr. Hamid TORPİ

Co-adviser: Assist. Prof. Dr. Salih DEMİREL

RF Front-end is the term basically used to refer to the parts in an RF receiver that comprise the initial stage before the intermediate frequency or base-band section. It is usually meant to cover the antenna, filter, mixer with local oscillator and amplifier units in a typical superheterodyne receiver. RF Front-end design is a prominent issue within the RF system design as it is closely linked to the system architecture and performance. Since it has a direct impact on the system performance, its design has always been an important task for the industry as well as attractive for the academia to study.

Recent scientific studies on the RF Front-end design indicates two mainstream trends; either the design, development and manufacturing of RF Front-end circuitry in the form of "System-on-a-Chip" architectures i.e increased integration or the application of various optimization algorithms on the design of RF Front-end sub-units like antenna and filter as well as the overall system design to obtain a better performance. In this study, we followed the second trend and studied "Ultra Wide Band - UWB" RF Front-end design issues in terms of design, implementation and concatenation of novel UWB antenna and filter units as they are common to all kinds of RF Front-end system architectures. Other parts that are used to complement and test the design are commercially (readily) available equipment with known electrical characteristics and performance.

The designed antenna is a compact (miniaturized) version of a "Vivaldi Shaped Partially Dielectric Loaded (VS-PDL) Transverse Electromagnetic (TEM) Horn antenna". It was specifically designed to achieve high gain levels around 10dBi over the UWB band of 1.5-10.6 GHz. Vivaldi antennas as well as the TEM Horn antennas are good candidates for UWB applications as they both have relatively simple geometry and high gain over a wide bandwidth.

The idea is to make use of combined respective advantages of Vivaldi and TEM horn antennas to achieve the desired goals by shaping the TEM horn antenna to look like a Vivaldi antenna. The antenna structure is further modified by a partial dielectric load in the center to increase the gain bandwidth. It is placed in a surrounding box made of a Perfect Electric Conductor (PEC) material to reduce the undesired side lobes and to obtain more directive radiation pattern.

The results are promising and the Vivaldi Shaped Partially Dielectric Loaded (VS-PDL) TEM horn antenna is proposed as a compact UWB antenna for systems using the newly established UWB (3.1-10.6 GHz) band and also for various applications including the RF Front-End parts of the communication systems using the popular bands like ISM, Wi-Fi and GSM.

Regarding the filter, a new methodology using a 3D Electromagnetic (EM) simulator-based Support Vector Regression Machine (SVRM) models of base elements is presented for band-pass filter (BPF) design. SVRM models of elements which are as fast as analytical equations and as accurate as a 3D EM simulator, are employed in a simple and efficient Cuckoo Search Algorithm (CSA) to optimize an ultrawideband (UWB) microstrip BPF. CSA performance is verified by comparing it with other Meta-Heuristics such as Genetic Algorithm (GA) and Particle Swarm Optimization (PSO). As an example of the proposed design methodology, an UWB BPF that operates between the frequencies of 3.1 GHz and 10.6 GHz is designed, fabricated and measured. The simulation and measurement results indicate in conclusion the superior performance of this optimization methodology in terms of improved filter response characteristics like return loss, insertion loss, harmonic suppression and group delay.

The concatenation of the antenna and the filter (as if they were part of a complete RF Front-end circuitry) without seeking any certain application is verified by the simulations using the CST STUDIO SUITE Electromagnetic (EM) Simulation software program first and then by the system level measurements within the laboratory environment. It has been observed that there were no significant waveform dispersion on the received pulse shape. This is an important issue in the UWB design and hence the measurement results are concluded as very satisfactory and in agreement with the simulation results indicating a successful UWB performance of the units under test.

Key words: RF Front-End, Ultra Wide Band (UWB), UWB Communication Antenna, TEM Horn Antenna, Vivaldi Antenna, Optimization, Cuckoo Search Algorithm, Band-Pass Filter (BPF), Support Vector Regression Machine (SVRM)

YILDIZ TECHNICAL UNIVERSITY

GRADUATE SCHOOL OF NATURAL AND APPLIED SCIENCES

ÖZET

RF ÖN UÇ UYGULAMALARI İÇİN ÖZGÜN, ÇOK GENİŞ BANDLI ANTEN VE FİLTRE TASARIMI VE GELİŞTİRİLMESİ

Mustafa İLARSLAN

Elektronik Mühendisliği Anabilim Dalı

Doktora Tezi

Tez Danışmanı: Yrd. Doç. Dr. Hamid TORPİ

Eş Danışman: Yrd. Doç. Dr. Salih DEMİREL

RF ön-uç temelde bir RF alıcısının, ara frekans veya baz-bant bölümünden önce ilk aşamasını oluşturan parçaları ifade etmek için kullanılan bir terimdir. Bu, genellikle, tipik bir süperheterodin alıcısının karıştırıcı / yerel osilatör ve düşük gürültülü yükselteç birimleri ile anten ve filtre birimlerini kapsamaktadır. RF ön-uç tasarımı, doğrudan sistem mimarisi ve performansını etkilediği için RF sistem tasarımında önemli bir konudur. Sistem performansı ile doğrudan bağlantılı olduğu için sanayinin ilgisini çektiği kadar akademik camia için de cazip bir çalışma alanı oluşturmaktadır.

Son bilimsel çalışmalar RF ön-uç tasarımında iki ana eğilimi göstermektedir; ya "Yongada Sistem (System-on-a-Chip)" formunda RF ön-uç devresi tasarım, geliştirme ve imalatı yani artan entegrasyon eğilimi ya da anten ve filtre gibi gibi RF ön-uç alt birim tasarımları ile genel sistem tasarımının çeşitli iyileştirme (optimizasyon) algoritmalarının uygulanması yoluyla geliştirilmesi ve genel bir performans iyileştirmesi elde edilmesi şeklindedir. Bu çalışmada ikinci eğilim takip edilmiş ve "Ultra Geniş Band - UGB" RF ön-uç tasarım hususları ele alınmıştır. Ayrıca, tüm RF ön-uç mimarilerinin hepsinde bulundukları için UGB anten ve filtre ünitelerinin özgün tasarımları gerçeklenmiştir. Tasarımı tamamlamak ve test etmek için kullanılan diğer cihazlar, bilinen elektriksel özelliklere ve performansa sahip Rafta Hazır Ticari (RAHAT) ürünlerdir.

Tasarlanmış anten "Kısmen Dielektrik Yüklü Vivaldi şekilli Transverse Electromanyetik (TEM) Horn (VS-PDL)" antenin kompakt (küçültülmüş) bir

versiyonudur. Özellikle 1,5-10,6 GHz (UGB) bandında 10dBi civarında yüksek kazanç değerleri sağlayacak şekilde çalışmak üzere tasarlanmıştır. Vivaldi ve TEM Horn antenler nispeten basit geometrileri ve geniş bir bantta sağlayabildikleri yüksek kazanç değerleri nedeniyle UGB uygulamaları için uygun adaylardır.

Çalışmanın bu bölümü, TEM Horn antenler ile Vivaldi antenlerin karşılıklı avantajlarından yararlanarak istenen performans hedeflerine ulaşmak amacıyla TEM Horn antenin Vivaldi anten gibi şekillendirilmesi esasına dayanmaktadır. Anten yapısına, kazanç ve bant genişliğini artırmak amacıyla ortasından kısmi dielektrik yüklemesi yapılmıştır. Anten, daha iyi yönlendirilmiş bir ışıma diyagramı elde etmek ve istenmeyen yan süzmeleri azaltmak için Mükemmel Elektriksel İletken (MEİ) bir malzemeden yapılmış bir kutu içine yerleştirilmiştir.

Sonuçlar başarılı bir seviyede olup "Kısmen Dielektrik Yüklü Vivaldi şekilli TEM Horn (VS-PDL)" anteni, yeni oluşturulan UGB (3,1-10,6 GHz) bandını kullanan sistemler için olduğu kadar ISM, Wi-Fi ve GSM gibi popüler bantları kullanan iletişim sistemlerinin RF Ön-uç bölümlerinde de kullanılabilecek kompakt bir anten olarak önerilmiştir.

Filtre ile ilgili olarak, bant-geçiren filtre (BGF) tasarımı için, baz elemanlarının, 3B Elektromanyetik (EM) simülatör tabanlı Support Vector Regression Machine (SVRM) modellerini kullanan yeni bir metodoloji sunulmuştur. Analitik denklemler kadar hızlı ve 3B EM simülatörü kadar doğru SVRM model elementleri, Ultra Geniş Bant mikrostrip BGF'yi optimize etmek için basit ve etkili bir Guguk Kuşu Arama (GKA) Algoritmasında kullanılmıştır. GKA performansı, Genetik Algoritma (GA) ve Parçacık Sürü Optimizasyonu (PSO) gibi diğer Meta-Heuristic'lerin sonuçları ile karşılaştırarak doğrulanmıştır. Önerilen tasarım metodolojisine bir örnek olarak, 3.1 GHz ve 10.6 GHz frekansları arasında çalışan bir UGB BGF tasarlanmış, üretilmiş ve ölçülmüştür. Simülasyon ve ölçüm sonuçları paralellik arz etmekte olup, dönüş kaybı, ekleme kaybı, harmonik bastırma ve grup gecikmesi gibi filtre tepki karakteristikleri açısından da bu optimizasyon metodolojisinin daha üstün performansına işaret etmektedir.

Özgün tasarlanan UGB anten ve filtre ünitelerinin ardışık olarak birlikte çalışma performansları (sanki komple bir RF ön-uç devresinin bir parçalarıymış gibi) özel bir uygulama amacı düşünülmeden, CST STUDIO SUITE Elektromanyetik (EM) Simülasyon yazılımı kullanılarak simule edilmiş ve ayrıca laboratuar ortamında gerçekleştirilen ölçümler ile doğrulanmıştır. Alınan dalga şekillerinde ciddi bir dağılma /bozulma gözlemlenmemiştir. Bu husus UGB tasarımında önemli bir noktadır. Dolayısıyla, ölçüm sonuçları, simülasyon sonuçları ile uyum içerisinde ve çok tatmin edici bir seviyede olup başarılı bir UGB performansına işaret etmektedir.

Anahtar Kelimeler: RF Ön-Uç, Ultra Geniş Bant (UGB), UGB Haberleşme Anteni, TEM Horn Anteni, Vivaldi Anteni, Optimizasyon, Guguk Kuşu Arama Algoritması, Band-Geçiren Filtre (BGF), Support Vector Regression Machine (SVRM)

CHAPTER 1

INTRODUCTION

1.1 Literature Review

1.1.1 What is RF Front-End?

The RF front end is one of the most critical subsystems in any communication system. It is part of an overall radio receiver-transmitter or transceiver system. It is generally defined as everything between the antenna and the digital baseband system. For a receiver, this “between” area includes all the filters, low-noise amplifiers (LNAs), and down-conversion mixer(s) needed to process the modulated signals received at the antenna into signals suitable for input into the baseband analog-to-digital converter (ADC). For this reason, the RF front end is often called the analog-to-digital or RF-to-baseband portion of a receiver.

Radios work by receiving RF waves containing previously modulated information sent by an RF transmitter. The receiver is basically a low noise amplifier that down converts the incoming signal. Hence, sensitivity and selectivity are the primary concerns in receiver design.

Conversely, a transmitter up converts an outgoing signal prior to passage through a high power amplifier. In this case, non-linearity of the amplifier is a primary concern. Yet, even with these differences, the design of the receiver front end and transmitter back end share many common elements — like antenna and local oscillators.

Why is the front-end so important? It turns out that this is arguably the most critical part of the whole receiver. Trade-offs in overall system performance, power consumption, and size are determined between the receiver front end and the ADCs in the baseband (middle end). In more detail, the analog front end sets the stage for what digital bit-error-rate (BER) performance is possible at final bit detection. It is here that the receiver can, within limits, be designed for the best potential signal-to-noise ratio (SNR) [1].

1.1.2 Building Blocks of RF Front-End

If we look inside any modern mobile phone, multimedia device, or home-entertainment control system that relies on the reception and/or transmission of wireless signals, we'll find an RF front end. In the RIM Blackberry PDA, for example, the communication system consists of both a transceiver chip and RF front-end module (Figure 1.1) [1]. The front-end module incorporates several integrated circuits (ICs) that may be based on widely different semiconductor processes, such as conventional silicon CMOS and advanced silicon germanium (SiGe) technologies. Functionally, such multichip modules provide most if not all of the analog signal processing — filtering, detection, amplification and demodulation via a mixer. (The term " system-in-package " or SIP is a synonym for multichip module or MCM)

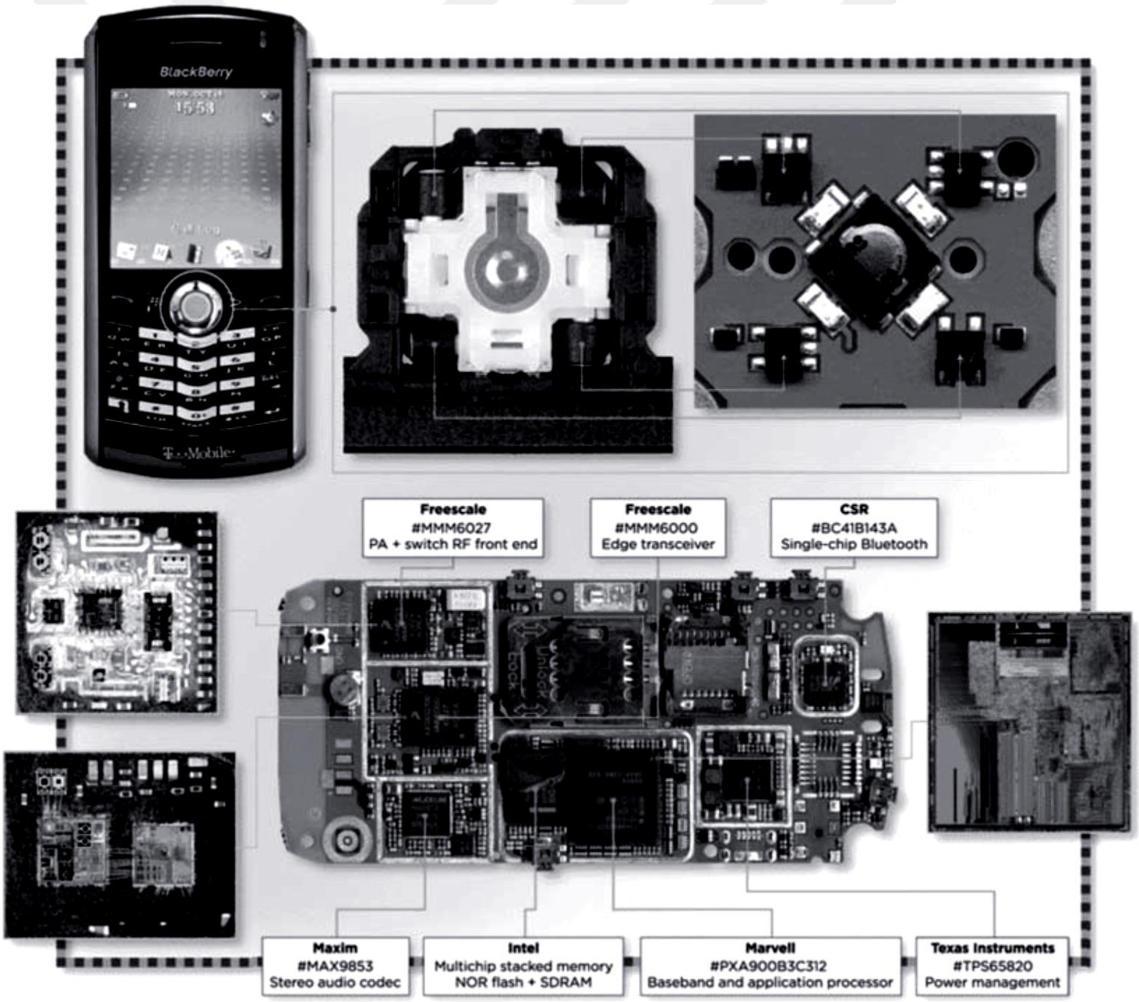

Figure 1.1 Tear down of modern mobile device reveals several RF Front-end chips

Multichip front-end modules demonstrate an important trend in RF receiver design, namely, ever-increasing levels of system integration required to squeeze more functionality into a single chip. The reasons for this trend — especially in consumer electronics — come from the need for lower costs, lower power consumption (especially in mobile and portable products), and smaller product size. Still, regardless of the level of integration, the basic RF architecture remains unchanged: signal filtering, detection, amplification and demodulation. More specifically, a modulated RF carrier signal couples with an antenna designed for a specific band of frequencies. The antenna passes the modulated signals along to the RF receiver's front end. After much conditioning in the front-end circuitry, the modulation or information portion of the signal — now in the form of an analog baseband signal — is ready for analog to- digital conversion into the digital world. Once in the digital realm, the information can be extracted from the digitized carrier waveforms and made available as audio, video, or data.

Before the advent of such tightly integrated modules, each functional block of the RF Front-end was a separate component, designed separately. This means that there were separate components for the RF filter, detector, mixer-demodulator, and amplifier. More importantly, this meant that all of these physically independent blocks had to be connected together. To prevent signal attenuation and distortion and to minimize signal reflections due to impedance differences between function blocks, components were standardized for a characteristic impedance of 50 ohms, which was also the impedance of high-frequency test equipment. The 50-ohm coaxial cable interface was a trade-off that minimized signal attenuation while maximizing power transfer — signal energy — between the independently designed RF filter, LNA, and mixer. Before higher levels of functional integration and thus lower costs could be achieved, it was necessary to design and manufacture these RF functional blocks separately and deal with matching issues.

As mentioned earlier, the basic stages of an RF front end include an antenna, filter, detector demodulator, and amplifier. Each of these signal-conditioning stages contains unique circuit components. None of these components work in isolation and the performance of one component may well affect the performance of another. This is why we'll look at them in the context of several different radio architectures: detector, direct-conversion, and superheterodyne receiver configurations [1].

1.1.3 Basic Receiver Architectures

In Figure 1.2, the block diagram of an RF transceiver is presented. The receive path begins with an RF front-end. It has to suppress interferers, to amplify received high-frequency analog signals and to down-convert them to a low IF. The IF strip has to provide an additional filtering and amplification. At the end of the front-end, an Analog to Digital Converter (ADC) converts the low-frequency analog signals into the digital domain. In general, a Digital Signal Processing (DSP) block performs all or some of the following operations: demodulation, equalization, de-interleaving, decoding and voice decompression. Actually, the ADC is an interface between the analog and the digital part of an RF transceiver. ADC specifications have a strong influence on specifications of building blocks in the analog part of an RF transceiver. Therefore, the ADC is taken to be the last block in a front-end. A transmit path begins with a DSP block. It performs all or some of the following operations: voice compression, coding, interleaving and pulse shaping. Next, signals are converted to the analog domain using a Digital to Analog Converter (DAC). At the end, signals are up-converted to a high frequency and they are amplified by a power amplifier [2].

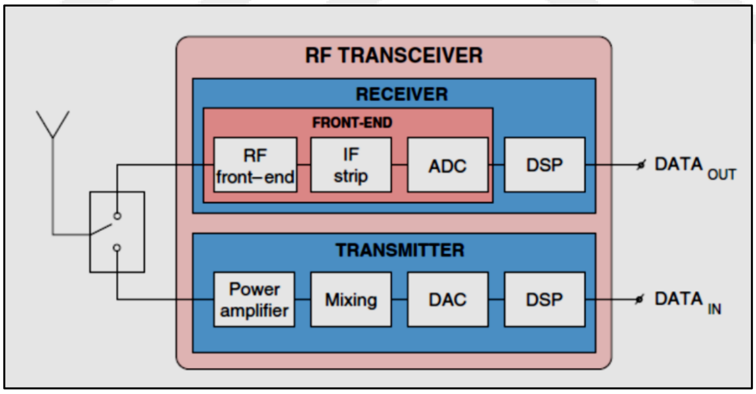

Figure 1.2 Block diagram of an RF transceiver

The block diagram of an RF front-end is presented in Figure 1.3 The fundamental operation of an RF front end is fairly straightforward: it detects and processes radio waves that have been transmitted with a specific known frequency or range of frequencies and known modulation format. The modulation carries the information of interest, be it voice, audio, data, or video. The receiver must be tuned to resonate with the transmitted frequency or frequencies in order to detect them. Those received signals are then filtered from all surrounding signals and noise and amplified prior to a process known as demodulation, which removes the desired information from the radio waves that carried it [1].

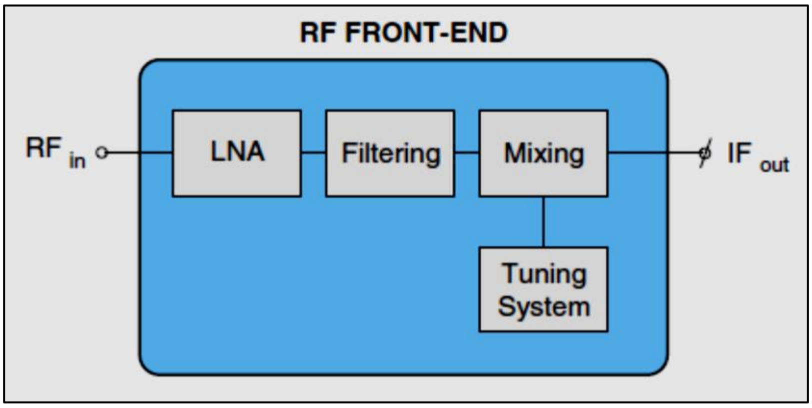

Figure 1.3 Block diagram of RF Front-end

These three steps — filtering, amplification and demodulation — summarizes the overall function of RF Front-end but its actual implementation (i.e. designing the physical RF receiver printed circuit board (PCB)) depends upon the type, complexity, and quantity of the data being transmitted. For example, designing an RF front end to handle a simple amplitude-modulated (AM) signal requires far less effort and hardware (and even software) than building an RF front end for the latest third-generation (3G) mobile telecommunications handset.

Because of the enhanced performance of analog components due to IC process improvements and decreasing costs of more powerful digital-signal-processing (DSP) hardware and software functions, the ways that different RF front-end architectures are realized has changed over the years. Still, the basic requirements for an RF front end, such as the frequency range and type of carrier to be received, the RF link budget, and the power, performance, and size restrictions of the front-end design, remain relatively the same in spite of the differences in radio architectures. Let's start by looking at the simplest of radio architectures or implementations [1].

1.1.3.1 AM Detector Receivers

One of the basic RF receiver architectures for detecting a modulated signal is the amplitude modulation (AM) detector receiver (Figure 1.4). The name comes from the fact that information like speech and music could be converted into amplitude (voltage) modulated signals riding on a carrier wave. Such an RF signal could be demodulated at the receiving end by means of a simple diode detector. All that is needed for a basic AM receiver — like a simple crystal radio — is an antenna, RF filter, detector, and (optional) amplifier to boost the recovered information to a level suitable for a listening device, such as a speaker or headphones. The antenna, which is capacitive at the low frequencies used for AM broadcasting, is series matched with an inductor to maximize current through both, thus maximizing the voltage across the secondary coil. A variable capacitance filter may be used to select the designed frequency band (or channel) and to block any unwanted signals, such as noise. The filtered signal is then converted to demodulate the AM signal and recover the information [1].

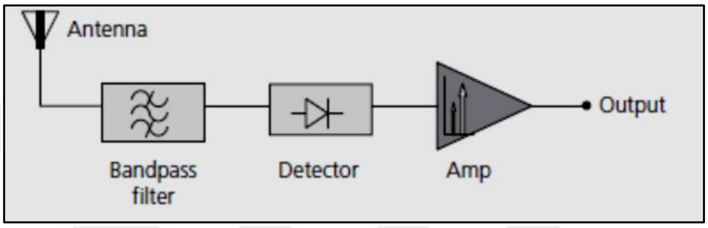

Figure 1.4 Simple amplitude modulation (AM) radio architecture

1.1.3.2 TRF Receiver

Moving up the scale in complexity, we come to the next evolutionary RF architecture: the tuned-radio-frequency (TRF) receiver (Figure 1.5). This early design was one of the first to use amplification techniques to enhance the quality of the signal reception. A TRF receiver consisted of several RF stages, all simultaneously tuned to the received frequency before detection and subsequent amplification of the audio signal. Each tuned stage consisted of a band pass filter with an amplifier to boost the desired signal while reducing unwanted signals such as interference.

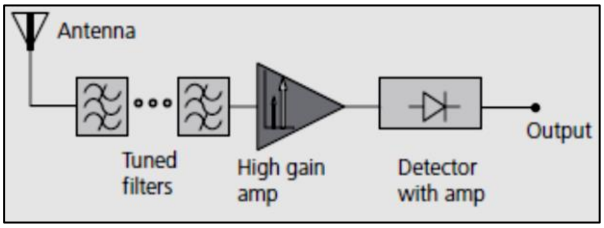

Figure 1.5 Tuned-Radio-Frequency (TRF) architecture emphasizes multiple tuned filters

The selectivity in a TRF receiver is not constant, since the receiver is more selective at lower frequencies and less selective at higher frequencies. Such variations in selectivity can cause unwanted oscillations and modes in the tuned stages. In addition, amplification is not constant over the tuning range. Such shortcomings in the TRF receiver architecture have led to more widespread adoption of other receiver architectures, including direct-conversion and superheterodyne receivers, for many modern wireless applications [1].

1.1.3.3 Direct Conversion Receiver

A way to overcome the need for several individually tuned RF filters in the TRF receiver is by directly converting the original signal to a much lower baseband frequency. In the direct conversion receiver (DCR) architecture, frequency translation is used to change the high input frequency carrying the modulated information into a lower frequency that still carries the modulation but which is easier to detect and demodulate. This frequency translation is achieved by mixing the input RF signal with a reference signal of identical or near-identical frequency (Figure 1.6). The nonlinear mixing of the two signals results in a baseband signal prior to the detection or demodulating stage of the front-end receiver.

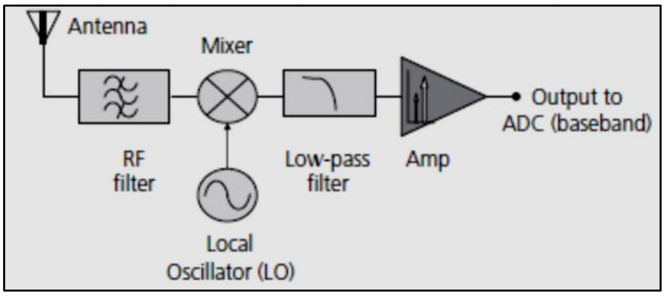

Figure 1.6 Direct-Conversion Receiver (DCR) architecture

The reference signal is generated by a local oscillator (LO). When an input RF signal is combined in a nonlinear device, such as a diode or field-effect-transistor (FET) mixer, with an LO signal, the result is an intermediate-frequency (IF) signal that is the sum or difference of the RF and LO signals. When the LO signal is chosen to be the same as the RF input signal, the receiver is said to have a homodyne (or “same frequency”) architecture and is also known as a zero-IF receiver. Conversely, if the reference signal is different from the frequency to be detected, then it’s called a heterodyne (or “different frequency”) receiver. The terms superheterodyne and heterodyne are synonyms (“super” means “higher” or “above” not “better”) [1].

1.1.3.4 Superheterodyne Receivers

In contrast to the simplicity of the direct-conversion receiver, the superheterodyne receiver architecture often incorporates multiple frequency translation stages along with their associated filters, amplifiers, mixers, and local oscillators (Figure 1.7). But in doing so, this receiver architecture can achieve unmatched selectivity and sensitivity. Unlike the direct conversion receiver in which the LO frequencies are synchronized to the input RF signals, a superheterodyne receiver uses an LO frequency that is offset by a fixed amount from the desired signal. This fixed amount results in an intermediate frequency (IF) generated by mixing the LO and RF signals in a nonlinear device such as a diode or FET mixer.

Although a superheterodyne receiver introduces problems with spurious responses that do not exist with the other receiver architectures, it is the ease and cost-effectiveness of filtering and boosting signals at IF that makes this configuration so attractive for wireless applications [1].

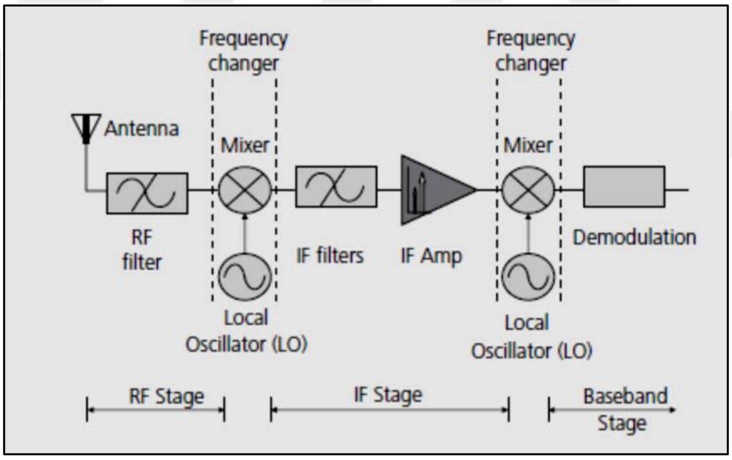

Figure 1.7 Superheterodyne architecture

1.1.4 Advanced Architectures

A typical modern communications transceiver and its front-end/back-end could be used to support modern cellular communication systems like 2G and 3G where they employ Code Division Multiple Access (CDMA) or Time Division Multiple Access (TDMA) systems in the same radio band which is possible since the processing and demodulation is performed in the post-baseband, digital section.

As the name implies, Time Division Multiple Access (TDMA) technology divides a radio channel into sequential time slices. Each channel user takes turns transmitting and receiving in a round-robin fashion. TDMA is a popular cellular phone technology since it provides greater channel capacity than its predecessor, Frequency Division Multiple Access (FDMA). Global System for Mobile Communications (GSM), an established cellular technology in Asia and Europe, uses a form of TDMA technology.

In a modern receiver front-end communication system, the received signal is amplified, mixed down to IF, and filtered before being mixed down to baseband where it is digitized for demodulation (Figure 1.8). A double (multi-mixer) superheterodyne architecture is typically used in a CDMA receiver whose basic receiver architecture is similar to TDMA. The RF front-end consists of the typical duplexer and low-noise amplifier (LNA) to provide additional signal gain to compensate for signal losses from the subsequent image-reject filter and then the first mixer. Two downconverter stages are used between the RF and baseband subsystems. The first mixer downconverts the signal to a first IF stage. The second mixer completes the downconversion from the IF stage to baseband. The I/Q outputs from the second mixer stage are digitally decoded and demodulated in the baseband DSP subsystem.

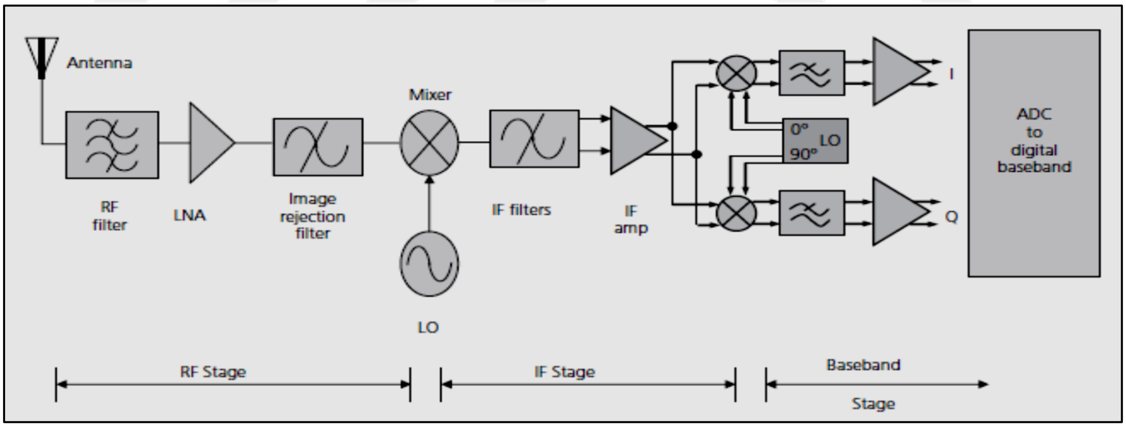

Figure 1.8 Block diagram of a modern RF communication receiver

In general terms, all receivers fall under the two main headings of TRF (tuned radio frequency) receivers, where the received signal is processed at the incoming frequency right up to the detector stage, and the superheterodyne receiver, where the incoming signal is translated (sometimes after some amplification at the incoming frequency) to an intermediate frequency for further processing. There are, however, a number of variants of each of these two main types. The dominant receiver architecture since the 1930s has been the superheterodyne in various forms, replacing the earlier TRF sets.

1.1.4.1 Software Defined Radios

In modern communication systems, we are more concerned with the reception or transmission of a single type of signal, even though some systems may use various different frequency bands, such as the three-band TV. Another example is a mobile phone base station, which is called upon simultaneously to receive from and transmit to a score of mobiles, using adaptive power control of the mobile-to-base station link, though they all use the same signal format or “air-interface standard”.

But there are cases where it is desirable or necessary to be able to receive transmissions on widely differing frequency bands and with widely differing modulation methods, data rates and bandwidths. In theory a receiver, using all conventional analog technology, could be designed such that it had a variety of different bandwidth filters and detectors to cope with a given range of signal types. But if then required to handle a new type of signal for which it had not been designed, it would be instantly obsolete.

An alternative approach is to design an SDR (software-defined radio) which can cover all bands from, say, 1 to 2000 MHz, with the signal converted, at a wideband IF following a quadrature mixer, to digital form in I and Q channel ADCs (analog to digital converters). A block diagram of such a receiver is shown in Figure 1.9.

The capability of creating RF front-end architectures that are controlled by software has become a reality, thanks to the continuing migration of analog functionality to digital chips and the performance improvements in DSP technology. Today, a designer can use SDR systems to process RF signals that were traditionally handled by analog and RF front-end circuitry. This new approach is being implemented in next generation, very high frequency (~6 GHz) applications that require flexible reconfiguration of the front end, like wireless base stations, mobile communication (often military) devices, and IPTV set-top boxes.

SDR technologies known as “frequency agile” systems allow the conversion of any analog wireless signal directly into digital baseband data, regardless of frequency. Semiconductor manufacturing processes have typically used gallium arsenide (GaAs) materials to demonstrate the RF-to-digital (RF/D) converter chips, though future production versions will convert the design to low-cost CMOS and BiCMOS technologies.

The great advantage of SDR systems is the on-the-fly interoperability among differing communications frequencies. In other words, a single RF receiver can communicate directly with different devices on multiple different frequency bands, using only software to receive, translate, and process the different signals [1].

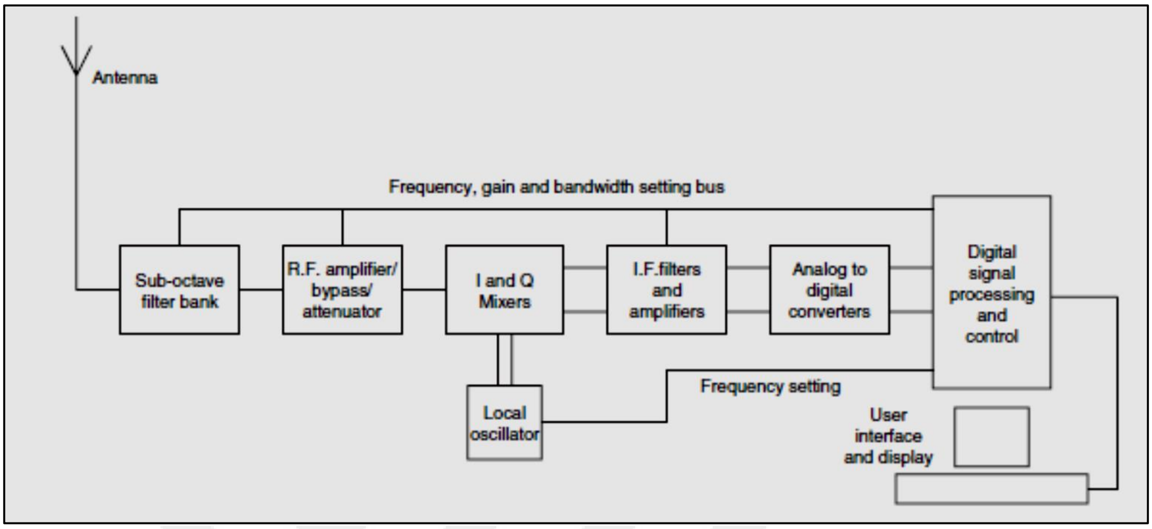

Figure 1.9 Simplified generic block diagram of the receiver portion of a SDR

1.1.5 The Trends for RF Front-End

Starting with the initial developments of superheterodyne architectures, radio front-ends have gone through many changes. Many researchers are working mostly toward implementing very low IF frequency and direct conversion radio front-ends for low power and compact implementations. Radio frequency receiver integrated circuits require a combination of expertise in the areas of circuit design and system architecture, and the choice of a suitable process technology for various applications.

It is noteworthy that the very basic principles of circuit design have not changed significantly from the 1920s, but their applications have. Experts are often tempted to call this technical advancement an “evolution” as opposed to a “revolution” [3].

A dominant trend in the field of wireless communications is that new standards are emerging very fast. In order to provide corresponding services to customers it is necessary to design hardware. Concerning hardware, two issues are important: Integrated Circuit (IC) technology and packaging. Basically, it is possible to implement hardware for wireless communications with discrete components. The disadvantages of this approach are: high price and large form factors. Integrated circuits bring cost reduction and miniaturization. When integrated circuits are produced, they have to be packaged in order to be protected and to be connected to other sub-systems.

Considering packaging, there are two important trends. The first one is “System-on-a-Chip (SoC)”. In this trend, the challenge is to try to achieve as high level of integration as possible. Reducing of the RF component count is a result of the SoC approach. The second is “System-in-Package (SiP)”. The main idea of SiP is to design and integrate different parts of a system in different technologies, but to put them in the same package. Considering the trends related to the IC technology, the most important trend concerns Complementary Metal Oxide Semiconductor (CMOS) technology. CMOS technologies scale down toward deep submicron processes. Trends in packaging and IC technology influence each other.

It is not possible to say which approach will be dominant in the future—probably both. If the satisfactory system performance can be achieved with CMOS technology, then SoC is the best solution. Likely, that is the case with RF transceivers for Zigbee, Bluetooth or even DECT. They have low-to-moderate system specifications and they have to be cheap. In the case that it is not possible to satisfy the system specifications with CMOS technology, SiP approach will remain the preferred solution.

The trends in the field of wireless communications, IC technology and packaging are thoroughly discussed in the previous section, and they are summarized in Table 1.1 [2].

Table 1.1 Overview of the main trends in the field of wireless communications, IC technology and packaging

Field	Main trends
Wireless Communications	New standards for wireless communications are emerging very fast
IC technologies	CMOS technologies scale down to deep submicron processes
Packaging	1. System on a chip (SoC) 2. System in package (SiP)

1.2 Objective of the Thesis

1.2.1 Issues with RF Front-end Design

Up to this point, we have introduced the design architectures common in most RF front-end receivers. We have defined a number of key parameters used to characterize the response of a receiver, including sensitivity and selectivity. In essence, the balance between filter losses and LNA gain in a superheterodyne receiver front end determines the overall selectivity and sensitivity of the receiver.

The sensitivity of a superheterodyne receiver is relative to an acceptable level of performance, such as the sensitivity for a given SNR in an analog radio front end or for a given bit-error rate (BER) in a digital radio front end. The sensitivity refers to the weakest possible signal level that a radio front end can process to achieve that agreed-upon SNR or BER. Sensitivity is affected by the level of noise external to the receiver and generated within the receiver itself. If the external noise is low enough, then the limit to receiver sensitivity will be established by the noise generated by the receiver's own components. Noise is contributed to a receiver by means of the receiving antenna, by contributions from the RF preselector filter and from the active devices in the receiving system, including the front-end LNA.

The RF front-end component most commonly connected to an RF or IF filter is an RF or IF amplifier, respectively. Depending upon its function in the system, this amplifier may be designed for high output power (in the transmitter) or low-noise performance (in the receiver). At the receiver, the receiver sensitivity will be a function of the ability of the preselector filter to limit incoming wideband noise and the front-end's low-noise amplifier (LNA) to provide enough gain to boost signal levels to an acceptable signal-to-noise ratio (SNR) for subsequent signal processing in the RF front end by mixers, demodulators, and/or ADCs.

Another important aspect of receiver design is achieving good selectivity, so that signals of interest are processed and unwanted spurious and interference signals are properly rejected or attenuated. Selectivity can be thought of as the capability of a receiver to separate a signal or signals at a given frequency or bandwidth from all other frequencies. Selectivity is generally a function of the matching networks between components, the filters, and the amplifiers in a front-end design.

Achieving good selectivity with a filter, for example, requires that the filter achieve a wide enough passband to channel the designed signals and their modulation, but provide a sharp enough response with adequate rejection to eliminate unwanted signals not falling in the desired passband. Selectivity can also be thought of as the amount of rejection needed to reduce the level of an unwanted signal to some required amount at some nominal frequency from the desired passband. Selectivity can be achieved at different stages in a superheterodyne receiver, by using selective components and devices at the RF, IF and baseband stages.

Receiver front-end selectivity should be as high as possible close to the antenna to remove large interfering signals before they enter the active devices in later stages and cause problems with distortion and overloading which what we did follow exactly. For selective filters, impedance matching can be difficult and can adversely affect the performance of the other components in the front-end signal chain, notably the mixers.

Filters are judged in terms of a number of performance parameters, including insertion loss, return loss (or VSWR), rejection, ripple, selectivity (amplitude-versus-frequency response), group delay (how long a signal takes to propagate through a filter), phase response, and quality factor (Q). In a bandpass filter, insertion loss is the amount of signal attenuation above a 0-dB level that would be represented by an ideal transmission line in place of the filter. Insertion loss occurs due to a filter’s dissipative elements (the resistors, inductors, capacitors, and transmission lines). Rejection is the amount of signal attenuation at specified points above and below the passband or center frequency, including the insertion loss. Bandpass filters are defined in terms of their center frequency and the width of their passband.

Analog-to-digital converters (ADCs) are commonly used in receivers for wireless applications for either IF or baseband signal sampling. The choice of ADC is generally determined by the rest of the receiver architecture, and can be affected by the selectivity of the filters, the dynamic range afforded by the front-end amplifiers, and the bandwidth and type of modulation to be processed [1].

The overall RF specifications of a front-end consist of noise figure, IIP3 (third-order intercept point), voltage gain, image rejection, receiver and channel filter selectivity and even the bit resolution of the ADC specifications. They are calculated based on the system specifications that include receiver sensitivity, interference performance, blocking performance and intermodulation performance. This high-level description of the RF front end reveals not only the basic functioning but also the potential system trade-offs that must be considered [2].

RF circuit design is a delicate process involving many time-consuming steps. In industry, whole design teams work on one radio. Therefore, it is important to limit the scope. Some of the most challenging and key RF blocks can be found in the receiver RF front-end which is investigated in the frame of this thesis.

1.2.2 The Motivation and Research Goals

The goal of this research is to investigate and understand the design issues with regard to RF front-ends for UWB systems of 3.1-10.6GHz band. By adapting the systems engineering methodology, it must follow a top-down approach: starting from the system level and coming up with the specifications for the antenna and RF circuits, respectively. We have chosen the antenna and filter units for implementation because they are mainly the basic, very first two building blocks of all kinds of different receiver RF front-ends regardless of their architectures and also the antenna is specifically mentioned as the most challenging part of an UWB design. As we did not try to implement a complete RF Front-end unit and did not seek any specific application for the developed hardware, we didn't impose any further requirements on them other than having an operational bandwidth of the FCC-approved UWB of 3.1-10.6GHz.

1.3 Hypothesis

As a result, designing an UWB antenna and UWB band-pass filter would be a good starting point for the design and implementation of a complete UWB RF Front-end regardless of a specific application. The research thus follows the steps as follows;

1. Investigate the RF Front-End Architectures' development as well as the development of UWB technologies and elaborate its impact on RF Front-end.

2. Design and Implement a novel UWB Antenna

3. Design and Implement a novel UWB BPF filter.

3. Simulate and measure the concatenation of antenna with filter to observe if any waveform dispersion occurs which is considered as the primary system level requirement for an acceptable UWB performance. This can also be considered as a

logical starting point for the design and development of a real UWB RF Front-End application and its associated hardware.

This thesis is composed of six chapters in total; following the introduction, Ultra-wideband (UWB) technologies in general terms and UWB RF Front-end in specific are described in the next chapter. The novel UWB antenna and filter designs are introduced in Chapter 3 and 4 respectively for a possible application on UWB RF Front-end systems. The system level functioning of novel UWB antenna and filter units are described in Chapter 5. The last chapter is for conclusions and discussions along with some recommendations for future work.

CHAPTER 2

UWB RF FRONT-END

2.1 Wireless Revolution

The explosive growth of commercial wireless communications has been driven mainly by consumer demand for enhanced functionality in smaller and more affordable handsets and for high-speed wireless data services. Wireless voice communication systems began in the early 1960s and now wireless systems pervade everything in our daily life. This enormous growth has been driven by three main criteria: (i) a higher data rate, (ii) enhanced user convenience, and (iii) lower cost. In the early days of wireless communication systems, reliable voice communication was the ultimate goal in system design. However, the success of wireless communication systems in the late twentieth century has transformed the design goal and redirected it toward replacing wired systems in every possible situation.

This goal of a wireless environment inevitably extends to a concept of ubiquity, which in terms of wireless communication can simply be defined as “anywhere at any time”. In a ubiquitous environment, communication devices will interact with each other seamlessly and users will use a simple platform to obtain information at any time without any awareness of a distinction between wireless and wired networks. To create this ubiquitous environment, future wireless communication systems will be characterized by a horizontal communication model to access different technologies such as cellular, cordless, wireless local area network (WLAN)-type systems, short-range connectivity and broadcast systems. These technologies will be integrated on a common platform in such a way as to optimally complement each other and to satisfy different service requirements in a variety of radio environments [4]. The Internet of Things (IoT) revolution will become possible only with the advent and application of these wideband wireless communication technologies.

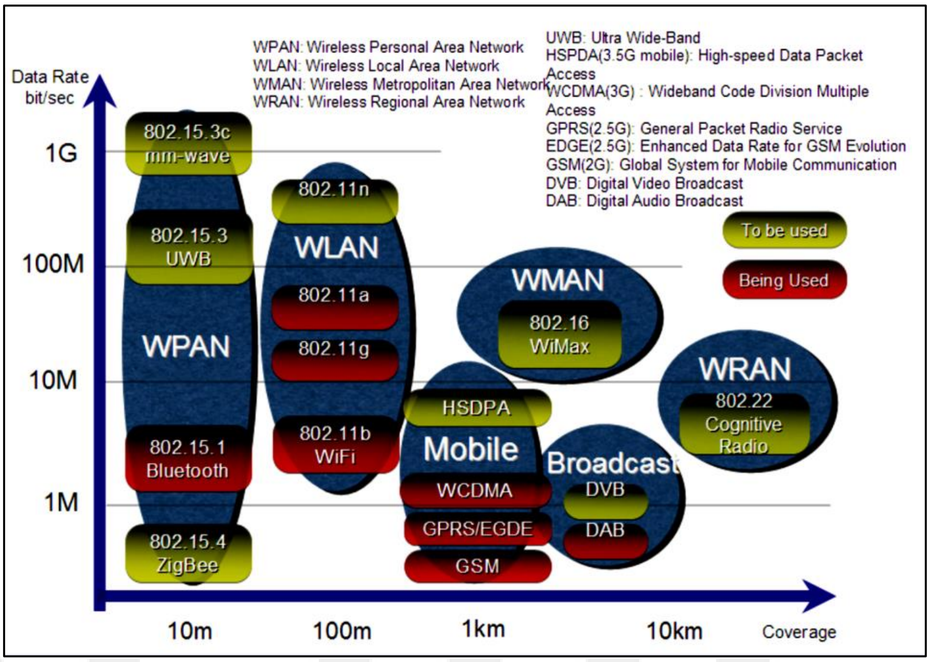

(a)

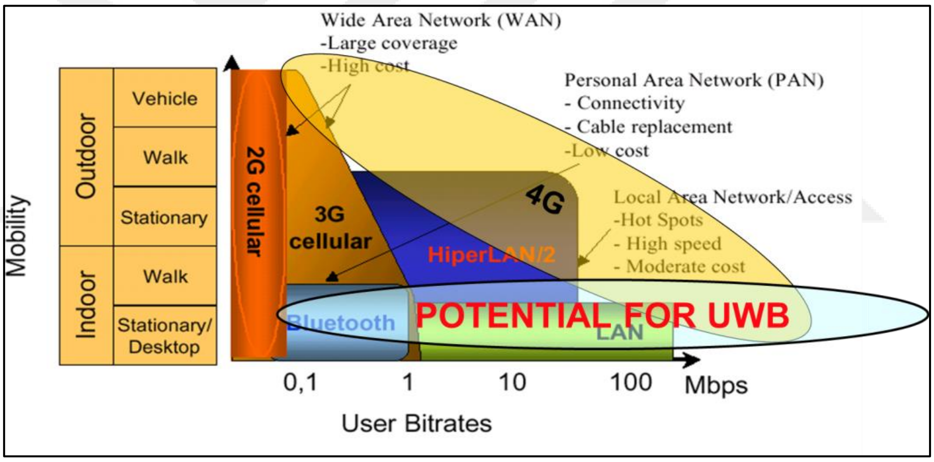

(b)

Figure 2.1 (a) and (b) Various wireless systems along with data rates and distances

Signs of movement in the direction of a common platform can be seen on today's cellular phones (what they call as smart phones) with their support for multi-standard integrated communication systems like Wi-Fi, multiband GSM, Bluetooth etc. Figure 2.1 shows currently developed or developing wireless communication systems. Various systems serve distinct purposes. For instance, a ZigBee application aims to deliver data at a very low rate but with extremely little power consumption. The application is suitable when the lifetime of a battery is important and the low data rate is nevertheless enough to serve its purpose.

On the other hand, mobile systems such as “Wideband CDMA – WCDMA” aim at reliable voice communication and proper data service over long distances. In the end, these various systems will be integrated into a single platform satisfying the various needs of users [4].

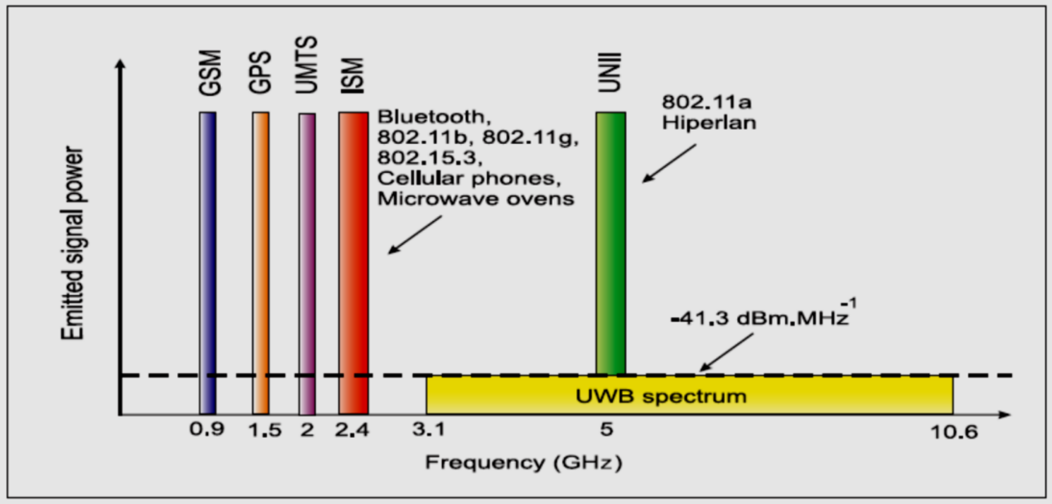

Figure 2.2 Allotted spectrum of various applications

Figure 2.2 shows the allotted spectrum for wireless applications. Each application occupies a different frequency range. This traditional approach of assigning a specific narrow frequency range to each type of system poses challenges to the integration of these systems on a common platform. From an implementation point of view, RF front-ends support these various systems in the simplest way possible to reduce implementation cost; this suggests that the active as well as the passive components of RF front-ends should cover the required wide frequency ranges while simultaneously satisfying the specifications of the different standards.

Moreover, FCC-allowance of the frequencies between 3.1GHz and 10.6GHz for UWB applications has brought into this frequency band and its various applications an increased level of interest and broadened the scope of research devoted to it. The availability of such high bandwidth would allow higher data throughput up to 500Mbps over short distances, which is desirable for HDTV and other wireless multimedia applications. Apart from high data rates, the other compelling features of UWB would be potentially lower cost and higher levels of integration.

To catch up with these trends and provide a viable solution in a timely manner, the issues in implementing the RF front-end for wideband applications such as a UWB system and a multiband, multimode system need to be investigated [4].

2.2 The History of UWB

As mentioned above, the rapid development in the wireless technology introduces new design challenges, such as low power consumption, high data rate, low cost, small dimension and multi-standard programmability.

According to Shannon's theorem, the channel capacity (C) characterized by the highest data rate of reliable transmission in bits per second (bps), is given by;

$$C = B \times \log 2\ (1 + S / N) \tag{2.1}$$

which indicates two fundamental factors setting the upper bound on the information transmission speed: the channel bandwidth B and the link signal to noise ratio (SNR) S/N. While the improvement of S/N is subject to various natural and implementation limitations, increasing B looks like a direct way to enhance achievable data-rate. This inspired the emergence of ultra-wideband (UWB) technology [5].

As a matter of fact, when radio was invented by Guglielmo Marconi more than a century ago, radio communications used enormous bandwidth in the course of conveying information by using spark-gap transmitters. The next milestone of UWB technology came in the late 1960s, when UWB radar systems were introduced in the search for high sensitivity to scatterers and low power consumption. Since Armstrong's invention of heterodyne techniques, most RF transceivers have switched over to narrowband approaches. As a result, until recently UWB technology has been used mostly for radar-based applications because the wideband nature of the signal results in very accurate timing information. However, recent developments in high-speed switching technology have made UWB more attractive for low-cost consumer communications applications as well.

The US Federal Communications Commission (FCC) allowed in 2002 a wide frequency spectrum of 3.1-10.6 GHz to be used for a communication system as long as the new system does not degrade the performance of previously existing communication systems. The huge "new bandwidth" opens the door for an unprecedented number of bandwidth-demanding position-critical low-power applications in wireless communications, networking, radar imaging and localization systems [6].

2.3 The Definition of UWB

Traditionally, UWB technology has been loosely defined as any wireless transmission scheme that occupies a bandwidth of more than 25% of a center frequency (fractional bandwidth) , or more than 1.5GHz. Clearly, this bandwidth is much greater than the bandwidth used by any current technology for communication. In 2002, the FCC has defined a UWB device as one with fractional bandwidths greater than 20% or one that occupies at least 500MHz of spectrum [7]. Furthermore, the FCC has regulated the spectral shape and maximum power spectral density of UWB radiation in order to limit interference with other systems, as shown in Figure 2.3.

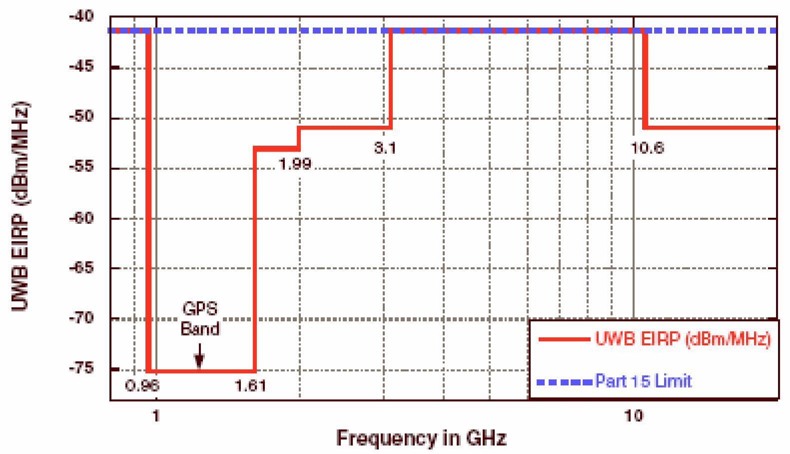

Figure 2.3 FCC spectral mask for indoor UWB systems

2.4 UWB Target Applications

The potential applications of UWB devices range from communications, measurement systems, vehicular radar systems, to imaging systems (ground-penetrating radar, wall-imaging systems, medical systems, and surveillance systems). It also expedites the potential for the use of UWB radios in short-range, high-speed access to the Internet and in such applications as accurate personnel and asset tracking for increased safety and security, precision navigation, imaging of steel reinforcement bars in concrete or detection of pipes hidden inside walls, surveillance, and medical monitoring of the heart’s actual contractions.

For wireless communications in particular, the FCC-regulated power levels are very low, which allows UWB technology to overlay already available services such as the GPS and the IEEE 802.11 wireless local area networks (WLANs) that coexist in the

3.1- 10.6 GHz band. Although UWB signals can propagate for greater distances at higher power levels, current FCC regulations permit high-rate (above 110MB/s) data transmissions over a short range (10-15m) at very low power. IEEE 802.15 Working Group leads the effort for standardizing UWB wireless radios for indoor multimedia transmissions [4].

Some applications that have been specifically related to UWB are discussed as follows [8]:

a. High Data Rate WPAN: In addition to the existing IEEE 802.11 WLAN (Wi-Fi) and Bluetooth-based IEEE 802.15 WPAN products, there is a variety of wireless networking products demanding high data rate. It has led to the development of standards for high-rate WPANs. As an example, the IEEE 802.15.3a WPAN standard is targeting at networks with a medium density of devices per room (5-10) transmitting at up to 100-500Mb/s data rate at a distance between 1 and 10 meters, mainly based on a peer-to-peer topology. The applications could include:

- Wireless replacement for Universal Service Bus (USB) connections among computers and peripherals in home and office environments.
- High-speed cable replacement, including downloading pictures from digital cameras to PCs and wireless connections between DVD players and projectors.
- Wireless video projectors and home entertainment systems with wireless connections between components.
- Coexistence and networking of audio, still video, and motion pictures for fixed and portable low-power devices.
- Home network of audio and video with Internet gateway.
- Multimedia wireless distribution system for dense user environments, such as multi-tenant units/multi-dwelling units.
- Office, home, auto, and wearable wireless peripheral devices.

b. Indoor Localization: The wide bandwidth of UWB signals implies a fine time resolution and avoids the difficulty of recognizing the signal due to multipath fading. It gives a great potential for high-resolution positioning applications. It is a promising technology for wireless sensor networks that deploy a high density of devices (intelligent sensors or tags) in industrial factories or warehouses transmitting low-rate data combined with position information. The data rate can be from 10Kbps to 100Kbps and the position accuracy is within 1m. The operating distance is typically within 100m between sensor nodes and a master station with a typical master-slave topology.

It can also implement intelligent wireless area networks that are characterized by a high density of devices in a domestic or office environment, covering distances over 30m. The devices feature very low cost (< 1 dollar/unit) and very low power consumption (1-10 mW) to provide users with access to intelligence distributed around the home/office. IEEE 802.15.4a standard has been formed to use UWB technology achieving low rate data transmission and locationing capability.

c. Stealthy Communication: The wide bandwidth afforded by UWB waveforms implies the data signals to be spread by a fast-running pseudorandom (PN) code. The processing gain available by correlating the PN sequence with a local reference at the receiver enables the low transmission power while achieving the same SNR. The resulting UWB signals are thus likely to be with power below noise floor and the possibility of being intercepted is dramatically reduced. It is one of the reasons that UWB has been applied for military purposes [8].

2.5 UWB Communication Technology

Traditional UWB systems rely on ultra-short waveforms that can be free of sine wave carriers and do not require IF processing because they can operate at base-band. Because information-bearing pulses with ultra-short duration have UWB spectral occupancy, UWB radios come with a unique advantage that has long been appreciated by the radar and communications communities. As mentioned above, the main advantages of the UWB systems are enhanced capability to penetrate obstacles, ultra-high precision ranging at the centimeter level, a potential for very high data rates along with a commensurate increase in user capacity, all available in a potentially small size and processing power.

UWB radio technology differs from conventional narrowband radio and spread-spectrum technologies in that the half power bandwidth of the signal is typically from 25% to 100% of the center frequency. Instead of transmitting a continuous carrier wave modulated with information (or with information combined with a spread code), which determines the bandwidth of the signal, a UWB radio transmits a series of very narrow impulses. The UWB radio has a distinct advantage over narrowband radio systems in resistance to signal degradation by multipath propagation. In environments having reflecting objects, the continuous carriers of narrowband systems are susceptible to destructive interference due to multipath signals. In an UWB radio system, the multipath signal energy arrives at a different time than the direct path energy, and cannot create destructive interference. A multiple correlator system can recover the multipath energy to enhance the system performance [3].

These systems use very low transmission power, spread over a bandwidth of several gigahertz. The very low transmission power and the large bandwidth usage enable UWB radio systems to coexist with other narrowband systems over the same frequency band without interfering with the narrowband systems. However, the narrowband systems may cause interference that can jam the UWB receiver. There have been efforts to develop narrowband interference suppression techniques for UWB radio systems [9].

Regarding the hardware developments for UWB technology, Figure 2.4 shows a very basic block diagram for the UWB receiver. The function of the correlator module is to recover the energy in the transmitted impulses and present a representative signal to the baseband module. The baseband module performs the functions of pulse integration and handling the timing offset during synchronization and reconstruction of the information signal. The timing module generates the precision master clock for all signal processing operations and provides the facility for the baseband module to time-shift the trigger signal to the correlator for synchronization. After synchronization is achieved, the pseudorandom code is included in the timing signal to the correlator, which strips off the transmitted signal’s pseudorandom coding. Till this point, the correlator output signal contains the information modulation and a DC component. The timer–correlator combination provides the critical element for reception of the time-modulated ultrawideband signal [3].

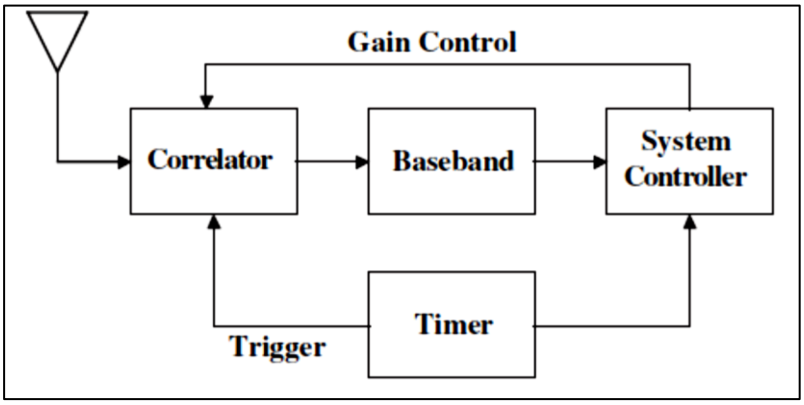

Figure 2.4 UWB receiver block diagram

Currently there are two approaches for implementing UWB systems to use the FCC-allowed UWB bands; namely a pulse-based system and a carrier-based system.

Following the traditional approach to use wide bandwidth, a pulse-based system uses a modulated pulse to transfer information; this has been the method used in conventional military applications and in impulse radios. Because of the characteristics of the pulse, the RF front-end of such systems tends to be simple, with this simplicity serving to eliminate the need for the up-conversion or down-conversion that was required for traditional narrow-band systems.

In contrast, the carrier-based system is a version of the traditional narrow-band system that has been extended to accommodate a wide bandwidth. Therefore, its RF front-end architecture closely resembles that found in conventional narrowband systems [4].

2.6 The Impact of UWB Technology on RF Front-End Design

To further elaborate the above discussion, the Direct-Sequence Ultra-wideband (DS-UWB) system is the one that adopts the traditional impulse-radio concept and transmits UWB pulses. The other one is the Multi-band Orthogonal Frequency Division Multiplexing (MB-OFDM) system that chops the 7.5GHz bandwidth into fourteen sub-bands which has a 528 MHz bandwidth and does frequency hopping in between different bands, while doing OFDM modulation in each band [8].

Each system gained multiple supports from industry but due to incompatible of two proposals, it experiences huge difficulties in commercialization of UWB technology. On the other hand, Impulse Radio UWB (IR-UWB) has become a hot research area in academia due to its low complexity and low power [10].

As UWB pulse itself does not contain information, one must add digital information to the analog pulse through modulation. The MB-OFDM systems are dealing with continuous ultra-wideband modulated signals while DS-UWB systems are transmitting discrete short pulses which cover ultra-wide bandwidth. On the other hand, IR-UWB is a carrierless pulse-based system (Figure 2.5) which means IR-UWB and DS-UWB are the two different categorizes of pulse based UWB. Pulse modulation scheme includes OOK (On Off Keying), BPSK (Binary Phase Shift Keying) and PPM (Pulse Position Modulation).

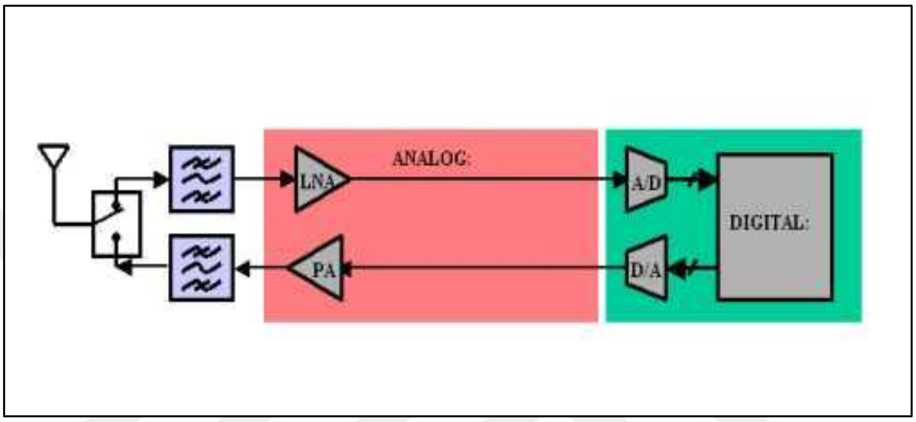

Figure 2.5 IR-UWB transceiver

Both DS-UWB (Figure 2.6) and MB-OFDM (Figure 2.7) are carrier-modulated systems, where a mixer is used to up/down convert the radio frequency (RF) signal; therefore it requires local oscillator (LO) synthesis. On the other hand, IR-UWB is a carrier-less pulse-based system, therefore, we can eliminate the fast hopping LO synthesis, thus reducing the complexity and power consumption of the entire radio. Furthermore, since the signal of a pulse-based UWB system is duty-cycled, the circuits can be shut down between pulses intervals which would lead to an even lower power design.

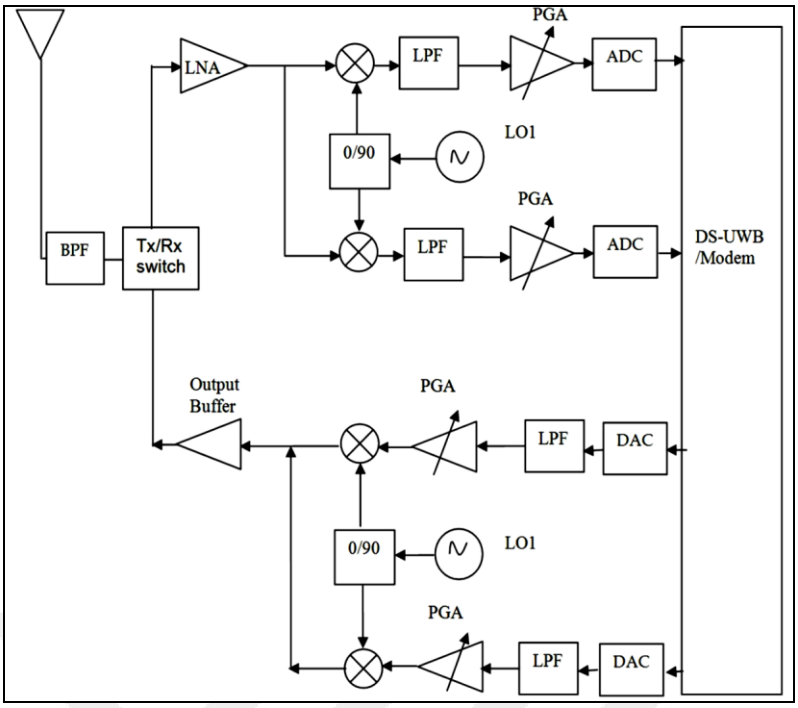

Figure 2.6 DS-UWB transceiver

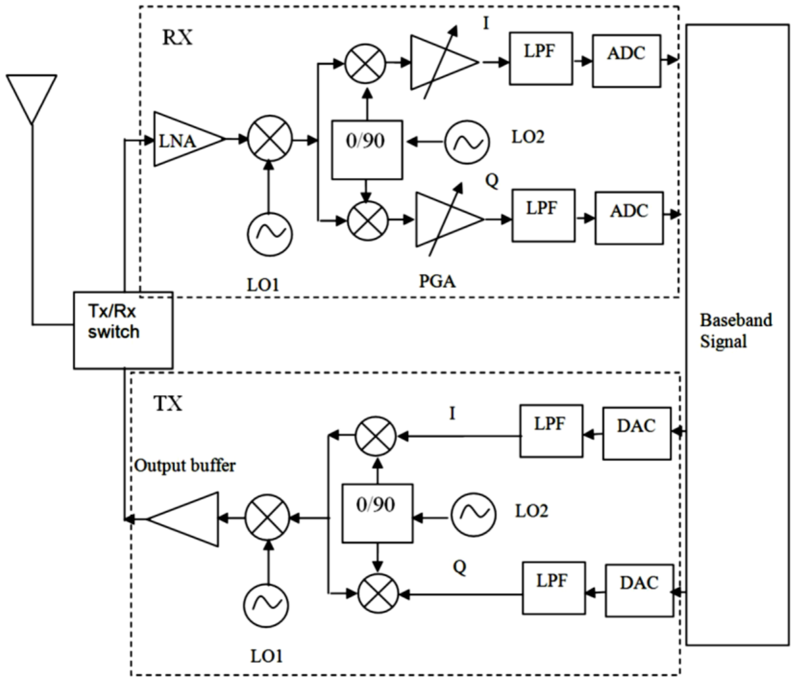

Figure 2.7 MB-OFDM Transceiver

Table 2.1 Candidate UWB systems specifications

UWB Technique	*OFDM*	*TDMS/FDMA Pulses*	*DSSS/CDMA*
Bands	3 to 13	3 to 13	2
Bandwidths	528 MHz	550 MHz	1.368 GHz, 2.736 GHz
Frequency ranges	3.168 GHz – 4.752 GHz 4.752 – 10.296	3.325 GHz – 4.975 GHz, 4.975 GHz – 10.475 GHz	3.1 GHz – 5.15 GHz 5.825 GHz – 10.6 GHz
Modulation Scheme	OFDM, QPSK	M-ary Bi-Orthogonal Keying (M-BOK), QPSK	BPSK, QPSK, M-BOK
Error correction	Convolutional code	Convolutional code, Reed-Solomon code	Convolutional code, Reed-Solomon code
Code rates	11/32 rate at 110 Mbps, 5/8 rate at 200 Mbps, ¾ rate at 480 Mbps	6/32 rate at 110 Mbps, 5/16 rate at 200 Mbps, ¾ rate at 480 Mbps	½ rate at 110 Mbps, RS(255,223) at 200 Mbps, RS(255,223) t 480 Mbps
Link margin	5.3/6 dB at 10 m / 110 Mbps, 10.7 dB at 4 m / 200 Mbps, 6.2 dB at 4 m / 480 Mbps	6.3 dB at 10 m / 108 Mbps, 8.0 dB at 4 m / 288 Mbps, 4.0 dB at 4 m / 577 Mbps	6.1 dB at 10 m / 110 Mbps, 11.1 dB at 4 m / 200 Mbps, 6.1 dB at 4 m / 600 Mbps
Symbol period	312.5 ns OFDM symbol	3 ns	23 or 17.5 ns (Low band), 11.7 or 8.9 ns (High band)
Multipath mitigation method	1-tap (robust to 60.6 ns delay spread)	frequency interleaving of MBOK chips; time frequency codes; feed forward filter	Decision feedback equalizer

The technical details of some candidate UWB systems are summarized in Table 2.1 for reference purposes. The wideband nature of the front-end architecture leads to a totally different design methodology from traditional narrow-band systems. Not only that expanding the bandwidth of the antenna and circuitry itself requires different techniques than the narrowband counterparts, but achieving ultra-low power consumption in the low-noise amplifier and pulse generator also becomes extremely important when the power consumption is not dominated by the radiation power anymore. New circuit topologies are thus needed in this situation.

In narrow-band systems, phase response is not crucial and the communication link budget can be calculated based on single values like power level and gain but for UWB systems, waveform dispersion needs to be characterized to ensure an accurate data correlation at the receiver, which implies the necessity of deriving the frequency dependent transfer function from the transmitter to receiver. This is because the concatenation of the antenna and front-end circuits may also introduce waveform dispersion that was never an issue in the narrowband systems. The traditional way of modeling antenna as a 50 ohm resistor is no longer valid [8].

An UWB communication system requires transmitter and receiver with a wideband antenna. Antennas are the fundamental component of a communication system, both at the receiver and at the transmitter, subject to performance requirements while at the same time supporting demand constraints to incorporate it in terminals or network access points. The contradiction between requirements and constraints make the selection or the design of an antenna something difficult in the UWB case as the large bandwidth imposes additional needs in comparison to narrowband radio. The second problem for the antenna designer is the lack of tools to evaluate the performance of an antenna embedded in a radio system, apart from tools intended to determine the antenna input impedance, gain, efficiency, and its radiation patterns. These tools are obviously quite important in order to describe where the direction of the radiation would go or would be received, and what signal power can be lost due to antenna losses, but nothing about the “matching” between the antenna and the channel. It is well known that matched filtering is a necessary requirement for optimal signal reception, therefore since both antennas and channels are filters that are involved in the transfer function between the signal to be transmitted and the signal at the receiver output. This means, we should analyze antenna performance and channel properties in a correlated manner, if optimization of the radio link performance is a goal to reach [10].

We now continue with design and development of a novel UWB antenna in the next chapter.

CHAPTER 3

THE UWB ANTENNA DESIGN

3.1 Introduction

UWB antennas are gaining prominence and becoming very attractive in modern and future wireless communication systems, mainly due to two factors. Firstly, people increasingly high demand for the wireless transmission rate and UWB properties such as high data rate, low power consumption and low cost, which give a huge boost to the UWB antennas' research and development in industry and academia since the FCC officially released the regulation for UWB technology in 2002. Secondly, now the wireless portable device need antenna operated in different frequencies for various wireless transmission functions, and operation bands and functions are increasing more and more, which may result in challenges in antenna design, such as antenna space limitation, multi antennas interference, and etc. One UWB antenna can be used to replace multi narrow-band antennas, which may effectively reduce the antenna number [11].

"Classical" antenna theory and practice is well understood and well developed for sinusoidal transmission and reception. Predicting and determining antenna radiation patterns for UWB signals is not as familiar to engineers because the effect of the antenna on the radiated signal is more critical—all antennas differentiate the input signal one or more times, depending on the antenna, and while derivatives of sinusoids are simply phase shifts of sinusoids, the whole shape of UWB waveforms can change due to the antenna. While existing antennas can radiate UWB baseband waveforms, they will not necessarily do so efficiently or with the desired pattern because of the wide bandwidth required. For that reason, it is recommended that antennas intended for UWB applications be specially designed for the waveform. The theory for such a design is basically known, but sometimes is controversial.

Generally, it is not desirable to generate UWB pulses by direct excitation of an antenna in which the shape and bandwidth of the pulse depends on the antenna configuration because inadvertent or intentional bending of the antenna, or bringing it near a metal surface, can change the center frequency of the waveform and cause significant interference to existing systems. Instead, the pulse shape should be determined by the transmitter circuitry before it reaches the antenna. This philosophy of antennas for UWB signals is dominant because of the FCC restrictions on UWB emissions, so the emphasis in antenna design and selection is in finding configurations that match the pulse generation circuitry well and have sufficient bandwidth [12].

As antennas are considered to be the largest components of integrated wireless systems; antenna miniaturization is necessary to achieve an optimal design as well [10].

The bandwidth is the antenna operating frequency band within which the antenna performances, such as input impedance, radiation pattern, gain, efficiency etc. are desired. The most commonly used definitions for the antenna bandwidth are the fractional bandwidth (for narrow or wideband definition) and the bandwidth ratio (for ultra-wideband definition) [11]. The fractional bandwidth is defined as;

$$BW = \frac{f_h - f_l}{f_c} \times 100\% \tag{3.1}$$

The bandwidth ratio is defined as;

$$BW = \frac{f_h}{f_l} : 1 \tag{3.2}$$

where;

fl – the lower frequency of the operation band.

fh – the higher frequency of the operation band.

fc – the center frequency of the operation band.

UWB antennas are obviously a vital part of UWB systems as they are closely linked to the system performance. In our case, they are basically needed to have a maximum gain over the specified bandwidth which is the FCC UWB. Other antenna features should be considered as application specific.

In this part of the thesis, our purpose is to design a compact (miniaturized) UWB antenna with a gain level close to 10 dBi over the bandwidth starting from 1.5 GHz up to 10.6 GHz. In the analog RF frontend, a high relative bandwidth and not necessarily a high absolute bandwidth poses new challenges to the RF system design. We therefore concentrate on this band where a large variety of system concepts are under investigation worldwide [13].

This chapter is composed of five sections in total; following the introduction, antenna design and implementation is described in Section 3.2, simulation and measurement results are given in Section 3.3 and finally Section3.4 is for the conclusions.

3.2 Antenna Design

This chapter is all about the design and development of a compact UWB antenna based upon Vivaldi and TEM horn antennas both of which have respective advantages for the possible UWB applications. The idea is to make use of these combined respective advantages of Vivaldi antennas and TEM Horn antennas to achieve the desired goals by shaping the TEM Horn antenna to look like a Vivaldi antenna.

3.2.1 The effect of partial dielectric loading

The antenna structure is modified by partially loading it in the center with a dielectric Teflon material of $\varepsilon r=2.1$ in order to decrease the lower frequency limit and by doing so increasing the frequency range of the antenna [14]. The dielectric filling or partial dielectric loading techniques are employed commonly as mentioned in the literature [15-17] to broaden the operational band up to twice and improve the directivity (gain) performance. It is noted that the partial dielectric loading operation should not result in altering the physical dimensions of the antenna (including its weight) in a negative manner [17].

To evaluate the impact of dielectric materials itself on the performance of the antenna, we have performed simulations by partially loading the antenna from the center with different kinds of dielectric materials. The Figure 3.1 presents the antenna gain and

VSWR results for (a, b) boxed and (c ,d) un-boxed configurations and gives reader the chance to make a comparison. It is very clear that for both configuration, the dielectric Teflon material of εr=2.1gives the best results in terms of gain and VSWR when compared to other dielectric materials of higher εr. Its performance is also quite stable over the UWB band of 3.1-10.6 GHz.

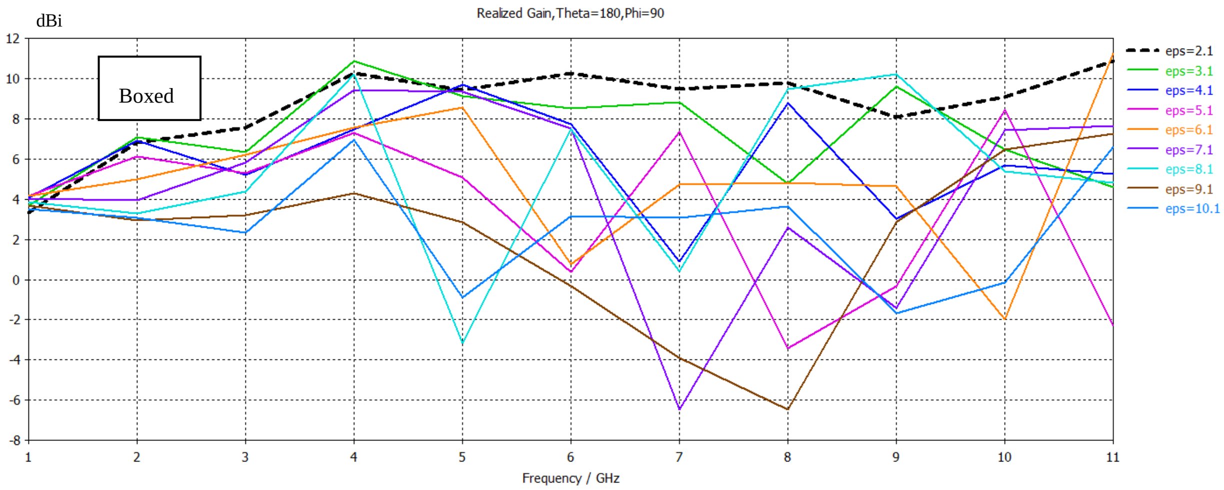

(a) Gain for boxed configuration

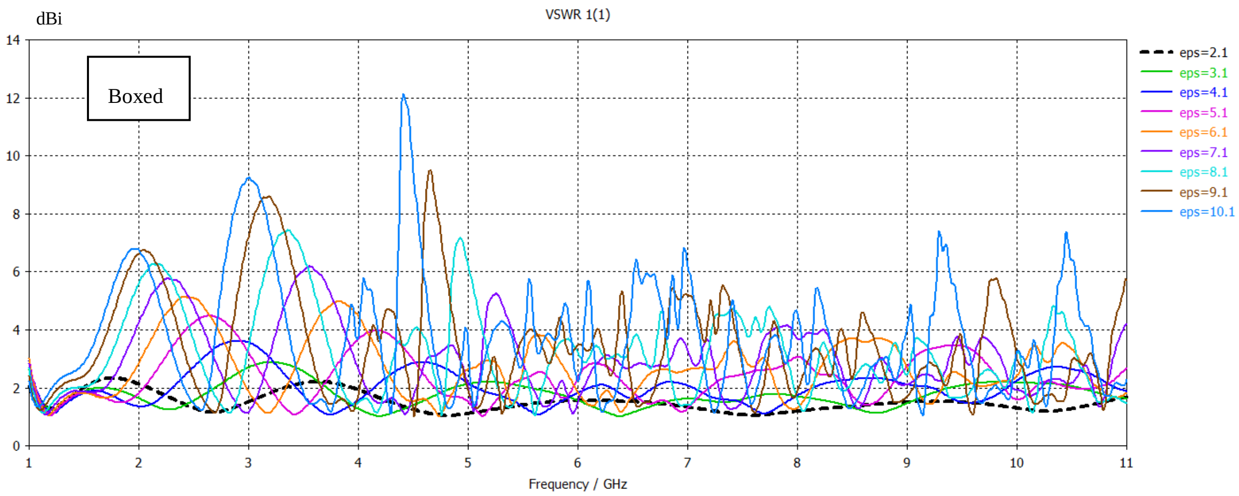

(b) VSWR for boxed configuration

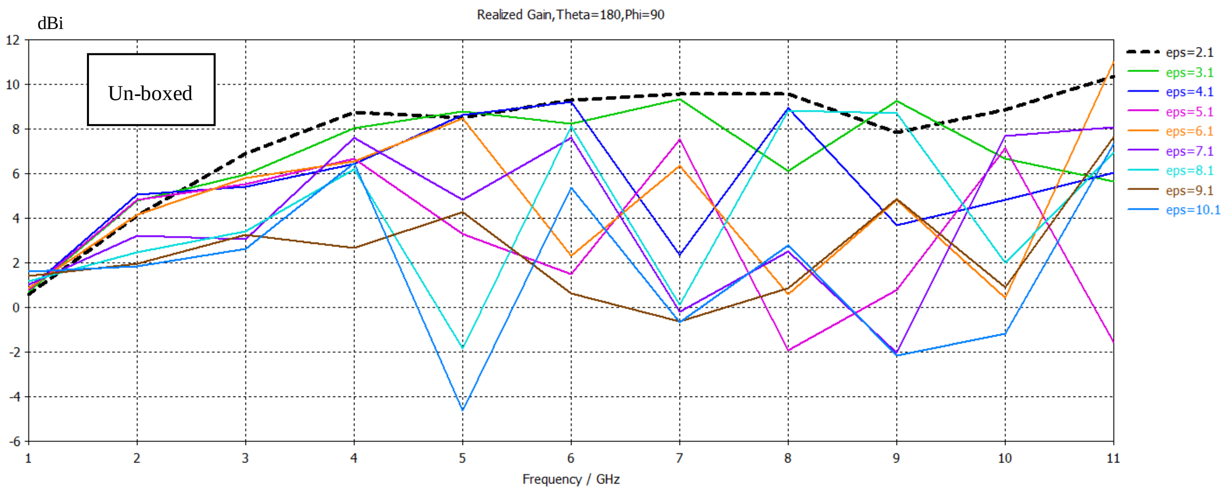

(c) Gain for un-boxed configuration

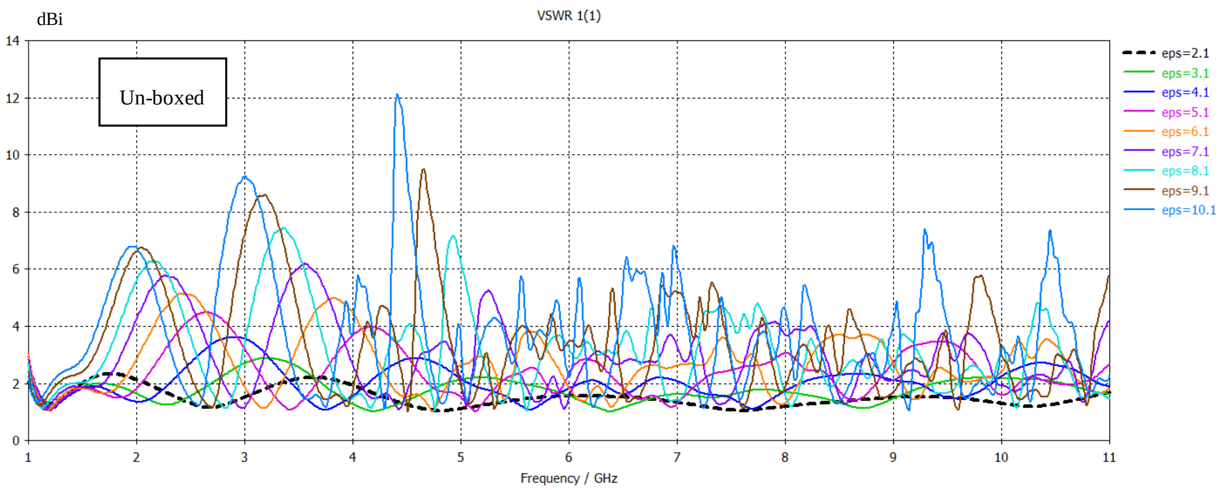

(d) VSWR for un-boxed configuration

Figure 3.1 (a - d) The impact of dielectric loading on the antenna performance for both "boxed" and "un-boxed" configurations

3.2.2 Antenna Implementation

The partially dielectric loaded TEM (PDTEM) horn, its Vivaldi shaped version (PDVA) and array combinations have been introduced by Turk as efficient UWB impulse radiators for GPR (Ground Penetrating Radar) operation to obtain UWB characteristics from 150 MHz to 10 GHz [15, 18, 19].

As a specific example, the partially dielectric-loaded Vivaldi antenna (PDVA) which yields ultrawide band antenna characteristics from 400 MHz to 10 GHz was introduced and referred to as PDVA10 (meaning an aperture depth length of 10 cm) in

[18] as given in Fig. 3.2. It had a positive gain over the specified bandwidth which came close to 10 dBi at higher frequencies. It was designed for multi-sensor adaptive-impulse GPR operation and its performance was promising when compared to the regular (no dielectric loading) TEM Horn and Vivaldi antennas.

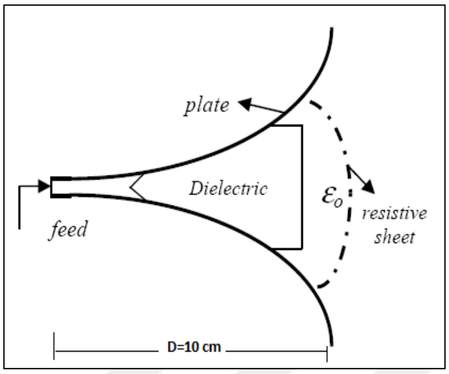

Figure 3.2 Vivaldi Shaped TEM Horn Antenna (PDVA10) [18]

However, it has the disadvantage of having a large size. Our purpose herein is to improve that design to make it smaller (compact) for some possible applications in UWB communication systems as it covers whole popular wireless frequency bands. To make it compact, the height of the antenna is reduced up to 8 cm to cancel the lower bands of the spectrum which were needed for GPR operations and the depth of the E-plane (flared vertically) horn antenna aperture has been changed from 8 cm down to 3 cm as the primary parameter affecting the antenna gain. The gain values have been examined by using CST STUDIO SUITE EM simulation software. The simulation results (Figure 3.3) showed that the antenna gain was decreasing especially for the band above 4.0 GHz and the radiation pattern was deforming as the antenna aperture depth shortened. As a result, an antenna structure with aperture depth D=5cm is decided as optimal by taking into consideration the fact that it was aimed to be constructed as compact as possible.

It is placed in a surrounding box made of PEC material to reduce the undesired side lobes and to obtain a more directive radiation pattern. It would also help to obtain physical protection and EM shielding in a possible application like wireless communication system to overcome the coupling affects between the Transmit/Receive antennas [19]. The final design of the VS-PDL TEM horn antenna with its dimensions is given in Fig. 3.4 (a) as vertically divided right-hand-side made transparent for the purpose of clarity while the manufactured antenna is shown in the Fig. 3.4 (b).

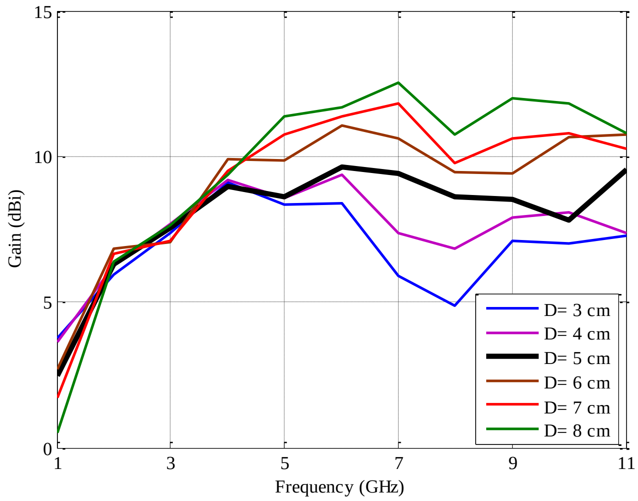

Figure 3.3 The Variation of Gain with respect to Frequency for various “Aperture Depth - D” values (Simulation Only)

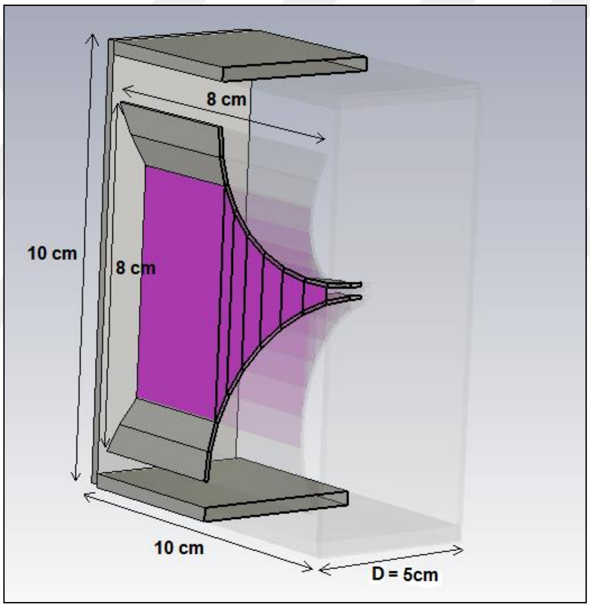

Figure 3.4 VS-PDL TEM Horn Antenna Design (Dimensions given on the Figure)

Figure 3.5 The Manufactured Antenna

3.3 The Simulation and Measurement Results

The simulation results show that the Vivaldi shaped partially dielectric loaded (VS-PDL) TEM horn antenna with 5 cm aperture depth as given in Fig.3.4 (a) achieves an optimum performance over the desired bandwidth while it is practically possible to implement it physically as a compact structure.

The simulated radiation patterns of the VS-PDL TEM horn antenna at selected frequencies within the 1.5-10.6 GHz band for “boxed” and un-boxed” configurations are given in Fig. 3.5 where the bolder line is for the “boxed” configuration.

It can easily be noticed from this figure that, with the metallic box, the radiation pattern becomes more directive especially at the higher frequencies. It offers superior gain performance starting from lower frequencies. The measured radiation patterns of the manufactured antenna verify the simulation results as shown in Fig. 3.6.

The simulated and measured gain values for the antenna are given in Fig. 3.7 while the simulated and measured VSWR plots are given in Fig. 3.8. The measured gain of the antenna remains above 7dBi over the practical band which is considered as a satisfactory gain performance.

Regarding the VSWR measurements, it remains below 2.0 throughout the operational band until 9.8 GHz but it exceeds that value for the rest of the band which can be considered as not satisfactory. On the other hand, as it does not impact the gain and radiation performance in a negative manner, it can still be considered as practically acceptable. It is also noteworthy to state that for “boxed” configuration, the box itself has a negative effect on VSWR performance at lower part of the bandwidth (1.5 to 2.5 GHz) resulting a higher VSWR values when compared to “un-boxed” case but still the “boxed” antenna has a satisfactory performance with VSWR values below 2.

Fig. 3.9 gives the time-domain characteristic of the proposed antenna for the measured received pulse case at various angles for 1.5-11.0 GHz. It denotes a smooth pulse shape with minimal ringing effects. The excitation pulse also is plotted within the Fig. 3.9.

If one evaluates the overall measured performance of the proposed antenna, one can easily conclude that it satisfies the requirements of a multitude of applications ranging from UWB communication to Electromagnetic Compatibility (EMC) measurement systems in terms of gain, VSWR and radiation performance due to its reduced size and shielded metallic box structure. Hence it can be considered as a good candidate for popular communication systems like cellular phone, SATCOM, Wi-Fi, Wi-Max/LTE and other systems using ISM and UWB (Table 3.1).

Table 3.1 Frequency bands of some of the popular wireless communication systems

806–960 MHz, 1,710–2,025 MHz, 2,110–2,200 MHz, and 2,500–2,690 MHz. (ITU-R approved bands)	1.227–1.575 GHz	2.3 GHz	2.4 GHz	868 MHz, 915 MHz, and 2.4 GHz	3.1–10.6 GHz	900 MHz, 1.8 GHz, 2.4 GHz, and 5.8 GHz
Cellular Phone Operations (GSM 3G and 4G (WiMax/LTE))	Global positioning system—GPS	Satellite radio	WiFi/802.11 b/g and Bluetooth	Zigbee/802.15.4	UWB	ISM (Industrial, scientific, medical)

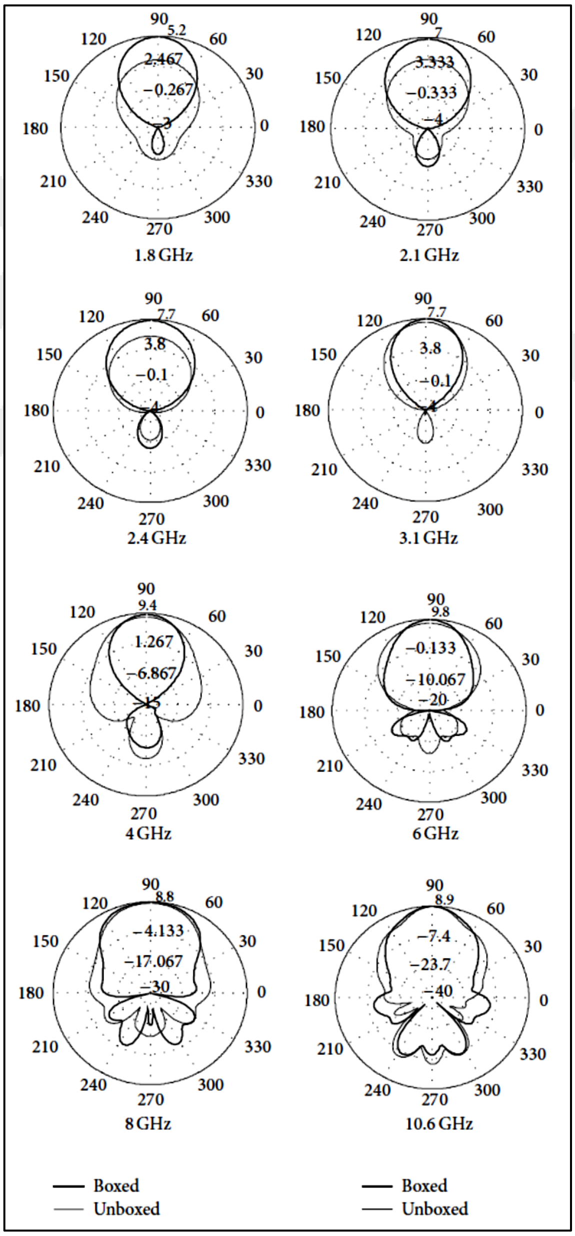

Figure 3.6 The Simulated Radiation Patterns of the VS-PDL TEM Horn Antenna for “boxed” and “un-boxed” configurations at various frequencies

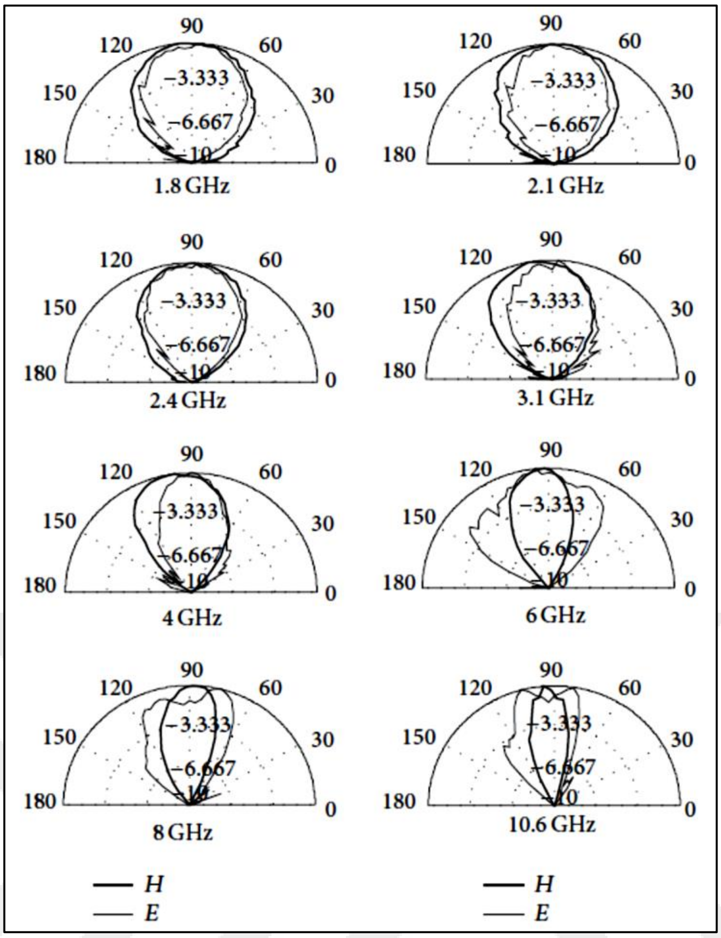

Figure 3.7 Measured E-plane and H-Plane (Normalized) Radiation Patterns of the proposed Antenna

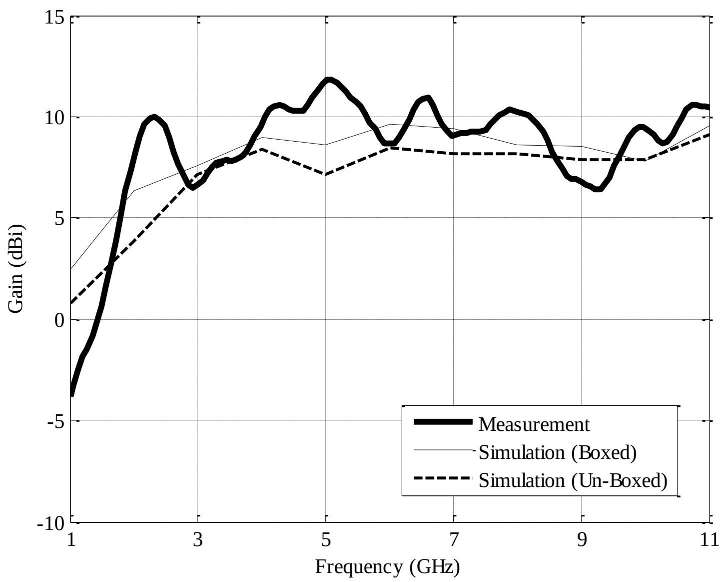

Figure 3.8 Gain Performance of the Antenna for Simulation (both boxed and un-boxed) and Actual Measurement Cases

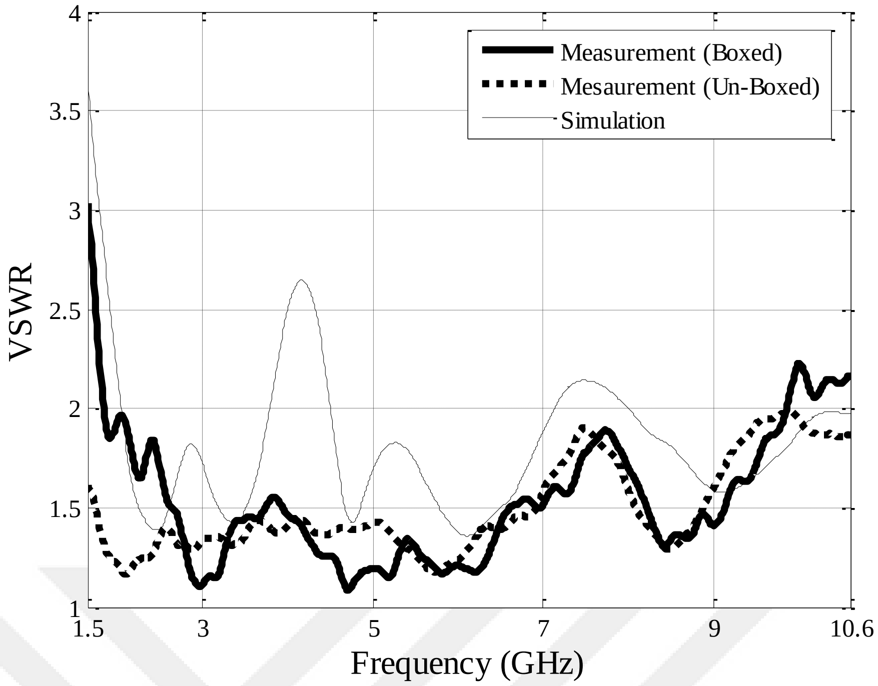

Figure 3.9 Simulated and Measured (for both boxed and un-boxed cases) VSWR plot of the Antenna

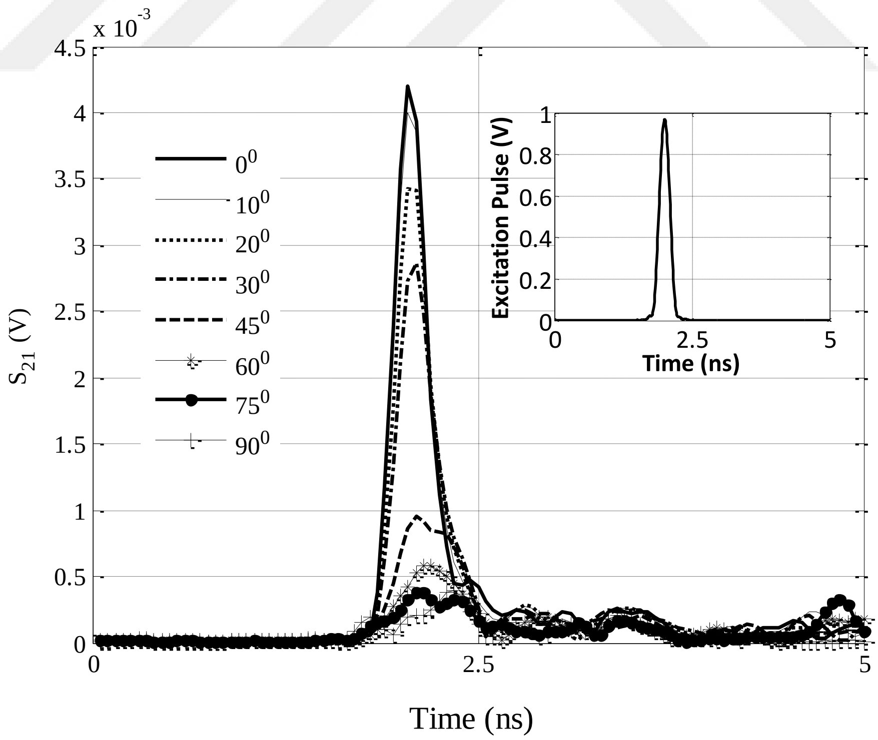

Figure 3.10 Time-domain Characteristic of the Proposed Antenna Measured on Received pulse for various angles and for 1.5-11.0 GHz (The excitation pulse is given within the figure as well)

3.4 Results and Conclusions

In this part of the thesis, a novel compact Vivaldi Shaped Partially Dielectric Loaded (VS-PDL) TEM horn antenna has been designed and developed for UWB communication systems of 1.5-10.6 GHz frequency band. We have shown that a new panel type quasi-planar design obtained by more bending the tapered Vivaldi shaped wings (shortened aperture depth) of the TEM horn antenna leads to a significant size reduction of the device. Furthermore, simulation and measurement results that were in coincidence showed that, when installed within a metallic box, VS-PDL TEM horn antenna with a 5 cm aperture depth has satisfactory far-field radiation characteristics and high gain/lower VSWR over the practical bandwidth. That means such a panel type quasi-planar antenna would be a good candidate for UWB applications as well as popular communication systems of GSM, GPS, ISM, Wi-Fi and SATCOM bands requiring satisfactory antenna performance.

CHAPTER 4

THE UWB FILTER DESIGN

4.1 Introduction

It is incontestable that one of the essential components in UWB RF Front-end modules is the band-pass filter (BPF) and hence, BPF design takes a critical role in UWB communication.

Band-pass filters are vital building blocks which allow a signal to pass at requested frequencies and repel the rest of frequencies in receiver and transmission systems. In RF and microwave communication systems, compactness, low insertion loss at the transmission band and high suppression at the rejection band are crucial parameters in order to design a well-suited BPF [20]. Different kinds of UWB BPF design methods and technologies have been investigated for many years in the literature [21-29]. As a filter realization technology, microstrips are thoroughly employed because of their low cost, easy fabrication and integration [30, 31].

Band-pass filters can be particularly important in an RF front-end design. BPFs are important components in all kinds RF Front-end receiver architectures. They provide frequency selectivity and affect receiver sensitivity.

RF and microwave filters suppress unwanted signals and separate signals of different frequencies. RF and microwave receivers and transmitters require numerous miniature filters for such functions as preselection in the case of a receiver front end, suppression of mixer spurious products, and suppression of transmitter parasitic signals, providing access to the passband and stopband characteristics in multiplexers.

4.2 Classification

Filters can be classified into five different categories of characteristics [1];

a. Frequency selection:

- Low-Pass Filter (LPF),
- High-Pass Filter (HPF),
- Band-Pass Filter (BPF),
- Band-Stop Filter (BSF);

b. Filter response:

- Chebyshev,
- Butterworth,
- Other (elliptical, Bessel, Gaussian, and so forth);

c. Percentage bandwidth:

- Narrow band (0% – 20%),
- Moderate band (10% – 50%),
- Wide band (over 50%);

d. Type of elements:

- Distributed elements,
- Lumped elements;

e. Construction types:

- Stepped impedance,
- Parallel coupled line,
- End-coupled line,
- Interdigital,
- Comb-line,
- Hairpin,
- Irregular line.

The low-pass and high-pass characteristics have the cutoff frequency, defined by the specified insertion loss in decibels, at which the passband ends. The LPF transfers energy to the load at frequencies lower than the cutoff frequency with minimal attenuation and reflects an increasing fraction of the energy back to the source as the frequency is increased above the cutoff frequency. The HPF transfers energy to the load at frequencies higher than the cutoff frequency with minimal attenuation and reflects an increasing fraction of the energy back to the source as the frequency is decreased below the cutoff frequency.

The band-pass and band-stop filter characteristics have two cutoff frequencies, or band-edge frequencies, which are defined by the specified insertion loss in decibels. In the BPF, energy is transferred to the load in a band of frequencies between the lower and upper cutoff frequencies. In the BSF energy transfers to the load in two frequency bands: from DC to the lower band-stop cutoff and from the upper band-stop cutoff to infinite frequency.

Accurate and fast UWB BPF design is a difficult optimization problem as each part of the circuit highly affects the frequency response of the filter to a certain extent. Since there are no analytical models of elements, 3D EM simulators should be used in the design process which thereby consumes a lot of time and CPU usage.

In this part of the thesis, an accurate and faster methodology for designing a microstrip UWB BPF is demonstrated. This method uses the very popular Support Vector Regression Machine (SVRM) which is trained by 3D EM simulator results of the desired microstrip shapes given as the basic design blocks and then combines the blocks to construct the BPF within an efficient and robust optimization process in accordance with the required design objectives. Thus, not only does this method avoids the slowness of 3D EM simulators, but is also as accurate as these simulators. Moreover, the easy implementation of different kinds of shapes and technologies like strip lines is one of the prominent features of this novel design methodology. As an application example, an UWB BPF is designed by using three base fundamental shapes; Shunt Stub (SS), Etched Square Stub (ESS) and Defected Ground Structure (DGS). SVRM and Cuckoo Search Algorithm (CSA) are utilized together in the analysis and design of the BPF.

In recent years, Cuckoo Search Algorithm has become very popular as a new optimization method amongst the academic communities of various engineering disciplines [32, 33]. It was first proposed by Xin-She Yang and Suash Deb in 2009 and its performance was tested by using standard test functions. The results were superior when compared with other popular meta-heuristic optimization methods like Genetic Algorithm (GA) and Particle Swarm Optimization (PSO).

In this chapter, the training data sets for the desired basis shapes are created first by using the 3D Computer Simulation Technology Microwave Studio (CST MWS) and then the SVRM model of each shape is constructed with these data sets. Then, the output of the obtained SVRM models are fed into the CS optimization algorithm until the BPF design is optimized according to the design goals. The performance of the CSA is compared with the standard Meta-Heuristics; Genetic Algorithm (GA) and Particle Swarm Optimization (PSO) methods. Finally, the designed UWB BPF is fabricated and measured.

This chapter is composed of 6 sections: After the introduction and the general classification chapters, the next section states the characteristics and design of the base elements and the SVRM model building. In the fourth section, the Cuckoo Search Algorithm (CSA) is presented for optimizing the defined cost function by making use of the SVRM models. The design procedure and fabrication of the UWB BPF is given in Section 4.5 and finally, the Section 4.6 is for the conclusion.

4.3 Base Elements

In this study, 3 kinds of resonator types which are illustrated in Fig. 4.1 – 4.3 are used as the base elements for the UWB BPF design. Shunt Stub (SS) behaves like high pass, Etched Square Stub (ESS) works like band stop, while Defected Ground Structure (DGS) shows band stop and low pass characteristics. Operational parameters of the resonators are manipulated by their geometrical dimensions within the limitations of the filter. These limitations could arise from the design objectives such as compactness and the frequency response of the filter. In the design, RO-4350 material which has a dielectric permittivity (ε_r) of 3.48, substrate thickness (h) of 1.52mm, copper thickness (t) of 35 μm and a tangent loss ($\tan\delta$) of 0.002 is utilized as the substrate.

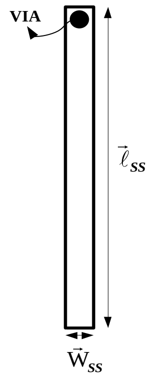

Figure 4.1 Shunt stub base element

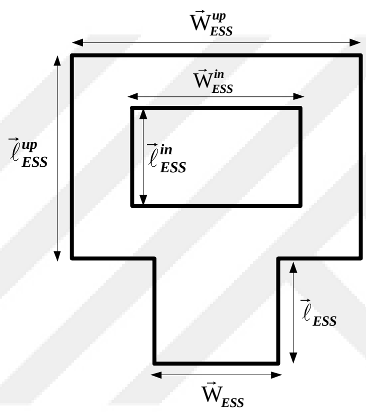

Figure 4.2 Etched Square stub base element

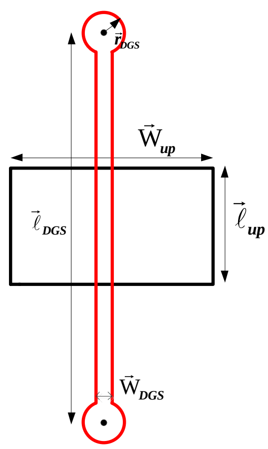

Figure 4.3 Defected Ground Structure with microstrip line base element

4.4 Design Synthesis and Optimization Process

4.4.1 Mathematical Bases of Support Vector Regression

Given the training dataset $(\vec{x}_i, y_i)$, i=1,2,...,λ where, $y_i \in R$ and λ is the size of the training data, Support Vector Regression Machine (SVRM) attempts to construct a continuous mapping function $f(\vec{x})$ from the independent p-dimensioned input variable vector $\vec{x}$ to the dependent output variable y by linearly combining the results of a nonlinear transformation of the input samples:

$$f(\vec{\boldsymbol{x}}) = \sum_{i=1}^{n_{sv}} (\alpha_i - \alpha^*_i)\ K(\vec{\boldsymbol{x}}_i, \vec{\boldsymbol{x}}) + b \tag{4.1}$$

where n_{sv} is the number of the Support Vector (SV)s, $\alpha_i \geq 0$, $\alpha^*_i \geq 0$ and b are the functional parameters, K is a kernel function which performs the nonlinear transformation and in practice, is directly defined. The measure of how well a sample is fitted by the function f is given by a so-called ϵ- insensitive loss function [34] described by;

$$L(f(\vec{\boldsymbol{x}}_i) - y_i) = \left| y_i - f(\vec{\boldsymbol{x}}_i) \right|_{\grave{o}} = \max \left| 0, \left(\left| y_i - f(\vec{\boldsymbol{x}}_i) \right| - \grave{o} \right) \right| \tag{4.2}$$

where ϵ is the radius of the regression tube and the distance among the predicted and target values for the training samples is defined as the empirical risk as follows:

$$\mathrm{R}_{emp} = \frac{1}{\lambda} \sum_{i=1}^{\lambda} L(\vec{\boldsymbol{x}}_i, y_i, f) \tag{4.3}$$

Therefore, in SV regression, the goal is to minimize R_{emp}. Using the standard Lagrange multipliers technique, the aforementioned minimization problem can be transformed into Constrained Quadratic Programming (CQP) in which the following function must be maximized with respect to the Lagrange parameters (α, α*) [34]:

$$MaximizeW(\alpha, \alpha^*) = -\frac{1}{2} \sum_{i,j=1}^{n_{sv}} (\alpha_i^* - \alpha_i)(\alpha_j - \alpha_j^*) K(\vec{x}_i, \vec{x}_j) - \int \sum_{i=1}^{n_{sv}} (\alpha_i + \alpha_i^*) + \sum_{i=1}^{n_{sv}} y_i (\alpha_i - \alpha_i^*) \tag{4.4}$$

subject to:

$$0 \leq \alpha_i \leq C,\ 0 \leq \alpha_i^* \leq C, \quad \sum_{i=1}^{\lambda} \alpha_i = \sum_{i=1}^{\lambda} \alpha_i^* \tag{4.5}$$

where index i represents support vector elements of the training data and index j represents irrelevant elements remaining from the training data. The parameter C>0 measures the trade-off between the capabilities of $f(\vec{x})$ to approximate the input samples and the error of the new samples. The CQP can be solved using standard optimization techniques subject to the conditions given by (4.5) and the result in λ Lagrange multiplier pairs (α_i, α_i^*). The parameter b can be computed by means of so-called Karush-Kuhn-Tucker conditions [34], [35], [36].

Since the insensitive loss function given by (4.5) applies the ϵ- tube selection process to the training dataset $(\vec{x}_i, y_i)$, i=1,2,...,λ, thus only for the samples satisfying $|f(\vec{\mathbf{x}}_i) - y_i| \geq \epsilon$, the Lagrangian multipliers (α_i, α_i^*) may be nonzero, and for the samples of $|f(\vec{\mathbf{x}}_i) - y_i| < \epsilon$, the Lagrangian multipliers (α_i, α_i^*) vanish. The samples $(\vec{x}_i, y_i)$, i=1,2, ..., n_{sv} that come with non-vanishing coefficients are called Support Vectors (SV). Therefore, we obtain a sparse expansion of the Lagrangian multipliers (α_i, α_i^*) in terms of the input variable vector $\vec{x}_i$. In other words, we perform generalization between the whole input $\vec{x}$- and output y- domains using only a small subset of the training data that ensures enormous computational advantages [34].

4.4.2 3D EM Simulation-based SVRM Microstrip Modeling

In order to obtain accurate and fast design UWB BPF, the SVRM model of basic elements is employed. Black-box models of each element are created, including geometrical dimensions of elements as input parameters and S parameters of element as output parameters. Input variable vectors of SS, ESS and DGS models are defined as; $\vec{W}_{SS}, \vec{\ell}_{SS}, f$, $\vec{W}_{ESS}, \vec{\ell}_{ESS}, \vec{W}_{ESS}^{up}, \vec{\ell}_{ESS}^{up}, \vec{W}_{ESS}^{in}, \vec{\ell}_{ESS}^{in}, f$ and $\vec{W}_{DGS}$, $\vec{\ell}_{DGS}, \vec{W}_{up}, \vec{\ell}_{up}, \vec{r}, f$, respectively. Output parameters of the element models are the same; $|S_{11}|, \angle S_{11}, |S_{21}|, \angle S_{21}$, the magnitude and phase of S parameters. Since the SVRM model has one output, a parallel operation is run to compose the element models. Therefore, each element model contains four machines which have the same input because of the four output parameters. Radial kernel function is exploited for the SVM regression which is described by;

$$K(\vec{x}_i, \vec{x}) = e^{-\gamma\|\vec{x}_i - \vec{x}\|^2} \tag{4.6}$$

where γ is the variance of the kernel function and will be chosen in the training phase. The training dataset of base elements is obtained by CST Microwave Studio within the physical ranges given in Table 4.1.

Table 4.1 Dimensional range of Base Elements for training data

Base Element	Input Variables	Min. Value	Max. Value	Interval	Data Number
SS	W_{SS} (mm)	0.2	1	0.2	5
	ℓ_{SS} (mm)	3	5	0.2	11
	f (GHz)	0.2	25.2	1	26
ESS	W_{ESS} (mm)	0.5	1	0.1	5
	ℓ_{ESS} (mm)	0.5	1	0.1	5
	$W^{up}{}_{ESS}$ (mm)	1.7	2	0.1	4
	$\ell^{up}{}_{ESS}$ (mm)	1	1.3	0.1	4
	$W^{dn}{}_{ESS}$ (mm)	1	1.4	0.2	3
	$\ell^{dn}{}_{ESS}$ (mm)	0.5	0.7	0.1	3
	f (GHz)	0.2	25.2	1	26
DGS	W_{DGS} (mm)	0.2	0.5	0.1	4
	ℓ_{DGS} (mm)	5	7	0.4	6
	W_{up} (mm)	1	2	0.2	6
	ℓ_{up} (mm)	2	4	0.2	11
	r (mm)	0.2	0.5	0.1	4
	f (GHz)	0.2	25.2	1	26

Total training data number of neural network for each frequency of SS, ESS and DGS are 55, 3.600 and 6.336, respectively. Furthermore, in Table 4.2, the accuracy of the models, the Support Vector numbers of $|S_{21}|$, are compared for different ϵ insensitive loss parameters, γ variance of the kernel function and C capability, respectively. Table 4.2 gives the used SVRM parameters, selection tube radius ϵ, number of the SVs and the resulted accuracy for the SVRM model of the S parameters for 7 GHz. The numbers of SVs used to train the SVRM model for SS, ESS and DGS are 14, 820 and 1223 respectively, with the accuracy of at least 96.0%. The simulation results show that SVRM models of the elements are not only as accurate as the 3D EM simulation model, but also approximately 280 times faster than the CST model.

Table 4.2 Accuracy with respect to SVRM parameters

Element	γ	C	ϵ	$\|S_{21}\|$ SVs Number	$\|S_{11}\|$ (%)	∟S_{11} (%)	$\|S_{21}\|$ (%)	∟S_{21} (%)
SS	0.001	10000	0.05	32	99.8	99.8	99.9	99.6
	0.001	10000	0.07	23	99.5	98.1	99.4	99.2
	0.001	10000	0.1	14	98.9	97.2	99.0	98.7
ESS	0.001	10000	0.05	1617	99.7	98.8	99.6	98.9
	0.001	10000	0.07	1272	99.3	98.6	99.1	98.8
	0.001	10000	0.1	820	98.1	97.9	98.3	98.5
DGS	0.001	10000	0.05	2915	99.2	98.1	99.0	97.5
	0.001	10000	0.07	2002	98.5	97.2	97.9	96.6
	0.001	10000	0.1	1223	97.2	96.1	96.8	96.0

4.4.3 Cuckoo Search Algorithm

Similar to other meta-heuristic optimization algorithms, it is a bio-inspired optimization algorithm based upon the obligate brood parasitism of some cuckoo species in nature which lay their eggs in the nests of other host birds. The Cuckoo Search which idealizes such breeding behavior was proposed by Xin-She Yang and Suash Deb in 2009 and since then, it has been applied extensively to various engineering optimization problems like antenna array optimization [37], data fusion in wireless sensor networks [38], welded beam and spring design optimization [36] and to multi-objective design optimization problems like reliable embedded system design [39]. It was also hybridized with quantum computing principles [40] and with power series [41] to obtain better performance.

In the CS, each egg in a nest represents a solution, and a cuckoo egg represents a new solution. The aim is to use the new and potentially better solutions (cuckoos) to replace a not-so-good solution (egg) in the nests. In the simplest form, each nest has one egg.

The CS is built upon the following three idealized rules:

- Each cuckoo lays one egg at a time and dumps its egg in a randomly chosen nest;
- The best nests with high-quality eggs will carry over to the next generation;
- The number of available host nests, n is fixed, and the egg laid by a cuckoo is discovered by the host bird with a probability $Pa \in (0,1)$. Discovering means

that some set of worst nests (eggs) will be thrown away and their corresponding solutions will be discarded from further calculations.

Yang and Deb also discovered that the random-walk style search is better performed by Lévy flights rather than by simple random walk. Many studies have shown that the flight behavior of many animals and insects has demonstrated the typical characteristics of Lévy flights [35], [36]. Lévy flight is defined as a random walk with the step-lengths based on a heavy-tailed probability distribution which enables CS to explore the whole solution space effectively. An important advantage of CS algorithm is its simplicity. In fact, compared with other population or agent-based meta-heuristic algorithms such as PSO and Harmony Search (HS), there is essentially only one parameter, *Pa* in CS as the population size (the number of available host nests, *n*) is fixed, making it very easy to implement and fast to converge. The Figure 4.4 depicts the flow chart indicating the main steps of the regular CS algorithm implementation [42].

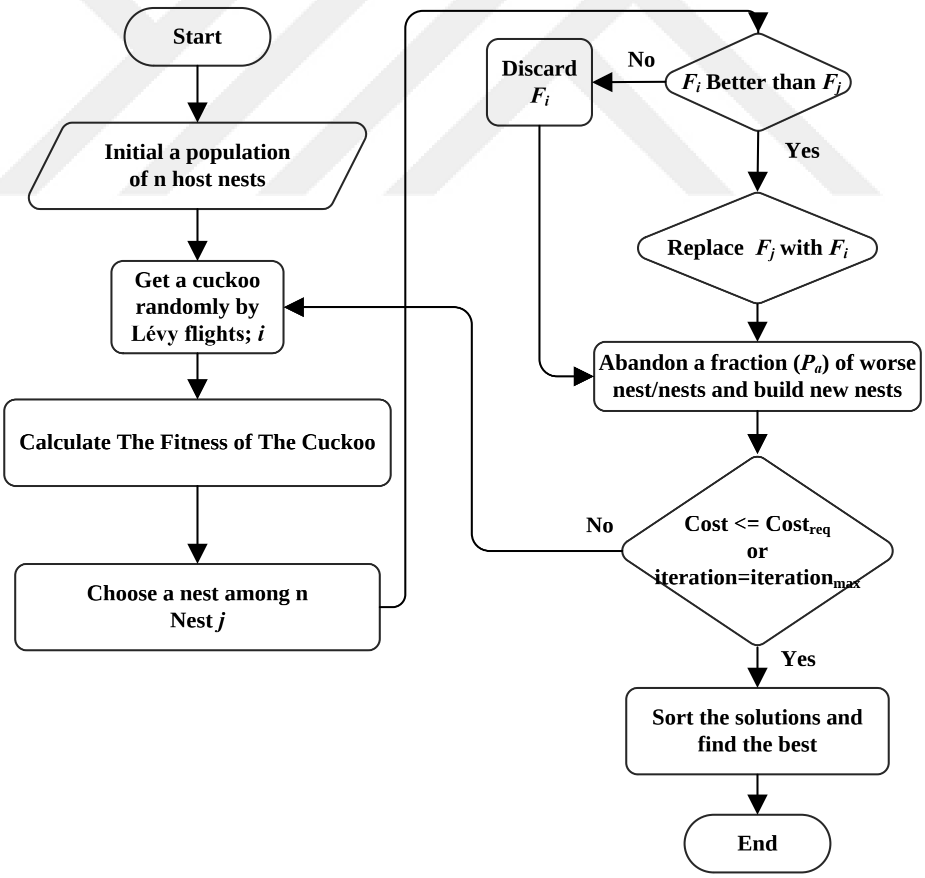

Figure 4.4 Flow chart of the conventional Cuckoo Search Algorithm

4.4.4 Cost function Evaluation and Updating Process

In microwave circuit design, two port structures could be demonstrated as cascaded connections of sub-structures. Thus, circuits can be solved by using ABCD parameters of each sub-structure. The total ABCD matrix of a circuit which is composed of cascaded n two-ports is described by;

$$\begin{bmatrix} A & B \\ C & D \end{bmatrix} = \begin{bmatrix} A_1 & B_1 \\ C_1 & D_1 \end{bmatrix} \begin{bmatrix} A_2 & B_2 \\ C_2 & D_2 \end{bmatrix} .... \begin{bmatrix} A_n & B_n \\ C_n & D_n \end{bmatrix} \tag{4.7}$$

In our case, UWB BPF could be considered by connection of each basic element in cascade form. The frequency response of the filter is calculated using (4.7) and the ABCD parameters of base elements are transformed from S parameters [43] which are obtained by SVRM models per the elements' dimensions and frequency. There are 2 of SS, 3 of ESS and 4 of DGS in our BPF design making the *n*=9. Therefore, the ABCD matrix of the filter is as follows (8-9);

$$[T]^n = \begin{bmatrix} A_n & B_n \\ C_n & D_n \end{bmatrix} \tag{4.8}$$

$$\begin{bmatrix} A & B \\ C & D \end{bmatrix}_{Filter} = [T]^1_{SS_1} [T]^2_{DGS_1} [T]^3_{ESS_1} [T]^4_{DGS_1} ....[T]^9_{SS_2} \tag{4.9}$$

S parameter of the filter is acquired using inverse transformation equations [43]. Meanwhile, there is no need to investigate full S parameters of base elements. The SVRM model results, which give us S_{11} and S_{21} of each elements, are enough to calculate ABCD parameters because of the reciprocity $S_{11}=S_{22}$ and $S_{12}=S_{21}$ [43].

In the design process, the optimal dimensions of the elements for the required UWB filter response are investigated by using the CS algorithm and SVRM models together under the analytical combination of ABCD parameters subject to cost function which is defined as follows (4.10);

$$\text{Cost Func.} = \omega_1.\Lambda_1 + \omega_2.\Lambda_2 + \omega_3.\Lambda_3 \tag{4.10}$$

$$\Lambda_1 = \left(1 - |S_{11}|\right)\Big|_{\Delta f_1} \tag{4.11}$$

$$\Lambda_2 = \left(1 - |S_{21}|\right)\Big|_{\Delta f_2} \tag{4.12}$$

$$\Lambda_3 = \left(1 - |S_{11}|\right)\Big|_{\Delta f_3} \tag{4.13}$$

where Δf_1 is picked as 0.2-3.1 GHz to provide suppression at a lower band (4.11), Δf_2 is selected as 3.1-10.6 GHz to obtain pass band characteristics (4.12) and Δf_3 is taken between 10.6-20 GHz to suppress the second and third harmonic of the filter (4.13). Moreover, $\omega 1$, $\omega 2$, $\omega 3$ (10) are chosen as 2/10, 1, 1/10, respectively. Optimization comes to the end when the iteration number is maximized or the cost value is minimized.

4.5 Design and Comparison of UWB Bandpass Filter

In this section, the UWB band pass filter design process is described and then the results of a specific design example are discussed. First, training data sets of bases elements are obtained with a 3D EM simulator in order to form fast and accurate SVRM models of SS, ESS and DGS within their physical limitations. Later, these models are employed in the CSA optimization process in order to obtain the required filter specifications which include rejection and pass band characteristics. The cost function of CSA is determined using analytical calculations of ABCD parameters for cascade-connected base element SVRM models. The CSA optimization process concludes when the iteration number or cost value reaches its limits. If the 3D model of basic elements is utilized instead of fast SVRM models, the duration of the optimization process would be extremely long.

The design procedure of the filter is shown in Figure 4.5.

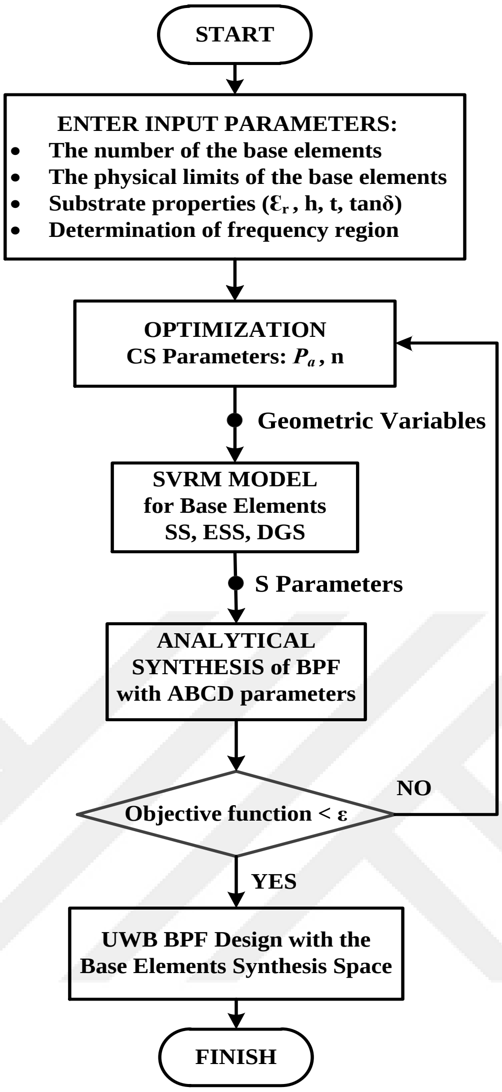

Figure 4.5 General Design Procedure for the BPF

RO-4350 material as mentioned in section 2 is used to fabricate the designed filter circuit. The aim is to design an UWB BPF that has an operational bandwidth between 3.1 GHz and 10.6 GHz. In order to achieve that, the dimensions of base elements of the filter are adjusted using the optimization process. After the optimization, the designed circuit is manufactured and measured. The total size of the filter whose scaled drawing and the actual picture can be seen in Figure 4.6 and Figure 4.7 respectively is about 2.5×1.5 cm2. The actual dimensions of each base element used in the design are given in Table 4.3.

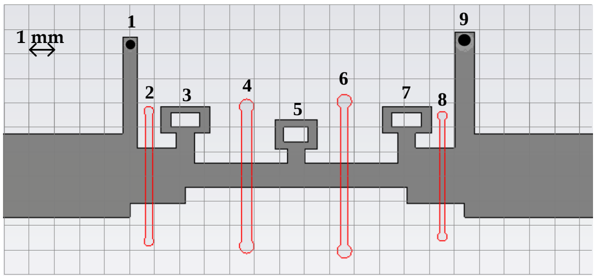

Figure 4.6 Scaled filter drawing with grid background

Table 4.3 Solution of the base elements

Base Element	Input Variables	1. Element	2. Element	3. Element	4. Element
SS	W_{SS} (mm)	0.6	0.8	-	-
	ℓ_{SS} (mm)	4	4.2	-	-
ESS	W_{ESS} (mm)	0.6	0.7	0.6	-
	ℓ_{ESS} (mm)	0.7	0.6	0.7	-
	W^{up}_{ESS} (mm)	2	1.7	2	-
	ℓ^{up}_{ESS} (mm)	1.1	1.2	1.1	-
	W^{in}_{ESS} (mm)	1.2	1	1.2	-
	ℓ^{in}_{ESS} (mm)	0.6	0.5	0.6	-
DGS	W_{DGS} (mm)	0.3	0.4	0.3	0.2
	ℓ_{DGS} (mm)	5.4	5.8	6.2	5
	W_{up} (mm)	1.6	1	1	1.6
	ℓ_{up} (mm)	2.4	3.8	3.8	2.4
	r (mm)	0.2	0.3	0.3	0.2

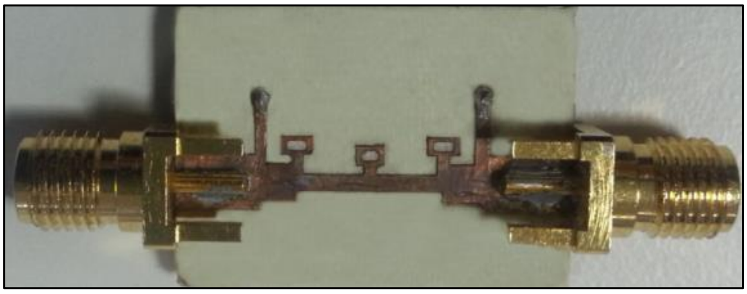

(a) Top layer

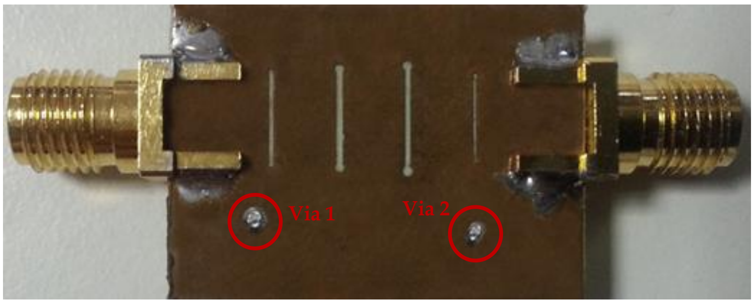

(b) Bottom layer

Figure 4.7 Photographs of the fabricated UWB BPF

The simulation and actual measurement results are in parallel with each other as given in Figure 4. 8. It is understood from the results that insertion loss, which increases with frequency, is better than -2 dB over the whole transition band and there is extra loss at the end of the transition band because of the SMA connectors utilized in the ports. Moreover, there is good suppression which is better than 10 dB until 25 GHz which contains the second and third harmonic at the rejection band. Return loss is under -10 dB at pass band. In addition, the low and high cut-off regions of frequency response show that the filter has good sharpness. Furthermore, the designed filter has a flat group delay over the whole operation band, as can be seen in Figure 4.9.

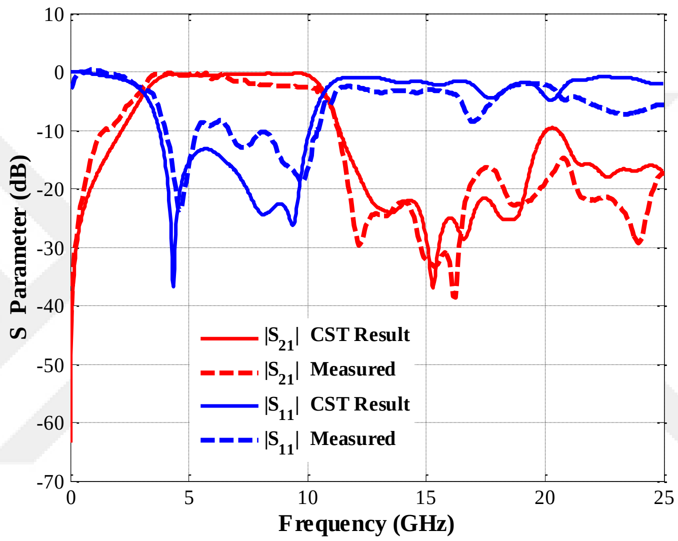

Figure 4.8 Simulated and measured S parameters of the designed UWB BPF

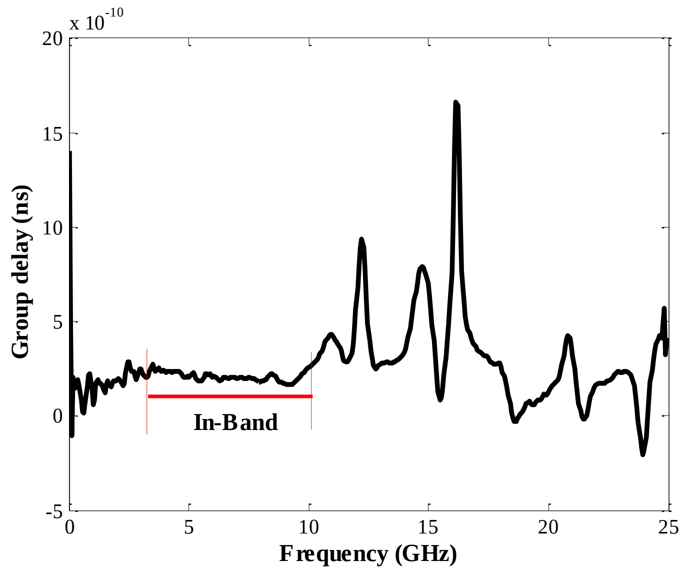

Figure 4.9 Measured group delay of the designed UWB BPF

In the CS optimization process, number of host nest (size of population), and fraction probability (*Pa*) is chosen as 50 and 0.25, respectively as they provided the best results.

In order to compare it with other Meta-Heuristics, the PSO optimizer is constructed with the population (particle number) equals to 50, max/min velocity of ±0.1 and learning factors set to 2.0, respectively. Similarly, the GA optimizer has a population (chromosome) of 50, crossover probability of 0.8, and mutation probability of 0.1. The cost results of 5-time tries and 120 iteration of CSA and other standard Meta-Heuristic algorithms and benchmarking at 120th iteration for best try with the corresponding execution times for the same filter are shown in Table 4.4.

Table 4.4 Comparison of the CSA performance with the Standard Meta-Heuristic Algorithms

Algorithm	Worst (max)	Best (min)	Average (mean)	Execution Time (s)
CSA	2.687	0.266	0.813	131
GA	4.999	0.677	2.017	180
PSO	2.158	0.301	1.110	136

A desktop computer with 'Intel Core i7 CPU, 2.20 GHz Processor, 8 GB RAM' is used for the design and optimization process. At end of the optimization, the iteration number reaches 72 and the cost value of the operation is equal to 0.271. It is clear from the Tab. 4 that CSA has a superior performance with respect to other popular Meta-Heuristics.

4.6 Results and Conclusions

In this part of the thesis, a novel design methodology which uses fast and accurate SVRM models of base elements based on a 3D EM simulator is presented to design and analyse a UWB BPF. The outputs of the built SVRM models are used as input by a straightforward, simple and efficient CS algorithm under the rules of circuit theory to solve the filter response. The designed filter is manufactured and measured to show that the actual results are in coincidence with the simulation results. Furthermore, the performance of the CS algorithm is compared with other popular methods like GA and PSO to demonstrate the efficiency of the CS algorithm. The suggested methodology could be used for different kind of element shapes and filter types. Consequently, the proposed design methodology could be considered as an important contribution to the UWB design literature.

CHAPTER 5

THE SYSTEM LEVEL TESTING

5.1 Simulations

The concatenation of the antenna and the filter (as if they were part of a complete RF Front-end circuitry) without seeking any certain application is verified by the simulations using the CST STUDIO SUITE Electromagnetic (EM) Simulation software program first and then by the system level measurements within the laboratory environment of the YTU Department of the Electronics and Communication Engineering.

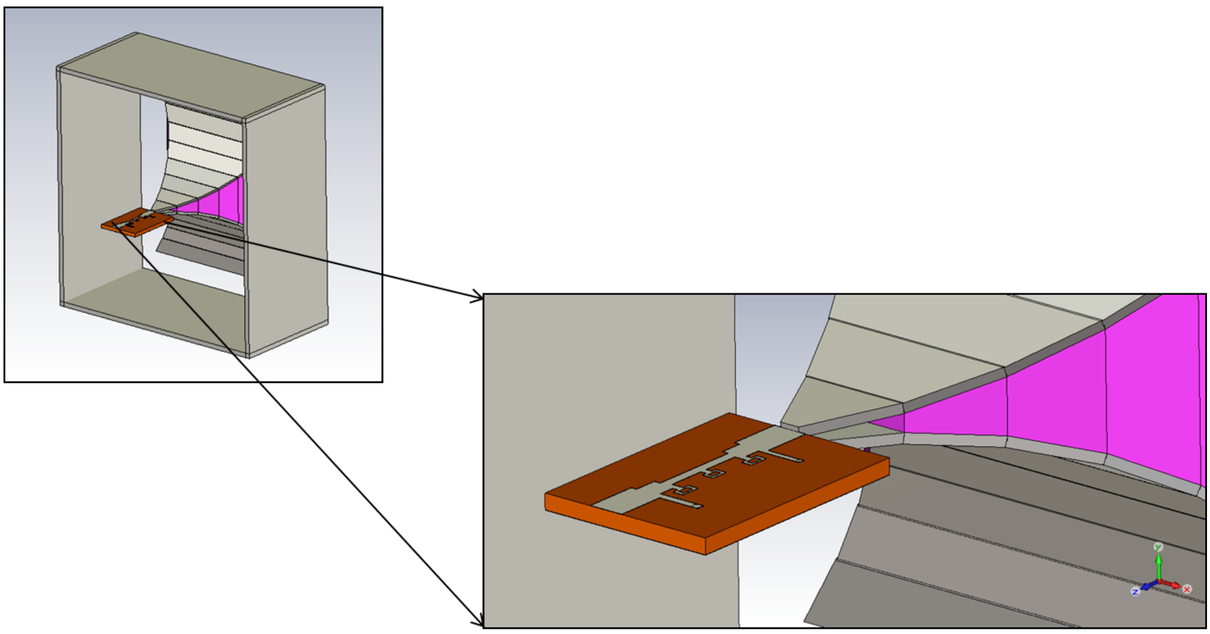

Figure 5.1 Antenna and the filter as attached to it

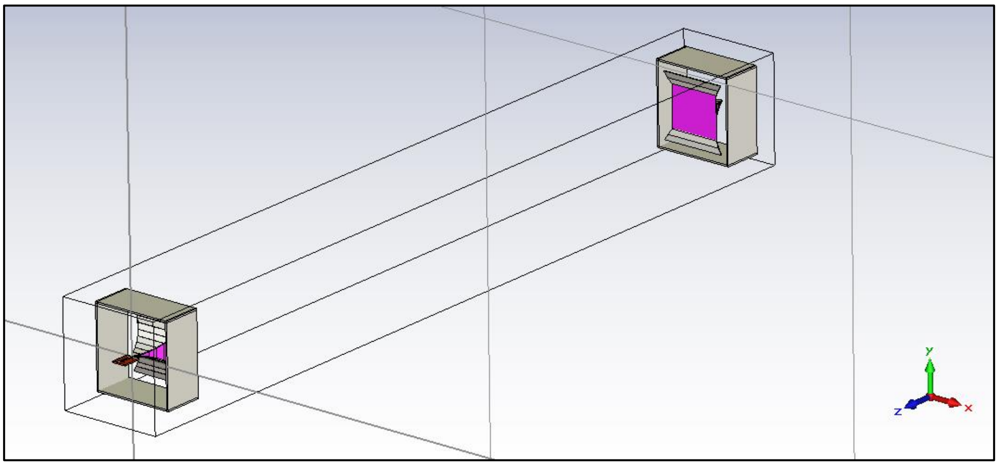

Figure 5.2 Simulation set-up

The Figure 5.2 gives an idea about the simulated set-up. The separation between the transmit and receive antennas is set to be 1 meter. The simulations are performed first for the frequency range of 1 to 11 GHz and then for 3.1 to 10.6 GHz band.

The simulation and measurement results are presented in the following figures for which (a) is for the frequency range of 1-11 GHz and (b) is for the frequency band of 3.1-10.6 GHz. Figure 5.3 depicts the transmitted signal which is a typical Gaussian pulse of duration of 100 psec. It has nominal maximum amplitude value of 1V. Figure 5.4 and 5.5 illustrate the received signals for antennas only and the filter attached to the antenna cases respectively.

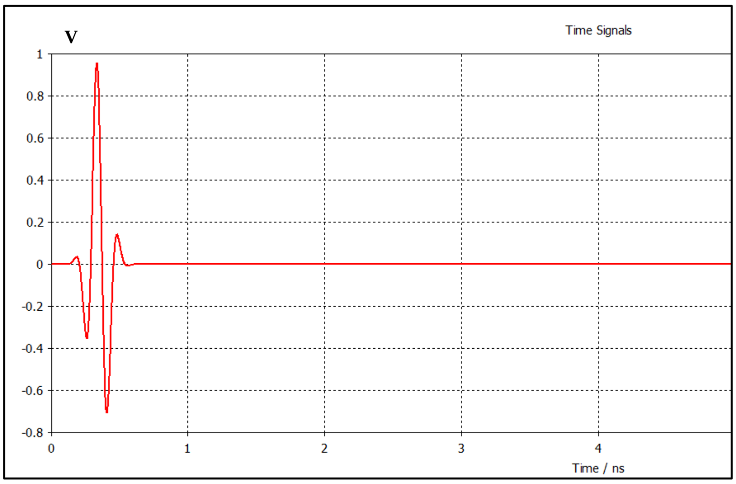

(a)

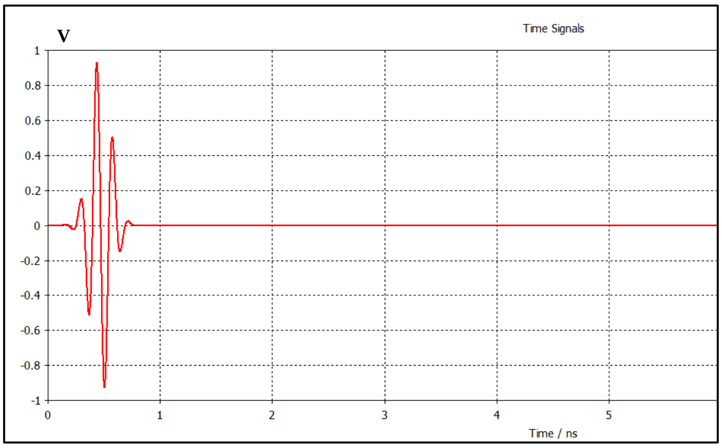

(b)

Figure 5.3 Transmitted Signal

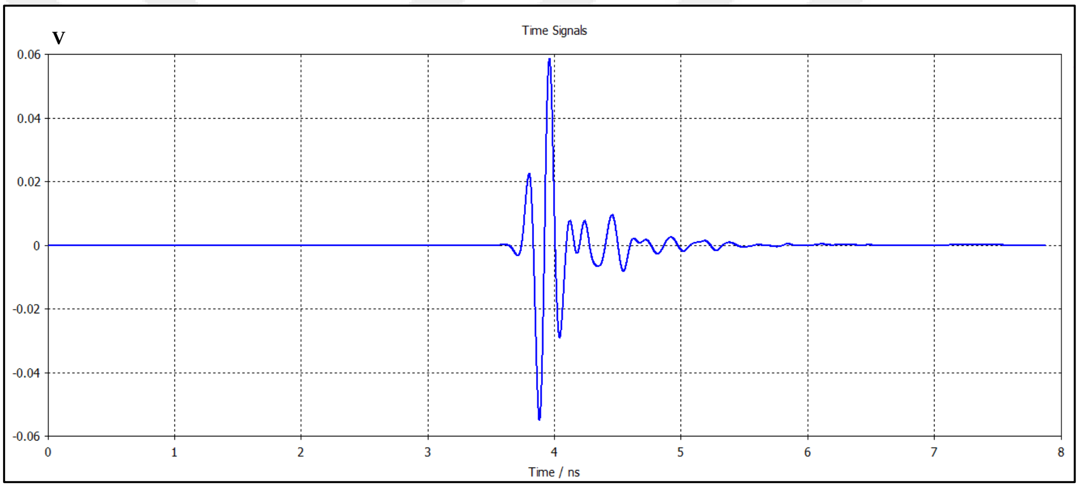

(a) 1-11GHz

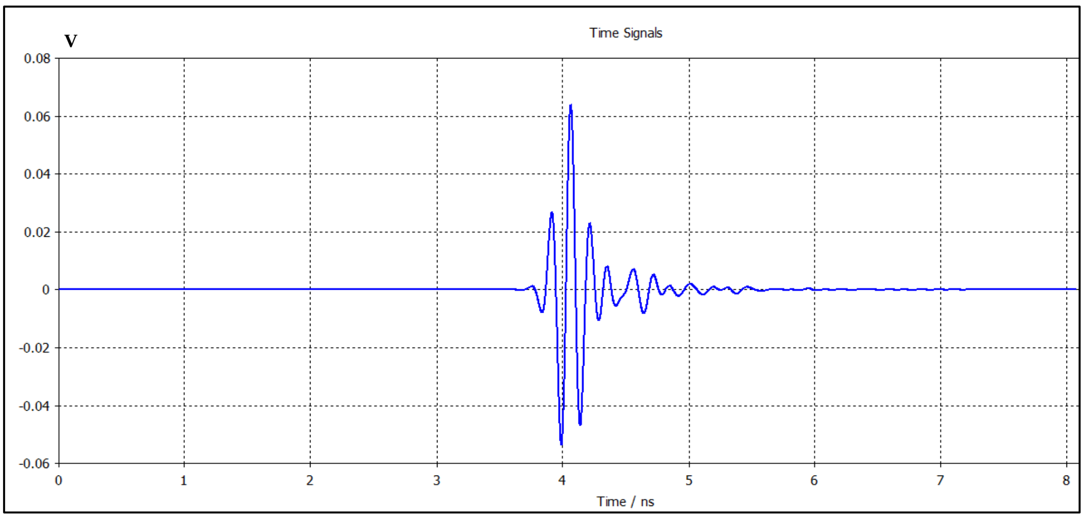

(b) 3.1-10.6 GHz

Figure 5.4 Received signal by the Antenna only

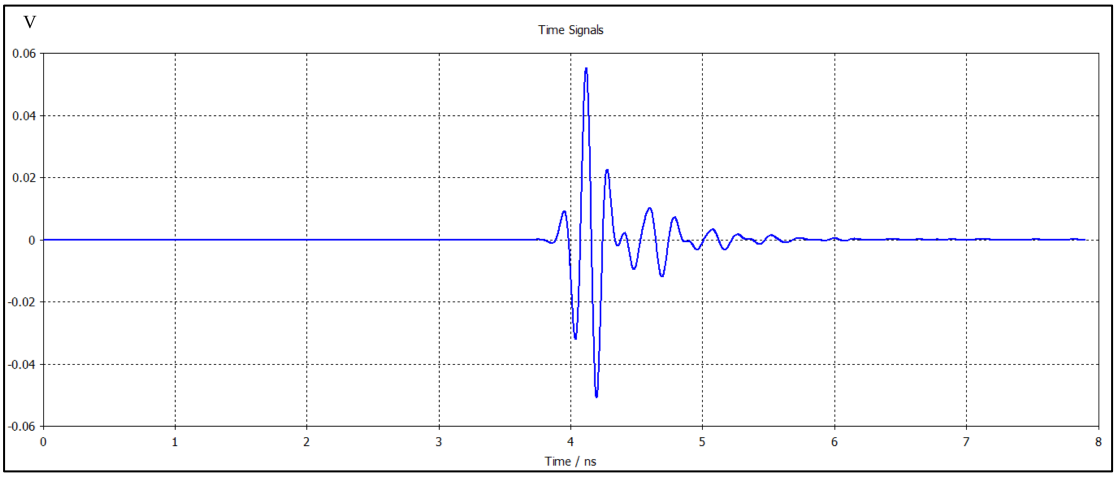

(a) 1-11 GHz

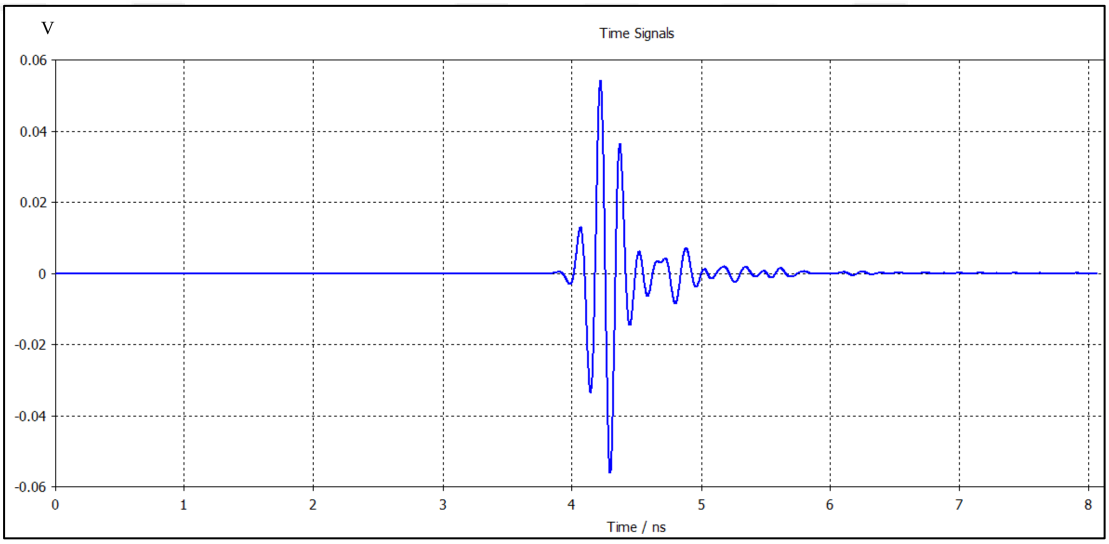

(b) 3.1-10.6 GHz

Figure 5.5 Received signal by the Antenna and the filter

5.2 Measurements

Regarding the physical measurements, they are taken place in the Antennas and Microwave Laboratory of the YTU Electronics & Communication Engineering department by using the actual hardware developed within the scope of this thesis.

Rohde-Schwartz ZVL-13 model Spectrum Analyzer is used for the measurements where a standart TEM Horn Antenna is used for transmitting the pulse. Figure 5.6 gives the picture of antenna and filter as attached to its back. Figure 5.7 (a) and (b) depicts the measurement set-up.

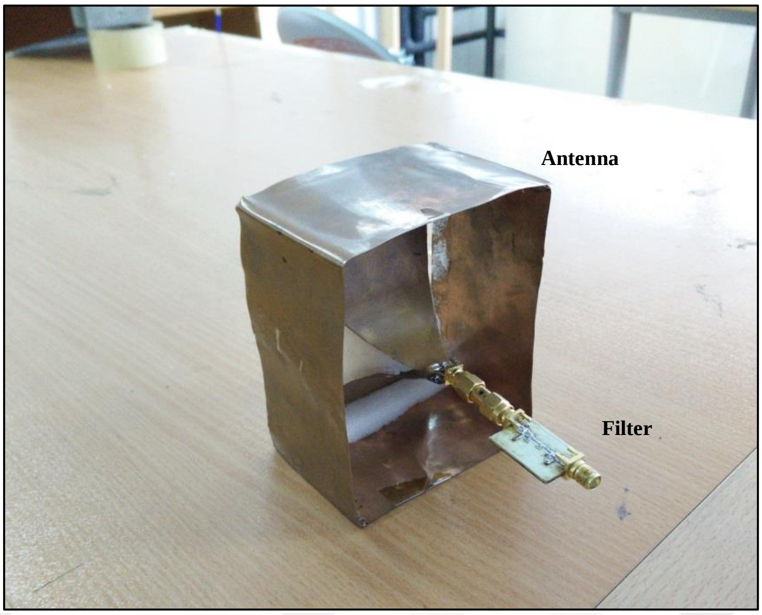

Figure 5.6 Antenna and filter units in concanetation

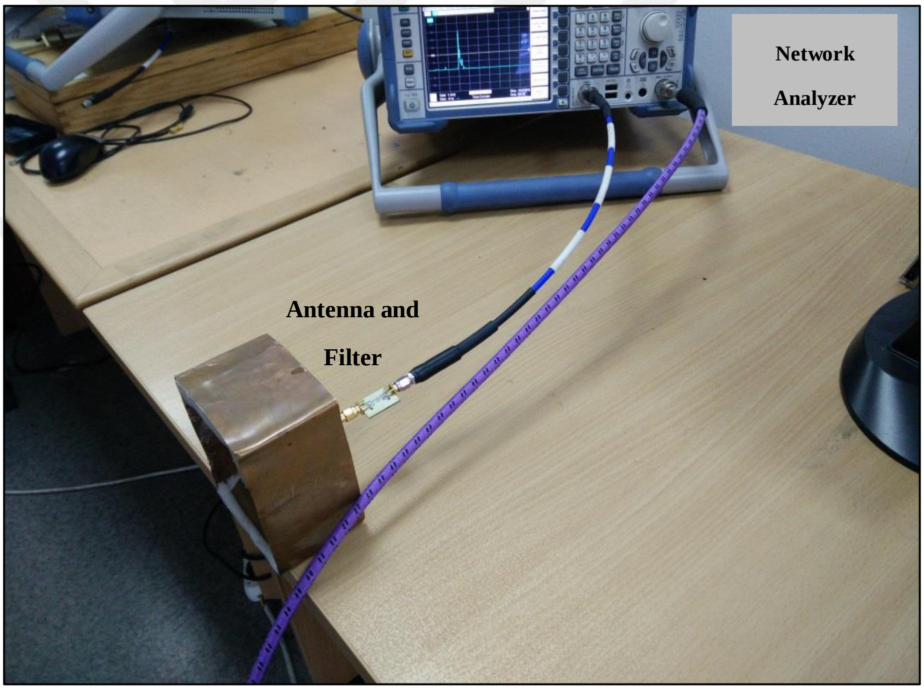

(a)

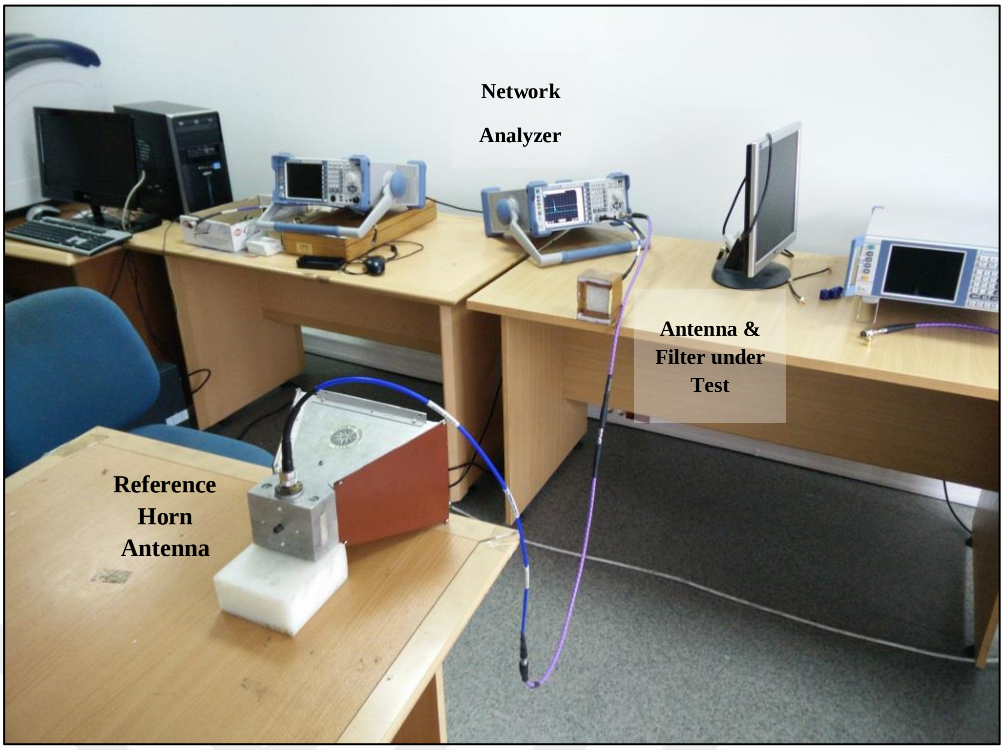

(b)

Figure 5.7 (a-b) Measurement set-up

The measurement results are given in the figures below. Figure 5.8 thru Figure 5.10 are for the frequency range of 1-11 GHz and they illustrate the transmitted pulse signal, the pulse fed-back thru the cables of the network analyzer (just to indicate the cable losses) and the pulses that are picked up by the antenna only and the antenna and the filter in concatenation respectively. The figures 5.11 thru 5.13 contain the same information but for the frequency range of 3.1 to 10.6 GHz.

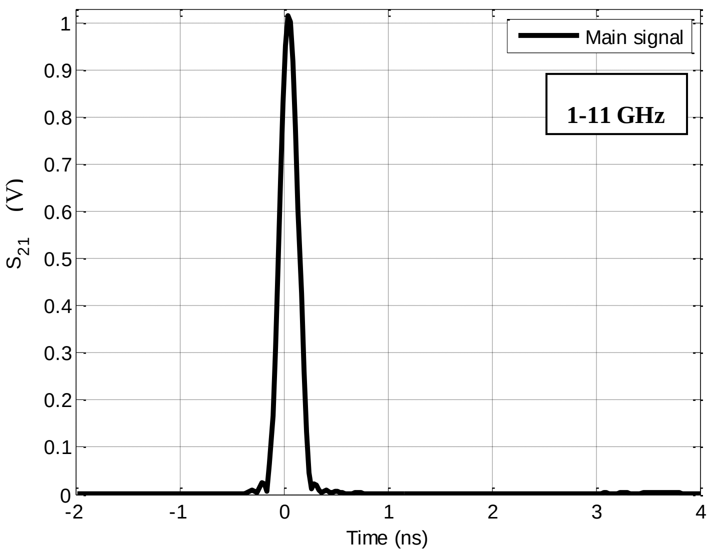

Figure 5.8 Transmitted Pulse

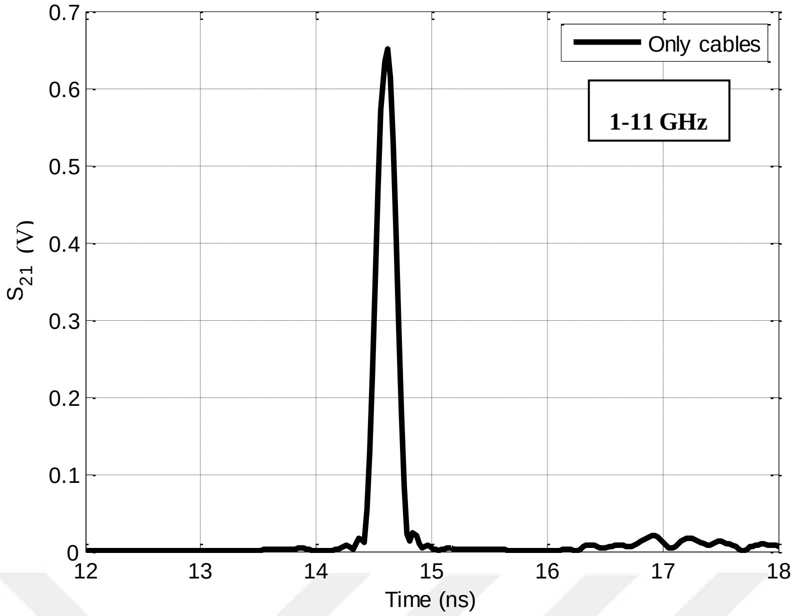

Figure 5.9 The signal fed-back thru the cables

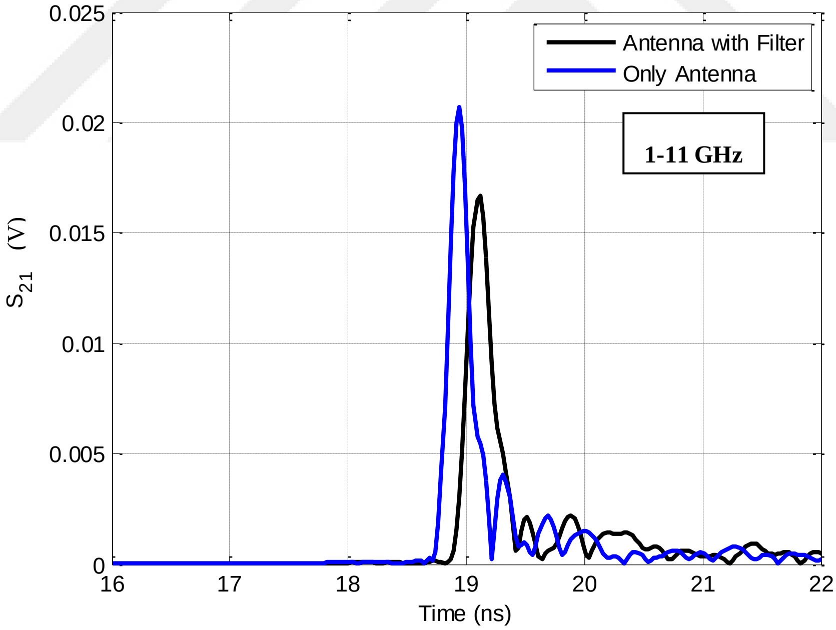

Figure 5.10 The signal picked-up by the antenna only and the antenna in concatenation with the filter

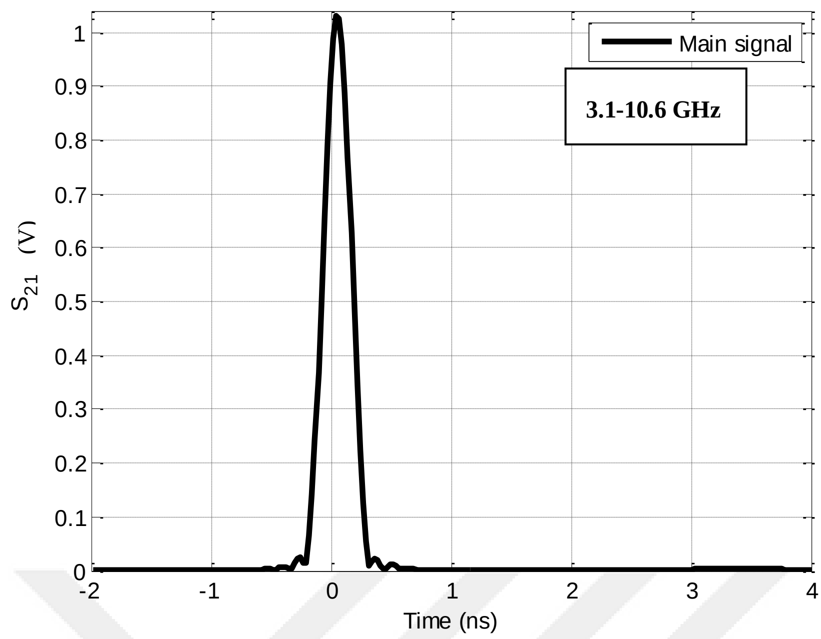

Figure 5.11 Transmitted Pulse

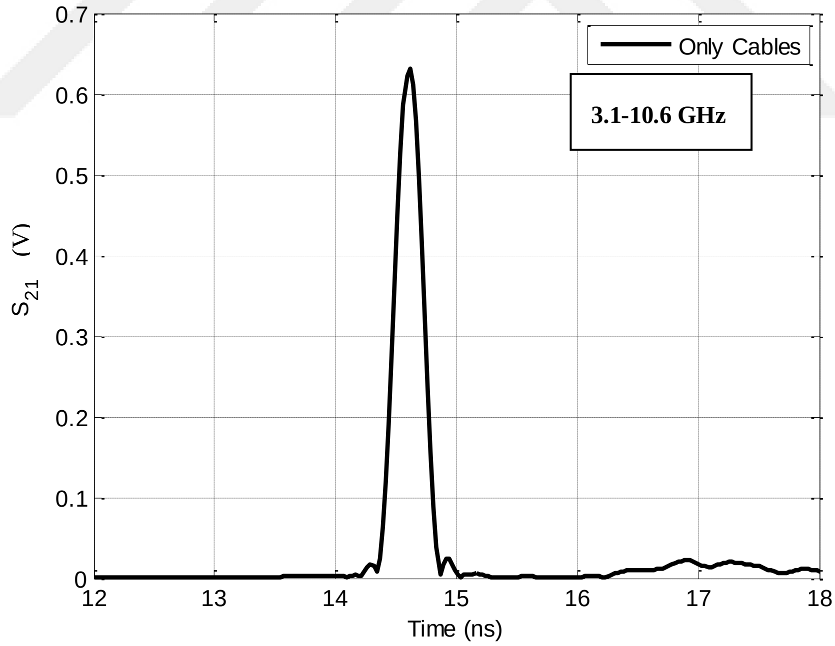

Figure 5.12 The signal fed-back thru the cables

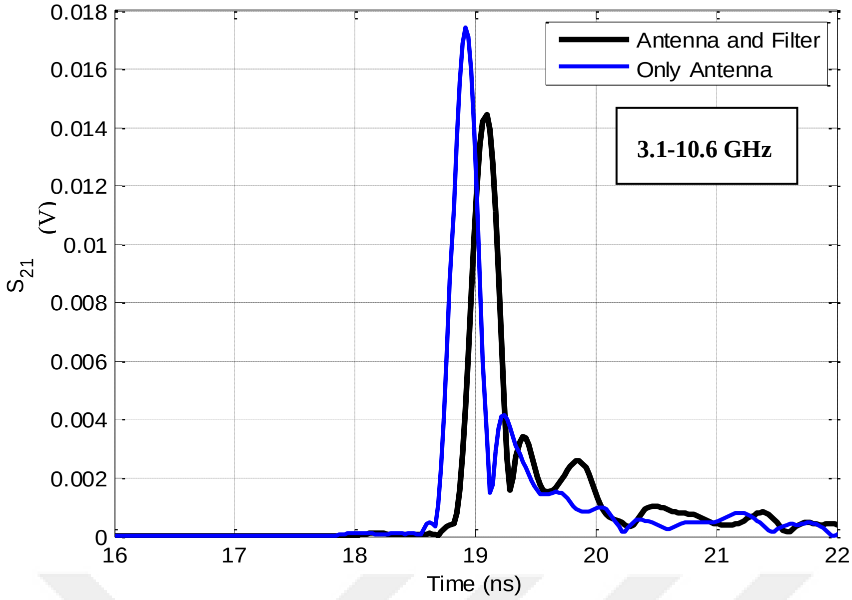

Figure 5.13 The signal picked-up by the antenna only and the antenna in concatenation with the filter

In order to evaluate the stop-band and transition-band performance of the filter, we have obtained measurements for the frequencies from 1 GHz to 2 GHz and then up to 3 GHz respectively. The same signal of figure 5.11 is used (transmitted) in this scenario too. The results are given in the figure 5.14 (a) for 1-2 GHz and (b) for 1-3 GHz. They indicate an expected stop-band performance for the filter. While the antenna picks up the transmitted signal successfully, when the filter is attached, it immediately rejects the parts of signal that are out of the pass-band of the filter (3.1 – 10.6 GHz). When the measurements are extended up to 3 GHz, it started to accept more parts of the signal meaning getting closer to the filter pass-band as obvious in figure 5.14 (b).

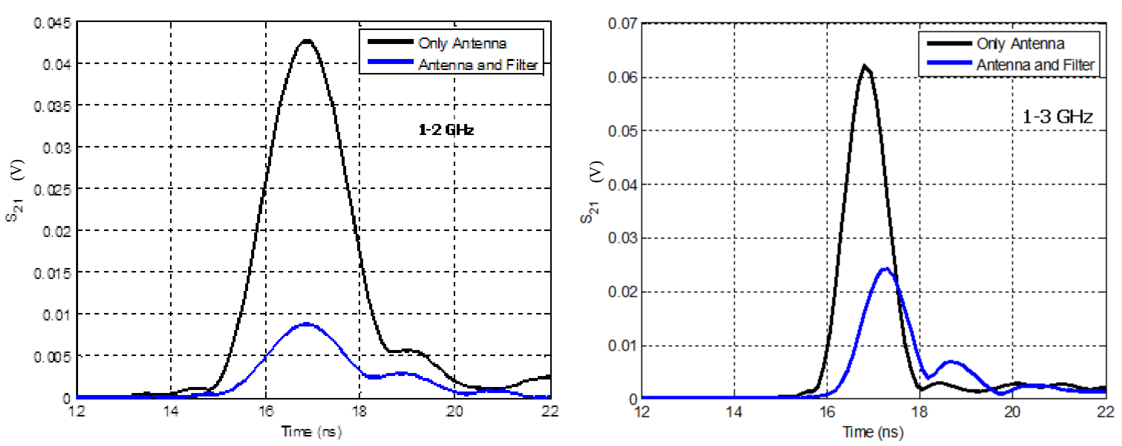

(a) (b)

Figure 5.14 The stop-band (a) and the transition-band (b) performance of the filter and its effect on the overall system performance

5.3 Results and Conclusions

The primary concern for this part of the study was to evaluate the dispersion on the waveform of the pulse throughout the transmission and reception process experimented with the developed antenna and filter units that are under investigation along with the laboratory equipment of network analyzer, standard TEM Horn antenna and cables.

Waveform dispersion becomes an issue in the UWB design because the shape of transmitted pulses is the vehicle itself to carry the information and if this happens due to RF Front-end hardware irregularities over the operational band, information cannot be extracted back from the received pulses.

It has been observed that even though the ringing effects are noticeable at the trailing edge of the received pulses for both configurations, there is no significant waveform dispersion for all cases and hence the measurement results that are in agreement with the simulation results can be considered as very satisfactory indicating a successful UWB performance for the novel antenna and filter units.

Another issue could be the signal level which could impact the S/N ratio in a negative manner and hence degrade the reception. At this level of RF frequencies, even the cable itself can have an important level of degradation over the transmitted pulse in terms of pulse-shape and signal level.

The cable alone costs the one-third of the transmitted signal level for one-way. Only the two-percent of the original signal level could be extracted after transmission thru the cables, standard TEM Horn antenna and the free space (air) medium of 1m range and reception thru the novel antenna, the filter and the cable again. There is no additional LNA in the line to boost the signal level except the one internal to the network analyzer. Nevertheless, the received signal level was enough for a successful reception.

For both of the performance criteria, there was no noticeable difference between the two different frequency bands, 1.5-11 GHz and 3.1-10.6 GHz namely. The former is the operational band of the antenna whereas the latter is for the filter. This was the issue for the investigation (to see if it has a negative impact on the overall system performance) but there was no difference in the performance with respect to operational band of frequency. This can be concluded as normal because the antenna band is wider and covers the filter band. This can even be considered as a requirement for a better selectivity.

CHAPTER 6

RESULTS AND DISCUSSION

RF circuit design is a delicate process involving many time-consuming steps. In industry, whole team could work on the design of a receiver. So, it is important to limit the scope of the study. As most of the challenging key RF blocks can already be found in the receiver RF front-end circuitry, it was decided to investigate in the frame of this thesis.

The goal of this research is to investigate and understand the design issues with regard to RF front-ends for UWB applications. The FCC-allowance of the frequencies between 3.1GHz and 10.6GHz for UWB applications in 2002 has increased the level of interest and broadened the scope of research devoted to it. UWB communication technologies promise low-cost implementation with fine time resolution and high throughput at short distances without interfering with other existing wireless communication systems.

As opposed to traditional narrowband radios, Ultra-Wideband (UWB) is a wireless digital communication system exchanging data using short duration pulses. However, the wideband nature of the front-end architecture leads to a totally different design methodology from traditional narrow-band systems. For example, if one employed the conventional narrow-band design approach, the UWB pulse waveform dispersion at the antenna/circuit interface cannot be captured.

Although we aimed for, we could not adapt the system engineering practices effectively because we did neither implement a complete RF Front-end circuitry nor have a specific target application to study. So we didn’t have top system level requirements from which one could derive the requirements for RF Front-end and for its sub-units like antenna and filter.

We have chosen the antenna and filter units for implementation because they are basically the most critical building blocks of all kinds of different receiver RF front-ends regardless of their architectures and targeted applications. The filter is needed to be a BPF over the UWB of 3.1-10.6 GHz. The developed antenna has even a wider operational frequency band of 1.5-10.6 GHz. So they could find place easily in a potential further work of designing a complete RF Front-end unit with a specific application.

One of the biggest challenges of implementing UWB systems is the design of UWB antennas [8]. It is required that a UWB antenna possess broad impedance bandwidth, high radiation efficiency, small size, omnidirectional radiation pattern (small directivity) and broad radiation pattern bandwidth (or frequency-independent radiation pattern). These properties are generally strong functions of the antenna electrical size.

At the same time, antennas are considered to be the largest components of integrated wireless systems making the antenna miniaturization necessary to achieve an optimal design.

Within the framework of this thesis, a novel compact (miniaturized) Vivaldi Shaped Partially Dielectric Loaded (VS-PDL) TEM horn antenna has been successfully designed and developed for UWB communication systems of 1.5-10.6 GHz frequency band. We have shown that a new panel type quasi-planar design obtained by more bending the tapered Vivaldi shaped wings (shortened aperture depth) of the TEM horn antenna leads to a significant size reduction of the device. Furthermore, simulation and measurement results that were in coincidence showed that, when installed within a metallic box, VS-PDL TEM horn antenna with a 5 cm aperture depth has satisfactory far-field radiation characteristics and high gain/lower VSWR over the practical bandwidth. That means such a panel type quasi-planar antenna would be a good candidate for UWB applications as well as the popular communication systems of GSM, GPS, ISM, Wi-Fi and SATCOM bands requiring satisfactory antenna performance.

Band-pass filters can be particularly important in an RF front-end design. BPFs are important components in all kinds RF Front-end receiver architectures. They provide frequency selectivity and affect receiver sensitivity.

As part of the thesis, a novel design methodology which uses fast and accurate SVRM models of base elements based on a 3D EM simulator is presented to design and analyze an UWB BPF. The outputs of the built SVRM models are used as input by a straightforward, simple and efficient CS algorithm under the rules of circuit theory to solve the filter response. The designed filter is manufactured and measured to show that the actual results are in coincidence with the simulation results. Furthermore, the performance of the CS algorithm is compared with other popular methods like GA and PSO to demonstrate the efficiency of the CS algorithm. The suggested methodology could be used for different kind of element shapes and filter types.

As the final part of the thesis work, we have simulated and measured the concatenation of antenna with filter to observe if any waveform dispersion occurs on the transmitted pulses. This is considered as the primary requirement for an acceptable UWB performance of the RF Front-end units regardless of their specific architecture or targeted application. It has been observed that there were no significant waveform dispersion and hence the measurement results were very satisfactory and in agreement with the simulation results indicating a successful UWB performance.

The future work to complement the work done within the scope of this thesis can be listed as follows;

- It would make sense to design a complete UWB RF Front-end unit for a specific target application and to evaluate the performance of the developed antenna and filter units within this complete system and to study design issues like impedance matching accordingly.
- The research presented in this thesis demonstrates some part of the RF section of the UWB systems. There can be lots of more issues when it is integrated with the rest of the system either the remaining RF units like LNA and I/Q mixer or the non-RF parts. Integrating the analog and digital parts is a big issue with the entire digital switching noise coupling into the RF/analog circuitry.
- The design trade-offs at system and sub-system levels could be investigated case by case. For example, if the antenna size needs to be further reduced, the performance degradation on both the transmitter and receiver front-ends needs to be taken into account and may need to be compensated by better circuit performance in the following chain.

- More robust antenna design can be targeted because the antenna characteristics such as input impedance and radiation pattern depend heavily on the environment, especially near field. How to make sure a radiation spectrum independent of the environment is quite challenging and definitely will lead to the design consideration of the whole UWB system where a tight coupling between RF front-end and the rest of the circuits exists.

REFERENCES

[1] Love, J.S., (2009). RF Front-end World Class Designs, First Edition, Elsevier Inc. Oxford, UK.

[2] Vidojkovic, V., Van der Tang, J., Leeuwenburgh, A. and Van Roermund, A., (2008), Adaptive Multi-Standard RF Front-ends, First Edition, Springer Science + Business Media B.V., Netherlands.

[3] Laskar, J., Matinpour, B. and Chakraborty, S. (2004). Modern Receiver Front-ends, First Edition, John Wiley & Sons, Inc., Hoboken, New Jersey, USA.

[4] Park, Y., (2005). Direct Conversion RF Front-End Implementation for Ultra-Wideband (UWB) and GSM/WCDMA Dual-Band Applications in Silicon-Based Technologies, PhD. Thesis, School of Electrical and Computer Engineering, Georgia Institute of Technology, USA.

[5] Guan, X., (2008). Development of RF CMOS Receiver Front-ends for Ultrawideband, PhD. Thesis, Office of Graduate Studies of Texas A&M University, USA.

[6] Yang, L. and Giannakis, G.B., (2004). "Ultra-wideband Communications: An idea whose time has come", IEEE Signal Processing Magazine, 21(6):26-54.

[7] Federal Communications Commission, http://www.fcc.gov, 20 November 2014.

[8] Wang, S.B-T., (2005). Design of Ultra-Wideband RF Front-End, PhD. Thesis, Graduate Division of the University of California, Berkeley, USA.

[9] Bergel, I., Fishler, E. and Messer, H., (2002). "Narrow-band interference suppression in time-hopping impulse-radio system", IEEE Conference on Ultrawideband Systems and Technologies, 20-23 May 2002, Baltimore, Maryland, USA, 2:303–308.

[10] Matin, M.A., (2012). Ultra-Wideband RF Transceiver, Ultra Wideband - Current Status and Future Trends (Chapter-1), InTech open book publishing, http://www.intechopen.com/books/ultra-wideband-current-status-and-future-trends/ultra-wideband-rf-transceive, 12 October 2014.

[11] Liang, X.L., (2012). Ultra-Wideband RF Transceiver, Ultra Wideband - Current Status and Future Trends (Chapter-7), InTech open book publishing, http://www.intechopen.com/books/ultra-wideband-current-status-and-future-trends/ultra-wideband-rf-transceive, 12 October 2014.

[12] Miller, L. E., (2003). “Why UWB? A Review of Ultrawideband Technology”, Report to NETEX Project Office, DARPA prepared by Wireless Communication Technologies Group, National Institute of Standards and Technology (NIST), Gaithersburg, Maryland, USA.

[13] Zwick, T., Wiesbeck, W.,Timmermann, J. and Adamiuk, G., (2013). Ultra-wideband RF System Engineering (EuMA High Frequency Technologies Series), Cambridge University Press, UK.

[14] Teggatz, A., Jöstingmeier, A. and Omar, A.S., A New TEM Double-Ridged Horn Antenna for Ground Penetrating Radar Applications, http://duepublico.uni-duisburg-essen.de/servlets/DerivateServlet/Derivate-14694/Final_Papers/GM0023-F.pdf, 16 October 2013.

[15] Turk, A.S. and Sahinkaya, D.S.A., (2007). Partial Dielectric Loaded TEM Horn Design for Ultra-Wideband Ground Penetrating Impulse Radar Systems, Ultra-Wideband Short-Pulse Electromagnetics Series 7 (Chapter 34), Springer Link, Berlin, Germany.

[16] Scheers, B., Acheroy, M. and A.V. Vorst, (2000). “Time-domain simulation and characterization of TEM horns using a normalized impulse response”, IEE Microwave Antennas & Propagation, 147(6):463-468.

[17] Yarovoy, A.G., Schukin, A.D, Kaploun, I.V. and Ligthart, L.P., (2002). “The dielectric wedge antenna”, IEEE Trans. on Antennas and Propagation, 50(10): 1460-1472.

[18] Turk, A.S., (2006). “Ultra-wideband Vivaldi antenna design for multi-sensor adaptive ground-penetrating impulse radar”, Microwave and Optical Technology Letters, 48(5):834-839.

[19] Turk, A.S., Sahinkaya, D.A., Sezgin, M. and Nazli, H., (2007). “Investigation of Convenient Antenna Designs for Ultra-Wide Band GPR Systems”, Proceedings of 4th International Workshop on Advanced Ground Penetrating Radar (IWAGPR), 27-29 June 2007, Naples, Italy, 192–196.

[20] Matthaei, G. L., Young, L. and Jones, E. M. T., (1980). Microwave filters, impedance-matching networks, and Coupling Structures, Artech House, Norwood, USA.

[21] Oskouei, H. D., Forooraghi, K. and Hakkak, M., (2007). “Guided and leaky wave characteristics of periodic defected ground structures”, Progress In Electromagnetics Research – PIER, 73:15–27.

[22] Wu, B., Li, B., Su, T. and Liang, C. H., (2006). “Equivalent-circuit analysis and lowpass filter design of split-ring resonator DGS”, Journal of Electromagnetic Waves and Applications, 20(14):1943–1953.

[23] Ahn, D., Park, J. S., Kim, C. S., Kim, J., Qian, Y. and Itoh, T., (2001). “A design of the low-pass filter using the novel microstrip defected ground structure”, IEEE Trans. on Microwave Theory and Tech., 49(1):86–93.

[24] Lee, J. K. and Kim, Y. S., (2010). “Ultra-wideband bandpass filter with improved upper stopband performance using defected ground structure”, IEEE Microwave Wireless Components Letters, 20(6):316–318.

[25] Deng, H. W., Zhao, Y. J., Zhang, X. S., Zhang, L. and Gao, S. P., (2010). “Compact quintuple-mode UWB bandpass filter with good out-of-band rejection”, Progress In Electromagnetics Research Letters, 14:111–117.

[26] Huang, J. Q. and Chu, Q. X., (2010). “Compact UWB band-pass filter utilizing modified Composite right/left-handed structure with cross coupling”, Progress In Electromagnetics Research, 107:179–186.

[27] Chou, T. C., Tsai, M. H. and Chen, C. Y., (2010). “A low insertion loss and high selectivity UWB bandpass filter using composite right/left-handed material”, Progress In Electromagnetics Research, 17:163–172.

[28] Wang, J. K., Zhao, Y. J., Qiang, L. and Sun, Q., (2010). “A miniaturized UWB BPF based on novel SCRLH transmission line structure”, Progress In Electromagnetics Research Letters, 19:67–73.

[29] Naghshvarian J. M. and Tayarani, M., (2008). “Miniature planar UWB bandpass filters with circular slots in ground”, Progress In Electromagnetics Research Letters, 3:87–93.

[30] Park, J., Kim, J. P. and Nam, S., (2007). “Design of a Novel Harmonic-Suppressed Microstrip Low-Pass Filter”, IEEE Microwave Wireless Components Letters, 17:424–426.

[31] Zhu, Y. Z. and Xie, Y. J., (2007). “Novel microstrip bandpass filters with transmission zeros”, Progress In Electromagnetics Research, 77:29–41.

[32] Yang, X. S. and Deb, S., (2009). “Cuckoo search via L´evy flights”, Proceedings of World Congress on Nature & Biologically Inspired Computing, 9-11 December 2009, India, 210-214.

[33] Yang, X. S. and Deb, S., (2010). “Engineering Optimisation by Cuckoo Search”, Int. Journal of Mathematical Modelling and Numerical Optimization”, 1(4):330–343.

[34] Vapnik V., (1995). The Nature of Statistical Learning Theory, Springer-Verlag, New York.

[35] Tokan, N. T. and Güneş, F., (2009). “Knowledge-based support vector synthesis of the microstrip lines”, Progress in Electromagnetics Research (PIER), 92:65–77.

[36] Güneş, F., Tokan, N. T. and Gürgen, F., (2010). “A knowledge-based support vector synthesis of the transmission lines for use in microwave integrated circuits”, Expert Systems with Applications, Elsevier journal, 37:3302–3309.

[37] Khodier, M., (2013). “Optimisation of antenna arrays using the cuckoo search algorithm”, IET Microwaves, Antennas & Propagation, 7(6):458–464.

[38] Layeb, A., (2010). “Hybrid Quantum Scatter Search Algorithm for Combinatorial Optimization Problems”, The journal of Annals, Computer Science Series, 8(2):227–244.

[39] Kumar, A. and Chakarverty, S., (2011). “Design optimization for reliable embedded system using Cuckoo Search”, Proceedings of 3rd International Conference on Electronics Computer Technology, 8-10 April 2011, India, 264–268.

[40] Layeb, A.A., (2011). “Novel quantum inspired cuckoo search for Knapsack”, International Journal of Bio-Inspired Computation, 3(5).

[41] Noghrehabadi, A., Ghalambaz, M. and Vosough, A., (2011). “A Hybrid Power Series – Cuckoo Search Optimization Algorithm to Electrostatic Deflection of Micro Fixed-fixed Actuators”, International Journal of Multidisciplinary Sciences and Engineering, 2(4).

[42] Najmy, K., Rani, A., Fareq, M., Malek, A. and Siew-Chin, N., (2012). “Nature-inspired Cuckoo Search Algorithm for Side Lobe Suppression in a Symmetric Linear Antenna Array”, Radioengineering, 21(3):865–874.

[43] Gonzales, G., (1996). Microwave Transistor Amplifiers: Analysis and Design, 2nd Edition, Prentice Hall, New Jersey, USA.

CURRICULUM VITAE

PERSONAL INFORMATION

Name Surname	: Mustafa İLARSLAN
Date of birth and place	:12.12.1966, Afyonkarahisar, TURKEY
Foreign Languages	: English
E-mail	: milarslan@yahoo.com

EDUCATION

Degree	**Department**	**University**	**Date of Graduation**
M.Sc.	Engineering Mng.	Eskişehir Osman Gazi Uni.	2007
M.Sc.	Electronics Eng.	Eskişehir Osman Gazi Uni.	2005
B.Sc.	Electronics Eng.	Middle East Technical Uni.	1989
High School	Cumhuriyet Lisesi	Afyonkarahisar	1984

WORK EXPERIENCE

Year	**Corporation/Institute**	**Enrollment**
Current	Turkish Air Force	1989

PUBLISHMENTS

Papers

1. Ilarslan, M., Demirel, S., Torpi, H., Keskin, A.K. and Caglar, M.F., (2014). "Optimization of Filter by using Support Vector Regression Machine with Cuckoo Search Algorithm", Radioengineering, 23(3):790-797.

2. Ilarslan, M., Turk, A.S., Demirel, S., Aydemir, M.E. and Keskin, A.K. (2014). "A Compact Vivaldi Shaped Partially Dielectric Loaded TEM Horn Antenna for UWB Communication", International Journal of Antennas and Propagation, 2014(9):1-6.

3. Aydemir, M.E., Ilarslan, M. and Gose, E., (2014). "Design and Development of the Avionics Experimentation Board for an Undergraduate Course on Avionic Systems", Journal of Society for Development of Teaching and Business Processes in New Net Environment in B&H, 9(3):714-720.

4. Ilarslan M., Bayrakceken K. and Arısoy, A, (2011). "Avionic System Design of mini VTOL UAV", IEEE Aerospace and Electronic Systems Magazine, 26(10):35-40.

5. Ilarslan, M., Turk, A.S. and Keskin, A.K. (2013). "Partial Dielectric Loaded TEM Horn and Reflector Antenna Designs for Ultrawide Band Ground Penetrating Radar Systems", The Journal of Applied Electronics, 2013(1):99-104.

6. Ilarslan M., (2007). "Testten Faal Geçti (TFG) karmaşası ve alınabilecek tedbirler", Türk Hava Kuvvetleri Uçuş ve Yer Emniyet Dergisi, 2(13).

Conference Papers

1. Aslan, A.R., Kalemci, E., Ilarslan, M., Umit, E. and Sofyalı,A., (2014). "QB50 Projesi Kapsaminda BeEagleSat Küp Uydusunun Geliştirilmesi", V. Ulusal Havacılık ve Uzay Konferansı - UHUK-2014, 8-10 Eylül 2014, Erciyes Üniversitesi, Kayseri.

2. Celik, O., Kilic, C., Sofyali, A., Aslan, A.R. and M. Ilarslan, (2013). "BeEagleSat Attitude Determination and Control System", 5th European CubeSat Symposium, 3-5 June 2013, The Royal Military Academy, Brussels, Belgium.

3. Ilarslan, M., Aslan, A.R. and Celebi, M., (2013). "Turkish University Consortium for Space Technologies and Education (UTEB) Prospects for Turkey", 6th International Conference on Recent Advances in Space Technologies-RAST 2013 (pp:335-338), 12-14 June, 2013, Istanbul / TURKEY.

4. Ilarslan, M., Aydemir, M.E., Gose, E. and Turk, A.S., (2013). "The Design and Simulation of a Compact Vivaldi Shaped Partially Dielectric Loaded (VS-PDL) TEM Horn Antenna for UWB Applications", IEEE International Conference on Ultra Wide-Band Systems-ICUWB 2013, 15-18 September 2013, Sydney, Australia.

5. Aslan, A.R. and Ilarslan, M., (2013). "Prospects for Turkish UNISEC and International Cooperation", United Nations / United Arab Emirates Symposium on Basic Space Technology, Small Satellite Missions for Developing Space Nations, 20-23 October 2013, UAE.

6. Aslan, A.R., Kalemci, E., Ilarslan, M., Umit, E. and Sofyalı,A., (2013). "A Double CubeSat with an X-Ray Detector for In-Situ Environmental Measurements of QB50", 5th Nano Satellite Symposium, 20-22 November 2013, Tokyo, Japan.

7. Sofyalı, A., Umit, E., Toktamış, B., Aslan, A.R. and Ilarslan, M., (2012). “Electrical Power and Attitude Determination and Control System for a 2U CubeSat for the QB50Mission”, 4th European CubeSat Symposium, 30 January - 1 February 2012, The Royal Military Academy, Brussels, Belgium.

8. Turk, A.S., Aydemir, M.E., Gose, E. and Ilarslan, M., (2012). “Practical design considerations for tri-band microstrip patch antennas”, IEEE International Symposium on Antennas and Propagation-ISAP 2012 (pp:1055-1058), 29 Oct.-2 Nov. 2012, Nagoya, Japan.

9. Aydemir M.E., Ilarslan M., Büyükatak K. and Duymaz E., (2011). "Swarm Intelligence in Solution of Impedance Matching Problem in Satellite Transmitters", 5th International Conference on Recent Advances in Space Technologies - RAST 2011, 09-11 June, 2011, Istanbul / Turkey.

10. Tola C., Aslan, A.R. and Ilarslan, M., (2011). “Development of a Mechanical De-orbiting System for a 3-Unit CubeSat”, 3rd Nano Satellite Symposium, 12-14 December, 2011, Kitakyushu, Japan.

11. Özdemir U., Yiğit A.,Tür Y., Aslan A.G., Özkan İ.G., Bayrakçeken, M.K., İlarslan M. ve Arısoy, A., (2010). “Otomatik Uçuş Kontrol Sistemlerinin Donanimli Simülasyonu”, 1nci Aviyonik ve Sistem Entegrasyonu Sempozyumu (ASES-2010) Bildiriler Kitabı, 29-30 Nisan 2010, Yeşilyurt/ İstanbul, 525-526.

12. Özdemir U., Yiğit A.,Tür Y., Aslan A.G., Özkan İ.G., Bayrakçeken, M.K., İlarslan M. ve Arısoy, A., (2010). “Dört Rotorlu Otonom Hava Aracı”, 1nci Aviyonik ve Sistem Entegrasyonu Sempozyumu (ASES-2010) Bildiriler Kitabı, 29-30 Nisan 2010, Yeşilyurt/ İstanbul, 521-524.

13. Bayrakceken, M.K., İlarslan, M., Arısoy, A. and Karamancıoglu, A., (2010). “HILSim for Attitude Control of a Quadrotor”, Proceedings of Unmanned Vehicles Workshop - UVW 2010, 10-12 June 2010, Istanbul/ TURKEY, 151-155.

14. Ilarslan, M., Bayrakçeken, M. K. and Arısoy, A., (2010). “Avionic System Design of a Mini VTOL UAV”, IEEE 29th Digital Avionics System Conference – DASC’2010, 03-07 October-2010, Salt Lake City, UTAH, USA, 6.A.3-1 - 6.A.3-7.

15. Arısoy, A., İlarslan, M., Savruk, S. and Yalçın, M.K., (2009). “The Experimental Setup for Altitude Control of a Quadrotor”, 5th Ankara International Aerospace Conference-AIAC-2009 (1/ 254), 17-19 August 2009, METU, Ankara, TURKEY.

16. Ilarslan, M., (2004). “Görev Bilgisayarları ve Milli olarak Geliştirilmesine Yönelik Değerlendirmeler”, Havacılıkta İleri Teknolojiler ve Uygulamaları Konferansı – HİTEK 2004, , 9–10 Aralık 2004, HHO, İstanbul, TÜRKİYE, 2:655-661.

Projects

1. Various Turkish Air Force Projects

2. 2012-2014, Measurement of Far field radiation pattern of a sea-based radar antenna by making use of a mini-UAV, supported by TUBİTAK-UME.

3. 2011-2016, QB50 – Development and launch of 50 nano satellites, EU-FP7 project managed by Von Karman Institute of Belgium. Turkish Air Force Academy, Istanbul Technical University and HAVELSAN are partners in this project.